RD
92
29

Report No. DOT/FAA/RD-92/29

COPY = 2

Project Report
ATC-193

Analysis of Surveillance Performance at Chicago O'Hare Airport

S.I. Altman
D.W. Burgess
R.G. Potts
R.G. Sandholm
M.L. Wood

FEDERAL AVIATION ADMINISTRATION
MAR 21 1994
TECHNICAL CENTER LIBRARY
ATLANTIC CITY INT'L AIRPORT, NJ 08405

28 January 1994

Lincoln Laboratory
MASSACHUSETTS INSTITUTE OF TECHNOLOGY
LEXINGTON, MASSACHUSETTS

Prepared for the Federal Aviation Administration.
Document is available to the public through
the National Technical Information Service,
Springfield, Virginia 22161.

This document is disseminated under the sponsorship of the Department of Transportation in the interest of information exchange. The United States Government assumes no liability for its contents or use thereof.

TECHNICAL REPORT STANDARD TITLE PAGE

1. Report No. ATC-193	2. Government Accession No. DOT/FAA/RD-92/29	3. Recipient's Catalog No.
4. Title and Subtitle Analysis of Surveillance Performance at Chicago O'Hare Airport		5. Report Date 28 January 1994 6. Performing Organization Code
7. Author(s) Sylvia I. Altman, Douglas W. Burgess, Richard G. Potts, Ronald G. Sandholm, M. Loren Wood, Jr.		8. Performing Organization Report No. ATC-193
9. Performing Organization Name and Address Lincoln Laboratory, MIT P.O. Box 73 Lexington, MA 02173-0073		10. Work Unit No. (TRAIS) 11. Contract or Grant No. DTFA-01-93-Z-02018
12. Sponsoring Agency Name and Address Department of Transportation Federal Aviation Administration Systems Research and Development Service Washington, DC 20591		13. Type of Report and Period Covered Project Report 14. Sponsoring Agency Code

15. Supplementary Notes

This report is based on studies performed at Lincoln Laboratory, a center for research operated by Massachusetts Institute of Technology under Air Force Contract F19628-90-C-0002.

16. Abstract

This report describes the results of RF measurements of the 1030 and 1090 MHz environment in the Chicago terminal area conducted by Lincoln Laboratory in October 1991. The measurements were made at the request of the FAA in response to reports by controllers in Chicago that TCAS interrogations are affecting the surveillance performance of the Chicago Secondary Surveillance Radar (SSR). The Airborne Measurements Facility (AMF), developed at Lincoln Laboratory, was used to gather TCAS and SSR interrogation and reply data in the vicinity of O'Hare Airport during periods of active TCAS operation. Simultaneously, local aircraft track data were collected using the Automated Radar Terminal System (ARTS) data recording facility.

Analysis of both the AMF data and the ARTS data show that TCAS interrogations do not cause a significant degradation in SSR surveillance performance and that the average Chicago ARTS track performance in the presence of TCAS-equipped aircraft is comparable to earlier measurements of track performance in Chicago as well as at a number of other high-density terminal areas. Specific regions within the Chicago surveillance area were observed to contain concentrations of poor ARTS track performance, and analysis of the data has shown the cause to be differential vertical lobing associated with the SSR antenna and faulty Mode S transponders on certain aircarrier aircraft. Both of these problems have subsequently been corrected.

17. Key Words			18. Distribution Statement
TCAS	ARTS III/A	interference limiting	This document is available to the public through the National Technical Information Service, Springfield, VA 22161.
Mode S	ATCRBS	interrogation rates	
AMF	fading	vertical lobing	
SSR	target coast	surveillance performance	
blip/scan	interference	SSR runlength	

19. Security Classif. (of this report)	20. Security Classif. (of this page)	21. No. of Pages	22. Price
Unclassified	Unclassified	121	

FORM DOT F 1700.7 (8-72) Reproduction of completed page authorized

EXECUTIVE SUMMARY

During 1991, air traffic controllers at several terminal areas, particularly Chicago, began reporting a noticeable decrease in Secondary Surveillance Radar (SSR) track performance. The controllers have attributed this degradation to interrogation channel interference caused by increased numbers of operational Traffic Alert and Collision Avoidance System (TCAS) II-equipped aircraft. The controller assertion that the SSR problems are TCAS-related is a concern since the TCAS design includes provisions to prevent such interference. Coincidentally, the Great Lakes Regional Office and O'Hare Radar Airway Facilities (AF) personnel have been engaged, for several years, in a program to improve the SSR performance in Chicago. They have been successful in achieving reasonably good SSR track-performance, consistent with that observed at other installations, despite inherent limitations in the capability of the current SSR equipment and site-related problems that are beyond their control.

On 16 July 1991, the Federal Aviation Administration (FAA) TCAS Program Office requested that Lincoln Laboratory evaluate the reported impact of TCAS on Chicago SSR track performance, confirm suspected siting problems and assist Airways Facilities personnel in characterizing the Chicago SSR interrogation performance. The FAA also requested that Lincoln Laboratory attempt to determine and resolve the causes responsible for the controller complaints.

To support the investigation, Lincoln Laboratory reactivated an instrumented airborne data collection facility, the Airborne Measurements Facility (AMF) developed in the 1970's, in order to collect data necessary to evaluate simultaneous TCAS and SSR interactive operations on the 1030 MHz interrogation channel. The AMF equipment provides the capability of measuring interrogation rates from all sources in order to determine the impact of these interrogations on the availability of a transponder for SSR surveillance and to evaluate SSR interrogator characteristics.

Visits were made to the Chicago Regional Office and O'Hare Terminal Radar Approach Control (TRACON) during July and August 1991 to exchange information, to observe problems on the air traffic displays, and to plan and coordinate the flight testing in the Chicago area.

On 22 and 23 October 1991, Lincoln Laboratory flew pre-planned flight tests in the Chicago area with the AMF equipment. The flight tests were organized to collect data in critical areas that have been designated as problematical by either controllers or FAA facilities and regional personnel. Flights were conducted during the busy morning rush period in heavy traffic density areas to evaluate TCAS interference and at night in order to evaluate SSR interrogation performance along specially designated radials to the SSR.

The data collected during the AMF flight test period consisted of AMF recordings of 1030 MHz signals and Automated Radar Terminal System (ARTS) data recordings. The analysis of the data was organized into the following three principal areas of investigation:

(a) Examination of AMF data recorded during the busy morning period to evaluate the impact of large numbers of TCAS aircraft on SSR surveillance.

(b) Examination of AMF data recorded during the evening radial flights to determine the extent of SSR antenna vertical differential lobing, SSR power adequacy and to evaluate these in terms of SSR target update reliability. AMF and ARTS data on targets-of-opportunity were also examined to determine the impact of differential lobing on SSR performance.

(c) Examination of ARTS data recorded during the AMF flights in order to evaluate the SSR ARTS blip/scan performance and to investigate and associate possible causes with ARTS coasting.

Analysis of both the AMF data and the ARTS data collected in Chicago has resulted in the following conclusions:

(a) TCAS Is Not Causing Significant SSR Degradation

TCAS interrogation rates observed during a busy morning period in Chicago were such that a victim transponder would be occupied by a TCAS interrogation 0.76% of the time. AMF data also indicate that actual preemption of the O'Hare SSR interrogation at the AMF by a TCAS interrogation occurred 0.6% of the time. The amount of interference caused by TCAS in the Chicago area is less than the 1% average interference limit allocated to TCAS. By contrast, examination of ground interrogator rates indicate that a transponder would be occupied by a ground interrogation or suppression 1.6% of the time.

TCAS interrogation rates showed occasional peaks in the total TCAS interrogation rate with the highest peak reaching about 500 TCAS interrogations per sec. This peak is not significant because the total TCAS interrogation rate would have to reach 10,000 interrogations per sec (20 time higher) before it would degrade the SSR surveillance track reliability of a transponder by 2%.

(b) Beacon Antenna Lobing Is Causing Serious Coasting

Serious differential lobing occurs along a 65-degree radial to the SSR and examination of the terrain surrounding the SSR indicates that differential lobing can also be a problem within a 40- to 85-degree azimuth sector relative to the SSR. The differential lobing is seen to cause main-beam suppression by the transponder due to low P1/P2 ratios and shortened main-beam run lengths due to destructive interference between the Improved Interrogation Side Lobe Suppression (I^2SLS) P1 and the mainbeam P1 close to the beam edge. Both AMF and ARTS data collected on targets-of-opportunity support the observation that much of the coasting on Victor 84 is due to differential lobing.

(c) Average O'Hare Track Performance Is Good

The overall blip/scan ratios measured on O'Hare ARTS tracked targets that are within 0.5- and 40-degrees elevation and 2- and 45-nautical mile (nmi) range were greater than 97% during both the busy morning period, which had large numbers of TCAS, and during the quiet late evening period, which had very few TCAS. This indicates that track performance in terms of blip/scan is independent of the number of TCAS. The blip/scan evaluation also showed that, in a few instances, individual tracks associated with a specific airline carrier had significantly lower blip/scan ratios. Analysis of air carrier aircraft coasts (failure to update a track) during the busy morning period and the quiet evening period has resulted in the successful association of a probable cause for each coast in over 90% of the situations. Most of the coasts in Chicago are determined to be caused by reply garble, low signal levels due to fading and differential lobing effects.

(d) Faulty Mode S Transponders Are Causing Serious O'Hare Beacon Coasts

A small percentage of the total coasts are due to aircraft with faulty Mode S transponders. These are associated with B-737S and DC-10 aircraft carrying one of two early models of a Mode S transponder having an improper reply rate limit circuit. Although the aircraft-specific coasts are a small percentage of the total, they persist for many SSR scans and deprive controllers of altitude information for an appreciable length of time.*

In summary, TCAS interrogations do not measurably interfere with the Chicago ATC surveillance function. Vertical lobing, siting problems, and faulty transponders have been identified as serious sources of SSR degradation and corrective action is underway.

---

* The manufacturer has since corrected this problem.

ACKNOWLEDGMENTS

The authors would like to acknowledge the following people who helped to restore the AMF equipment, recover AMF processing programs, plan and participate in the flight tests, participate in the data analysis, and, without whom, this effort would not have been possible.

Ann Drumm	-	who had the difficult task of determining TCAS equipage amongst the aircraft present in the Chicago area during the AMF flight tests.
Vic Gagnon	-	who coordinated the installation of AMF, helped plan the Chicago flight tests, and flew as an operator
Ralph Cataldo	-	who had the difficult task of restoring the AMF recording and playback facility
Joseph DiBartolo	-	who checked out and calibrated the AMF receiver
Arnold Kaminsky	-	who located most of the old AMF analysis software
Art Madge, FAATC	-	who established contacts and coordinated efforts with the Chicago personnel
Al Pratt	-	who piloted the AMF aircraft
Robert Hamilton	-	who co-piloted the AMF aircraft
Katharine Krozel	-	who edited this document

We would also like to acknowledge the Airways Facilities and Air Traffic personnel at the O'Hare ARTS and the Great Lakes Regional Office for their support and cooperation in the conduct of these flight tests.

LIST OF FIGURES

Figure No.		Page
1	O'Hare TCAS Activity	6
2a	AMF Range Track Relative to O'Hare Radar	7
2b	O'Hare TCAS Interrogation Rate Activity	7
3	SSR Target Report Eligibility vs TCAS Rate	8
4a	AMF Range Track Relative to O'Hare Radar	9
4b	O'Hare SSR Activity	9
5	SSR Vertical Lobing Pattern	13
6	SSR Azimuth Pattern, 1.75-Degree Elevation	16
7	SSR Azimuth Pattern, 1.75-Degree Elevation	17
8	SSR Azimuth Pattern, 1.75-Degree Elevation	18
9	SSR Azimuth Pattern, 2.4-Degree Elevation	19
10	SSR Azimuth Pattern, 2.4-Degree Elevation	20
11	SSR Azimuth Pattern, 2.4-Degree Elevation	21
12	SSR Azimuth Pattern, 2.4-Degree Elevation	22
13	Peak-of-Beam P1/P2 Ratio at AMF vs. Elevation Angle	23
14	SSR Elevation Pattern, 170-Degree Radial	27
15	SSR Elevation Pattern, 170-Degree Radial	29
16	View From the Main O'Hare SSR Antenna in the Direction of 165 Degrees Azimuth	31
17	SSR Elevation Pattern, 300-Degree Radial	33
18	View From the Main O'Hare SSR Antenna in the Direction of 215 Degrees Azimuth	35
19	Chicago Runlength	37
20	Chicago Runlength vs P1/P2 Ratio	38
21	SSR Horizontal Pattern: P1/P2 > 24 dB	41
22	SSR Horizontal Pattern: P1/P2 = 11 dB	42
23	SSR Horizontal Pattern: P1/P2 = 6 dB	43
24a	Radar Tracks Along V84	45
24b	Fresnal Zone Center Corresponding to Radar Tracks in Figure 24a	45
25	Mainbeam and Omni Antenna Elevation Patterns from AMF Measurements	49
26a	Radar Tracks Along V84	50
26b	Fresnal Zone Centers Corresponding to Radar Tracks in Figure 26a	50
27	Simple Block Diagram of Radar Data Processing and Storage	53
28	Single Track Blip/Scan Ratios - Major Airlines - High-Density Sample	56
29	Single Track Blip/Scan Ratios - Airlines - High-Density Sample	57
30	Single Track Blip/Scan Ratios by Major Airlines - Low-Density Sample	58
31	Single Track Blip/Scan Ratios - Airlines - Low-Density Sample	59
32	Single Track Blip/Scan Ratios Histogram - Airlines - High-Density Sample	60

LIST OF FIGURES
(continued)

Figure No.		Page
33	Single Track Blip/Scan Ratios Histogram - Airlines - Low-Density Sample	61
34	Total Track Reports and Blip/Scan Ratio vs. Azimuth - Both Data Samples	62
35	Total Track Reports and Blip/Scan Ratios vs. Elevation Azimuth - Both Data Samples	63
36	Total Track Reports and Blip/Scan Ratio vs. Ground Range - Both Data Samples	64
37	Blip/Scan Ratio vs. Time of Day - Both Data Samples	65
38	Distribution of High Coast Periods by Range	69
39	Distribution of High Coast Periods by Elevation	70
40	Maximum Single Track Coast Probabilities for Airlines	71
41	Maximum Single Track Coast Probabilities for Airlines	72
42	Maximum Single Track Coast Probabilities	73
43	Probability of Coasting vs. Slant Range for Selected Airline and Aircraft Type	74
44	Probability of Coasting vs. Slant Range for Selected Airline and Aircraft Type	75
45	Probability of Coasting vs. Slant Range for Selected Airline and Aircraft Type	76
46	Maximum Single Track Coast Probabilities	77
47	Maximum Single Track Coast Probabilities	78
48	High-Density Data Sample	82
49	Low-Density Data Sample	83
50	Coasts Associated with Low P1/P2 Ratio - High-Density Sample	84
51	ARTS Track Data	85
52	Chicago Radar Track	87
A-1	AMF Flight Test - Radials for Vertical Lobing Assessments (Test C)	95
D-1	AMF Airborne Subsystem Block Diagram	101

LIST OF TABLES

Table No.		Page
3-1	4/21/91 Coasts on V84	46
4-1	Coast Associations for High-Density Sample	80
4-2	Coast Associations for Low-Density Sample	81
A-1	Altitudes and Ranges for Radial Runs (Test C)	94

1. INTRODUCTION

During 1991, controllers at several terminal areas, including Chicago, began reporting a noticeable decrease in Secondary Surveillance Radar (SSR) track performance. The controllers attributed this degradation to interrogation channel interference caused by increased numbers of TCAS II-equipped aircraft. The degradation seen by the controllers was characterized by an increase in the number of coasted reports observed on TRACON displays. The controllers felt that the additional interrogations generated by the current numbers of TCAS units are using up transponder channel availability and preventing ground beacon radars from providing reliable surveillance. As a result the controllers were concerned about the final impact of a full TCAS implementation. The controller assertion that the SSR problems are TCAS-related was of serious concern since the TCAS design includes provisions to prevent such interference.

Coincidentally, the Great Lakes Regional Office and O'Hare Radar Airway Facilities personnel had a radar improvement program underway to increase the quality of SSR surveillance and to address problems reported by controllers. These problems include false tracks and the need to increase range coverage and were of concern before TCAS II deployment. They have been successful in achieving a reasonably good SSR track-performance level despite inherent limitations in the capability of the current SSR equipment as well as site-related problems that are beyond their control.

On 16 July 1991, the FAA TCAS Program Office requested that Lincoln Laboratory investigate the reported complaints, measure TCAS compatibility with the ATC system, and attempt to determine and resolve the causes responsible for the controller concerns. The FAA identified the O'Hare Airport in Chicago as the first terminal area to be investigated.

To conduct the measurements to support an evaluation of the impact of operational TCAS units on SSR-surveillance performance and to characterize SSR-interrogation performance relative to aircraft within O'Hare airspace, Lincoln Laboratory reactivated its Airborne Measurements Facility (AMF). The AMF was developed in the 1970s as part of the Mode S ground sensor development. It is an instrumented airborne test facility capable of detecting and recording at high speed all ATC interrogation pulses appearing on the 1030 MHz uplink or all ATC reply pulses appearing on the 1090 MHz downlink. Software post-processing programs are then used to associate the individually recorded pulses with their appropriate interrogation or reply waveforms. This permits a full characterization of either the 1030 MHz channel in terms of interrogator parameters and interrogation rates or the 1090 MHz channel in terms of transponder parameters and fruit reply rates.[1]

On 30 and 31 July 1991, Lincoln Laboratory staff made an initial visit to the FAA facilities at O'Hare Airport in Chicago. During this trip the staff presented a TCAS briefing to the FAA personnel, discussed the problems observed by the O'Hare controllers, gathered information on the O'Hare SSR characteristics, and spent time observing coasting problems on the TRACON display. A second visit was made to O'Hare on 8 August 1991 in order to become familiar with ARTS data extraction and analysis software and to conduct additional observations of the TRACON displays.

---

1 A *fruit reply rate* is an unsolicited reply elicited by another interrogator.

During the remainder of August and throughout September 1991, Lincoln Laboratory, with FAATC assistance, developed a flight test plan for the AMF aircraft flights in the Chicago area. The test plan was reviewed and finalized with O'Hare ATC and AF and FAA Regional Office personnel on 21 October 1991 (refer to Appendix A for a full description of the flight test plan).

Flight testing and data recording at O'Hare commenced on 22 October 1991 at 7:15am with several "racetrack" maneuvers in the vicinity of Victor 84 airway during the busy time that air carrier aircraft were approaching runway 22R along Victor 84. AMF then proceeded along the approach to 22R. This scenario was repeated in the vicinity of the approach to 14R and also included a departure along 9L. These locations were reported by controllers as being troublesome in terms of severe coasting. Approximately 2 hours of AMF data were recorded during this period. A series of VOR radial flights were then conducted from 9:00pm on 22 October 1991 to 12:30am on 23 October 1991 for the purpose of collecting SSR interrogation data to characterize the SSR antenna patterns and radiated power levels. Lincoln Laboratory also requested ARTS data recorded during the AMF morning and evening flight periods in order to examine and evaluate the coasting problems in detail.

The analysis of the AMF data and the ARTS data has been organized in this report into three principal investigation areas as follows:

(a) Section 2 investigates the impact of TCAS interrogations on the ability of the SSR to perform aircraft surveillance and to support air traffic control in the O'Hare terminal area. AMF data recorded during the peak morning traffic period are processed to determine the total interrogation rate associated with large numbers of TCAS aircraft as well as the interrogation rate associated with all of the observed ground interrogators in the vicinity of O'Hare. These data are used to compute the degree of "utilization" of a transponder by all TCAS units in its vicinity.

(b) Section 3 characterizes the interrogation performance of the O'Hare SSR in terms of the SSR radiated elevation and azimuth antenna patterns and the SSR interrogation power levels received at a transponder. AMF data collected during radial flights against the SSR are used to generate the antenna patterns and to determine received power levels. This information is examined for the occurrence of fades due to antenna pattern lobing nulls and main-beam suppression due to differential lobing between the main antenna and the SLS omni antenna. The information is also examined to determine whether the SSR is transmitting adequate power. AMF and ARTS target-of-opportunity data were also examined to characterize the effect of lobing on the generation of target reports and on the performance of target tracking.

(c) Section 4 presents an evaluation of target coasting as seen by ARTS III. ARTS data collected during the AMF flights are examined for coasting, and an attempt is made to associate each of the coast periods with a possible reason such as aircraft maneuver, code garble, fades or main-beam suppression due to vertical lobing and known problematical locations. Correlation of coasting with aircraft equipage is made to determine any relationship to Mode S or TCAS. The data are also used to calculate coast probabilities both in a global sense and for specific aircraft types (air carrier, airline, etc.) and geometric locations.

2. IMPACT OF TCAS ON SSR PERFORMANCE

Initially, a 9-minute segment of the 1030 MHz AMF pulse data, collected during the busy morning period of 22 October 1991, was analyzed to detect pulse sequences that had the spacing and relative amplitudes of ATCRBS Mode A, C and 2 interrogations, TCAS whisper/shout interrogations, Mode S short and long interrogations, and 2-pulse suppressions. The various sequences are referred to as "events." (The AMF recording format represents pulses that are longer than 2 microseconds as a sequence of 2-microsecond pulses. Therefore, a Mode S interrogation would be represented as a sequence of 10 or 17 consecutive pulses.)

The 9-minute segment contained 1,258,733 pulses of which 912,413 (72.4%) were associated with ATCRBS or TCAS events. An additional 294,616 pulses (23.4%) had nearest neighbors greater than 22 microseconds away and were generally near the detection threshold. They are probably attributable to ATCRBS or TCAS interrogations from sources so distant that, by chance, only one of the interrogation pulses made it above AMF threshold. Thus, about 95.8% of the pulses were accounted for.

The 1,258,733 pulses contained the following 262,663 events:

Event	Number	Rate/sec
2-Pulse Suppression	152,627	282.6
ATCRBS (P1,[P2],P3)	25,346	46.9
TCAS Whisper/Shout	43,994	81.5
TCAS Mode S Long or Short	38,217	70.8
Long Pulses (unknown origin)	2,477	4.6
Mode S All Call	2	0.0
	262,663	

The vast majority of the two pulse suppressions are I^2SLS transmissions from ATCRBS ground beacons.

If we consider that every event occupies a transponder for 50 microseconds, then (disregarding the long pulses) to a first approximation, the TCAS activity would occupy a victim transponder 0.76% of the time. The same transponder would be occupied by ground ATCRBS activity, including 2-pulse suppressions, 1.6% of the time. From this, we conclude that the TCAS activity appears to be well within the 1% allocated to TCAS, and the ATCRBS activity is more than twice the TCAS activity.

If the TCAS event rate of 152.3 events per second (81.5 + 70.8) were poisson distributed, then we would expect the probability of one or more TCAS events pre-empting an ATCRBS event to be 1-exp -[152.3 * 50 mic.sec] or 0.0076. Analysis of the AMF pulse data indicates that such preemption actually occurred 153 times in 25,346 opportunities, or with probability 0.0060. This low rate of preemption agrees with the poisson assumption, and would have no noticeable effect on the reliability of SSR ATCRBS target reports.

The rate of long Mode S interrogations, which are assumed to be TCAS broadcasts, was 5.1 per second. Since TCAS units transmit broadcast interrogations each 8 seconds, the number of TCAS aircraft is proportional to 8 times this rate divided by Q, where Q is related to whether the TCAS aircraft has a directional antenna, and could be any value from 1 to 4. From this, we can estimate that the number of TCAS aircraft within about 30 nmi of the AMF is between 10 and 40.

An examination of ARTS data for airline identification and a correlation of this information with known or estimated TCAS equipage indicate that the number of TCAS aircraft present during the above AMF analysis varied between 14 and 16 (see Figure 1).

In order to ensure that the initial 9-minute segment, analyzed in detail and described above is representative of a much longer period, ATCRBS and TCAS events were counted over the entire 2 1/2 hours of data. During this period, 4,232,526 events were identified and broken down as follows:

Event	Number	Rate/sec
2-Pulse Suppression	2,601,053	307.34
ATCRBS (P1,[P2],P3)	391,440	46.25
TCAS Whisper/Shout	565,598	66.83
TCAS Mode S Long or Short	608,886	71.9
Long Pulses (unknown origin)	65,530	7.7
Mode S All Call	19	0.0
	4,232,526	

The TCAS interrogation rates during the 2 1/2-hour period are plotted as a function of time in Figures 1 and 2. The TCAS interference limit threshold of 280 interrogations per sec, which represents a 1% SSR degradation limit, is indicated on the TCAS interrogation plot in Figure 1. Figure 1 also shows the overall ARTS track performance in terms of blip/scan and the total aircraft count over the same 2 1/2-hour period. Both the blip/scan and aircraft count were derived from ARTS data recorded during the same time period. The overall ARTS track performance remains within +/- 1% of 96% during this period and does not appear to be affected by the peak values associated with the TCAS interrogation rate.

Figure 2 shows the TCAS Mode S and whisper/shout interrogation rates separately along with a time plot of AMF range relative to the Chicago SSR. The peaks in the TCAS interrogation rate coincide with the times that the AMF aircraft is very close to O'Hare Airport. This appears to explain why the observed TCAS interrogation rate occasionally exceeds the interference limit. Each individual TCAS interference limiting algorithm is designed to limit the <u>average</u> reception rate of all TCAS interrogations at any transponder within detection range to 280 interrogations per sec. In addition, the practical implementation of the TCAS II interference limiting algorithm may approximate the algorithm by assuming a certain TCAS II antenna directionality. When the AMF is near the airport it is conceivable that a large number of TCAS aircraft are in very close proximity to AMF and that AMF is able to see most of the 83 whisper/shout interrogations from each nearby TCAS as well as those TCAS Mode S interrogations that are directed away from the AMF (i.e., the assumption of antenna directionality no longer holds true). The design philosophy behind the interference limiting algorithms is concerned with the average effect of the total of all TCAS

interrogations on the reply ratio of transponders under SSR surveillance and accepts that any one victim transponder will occasionally see TCAS interrogation rates in excess of 280 per sec for brief periods of time.

The highest peak TCAS interrogation rate observed in Chicago during the 21/2-hour period is just over 500 per sec. The impact of this rate on the ability of the SSR to provide adequate surveillance on a transponder-equipped aircraft is illustrated in Figure 3. A TCAS interrogation rate of 10,000 per sec at a victim transponder, nearly 20 times the rate observed, will degrade the SSR track reliability of that victim transponder by only 2%. The observed TCAS rate, therefore, has essentially no effect on the SSR in Chicago.

The AMF also measured the ATCRBS interrogation rates and the I^2SLS transmission rates over a 2 1/2-hour period from SSRs in the Chicago area. These are illustrated in Figure 4 along with the range track of the AMF aircraft relative to the O'Hare SSR. Peaks in the SSR interrogation and suppression rates all seem to coincide with times that AMF is close to the O'Hare SSR. Since the expected peak suppression rate observed from the O'Hare SSR is on the order of 400 per sec, it appears that the AMF is receiving transmissions from a number of SSRs in the Chicago area. It is interesting to note that the SSR transmission activity is nearly twice that of the TCAS activity.

To summarize, the 22 October 1991 measured SSR and TCAS activity at O'Hare demonstrates that TCAS is not degrading SSR track performance.

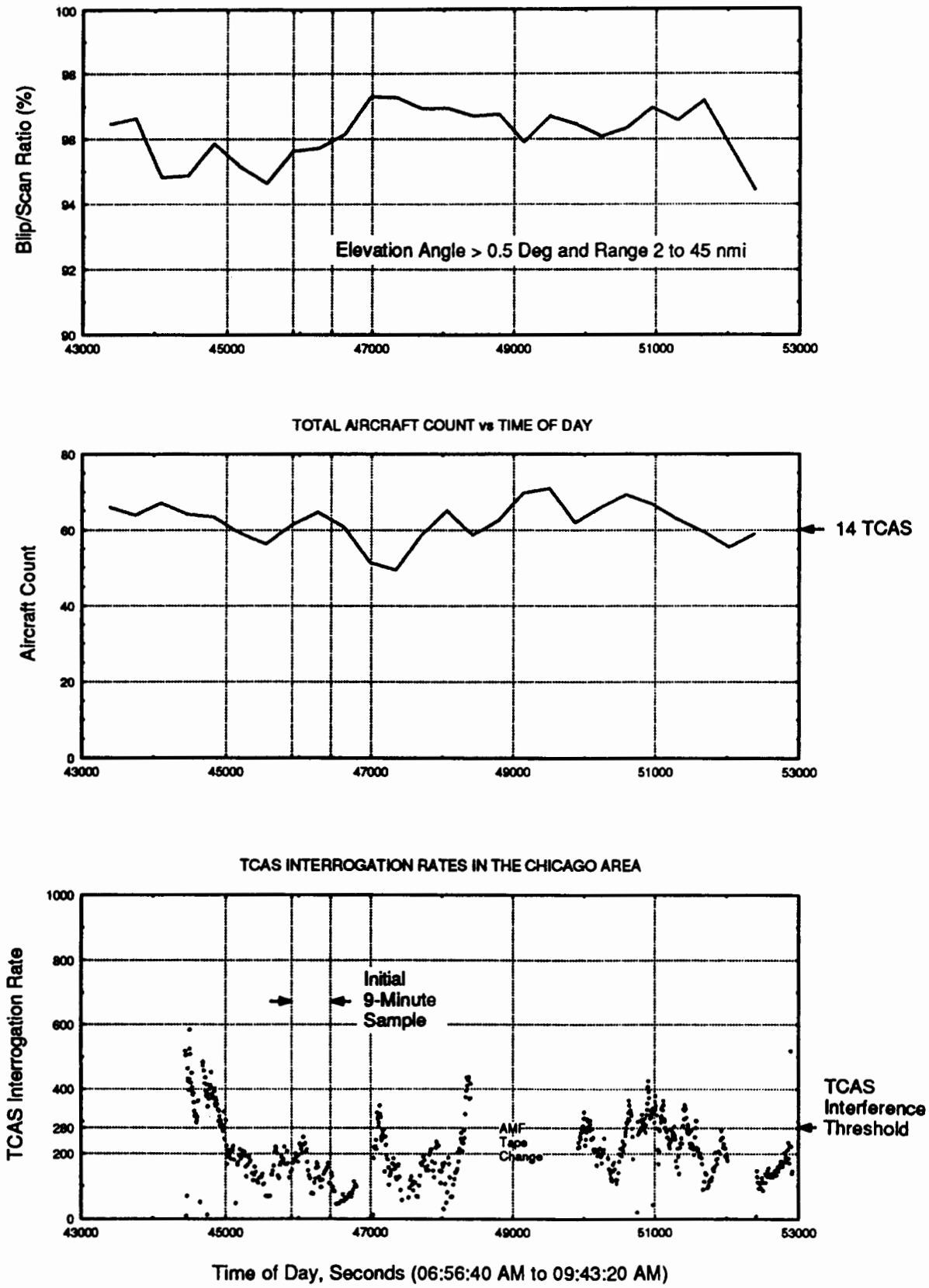

Figure 1. O'Hare TCAS Activity – 22 October 1991.

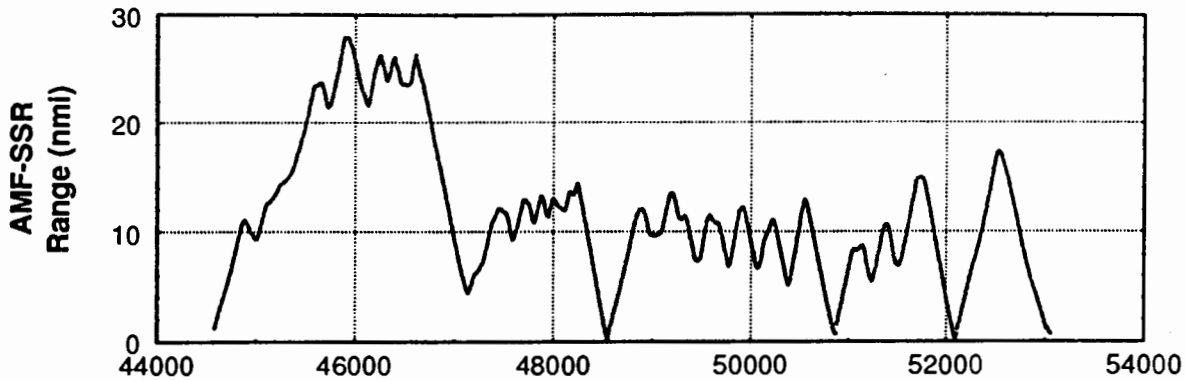

Figure 2a. AMF Range Track Relative to O'Hare Radar.

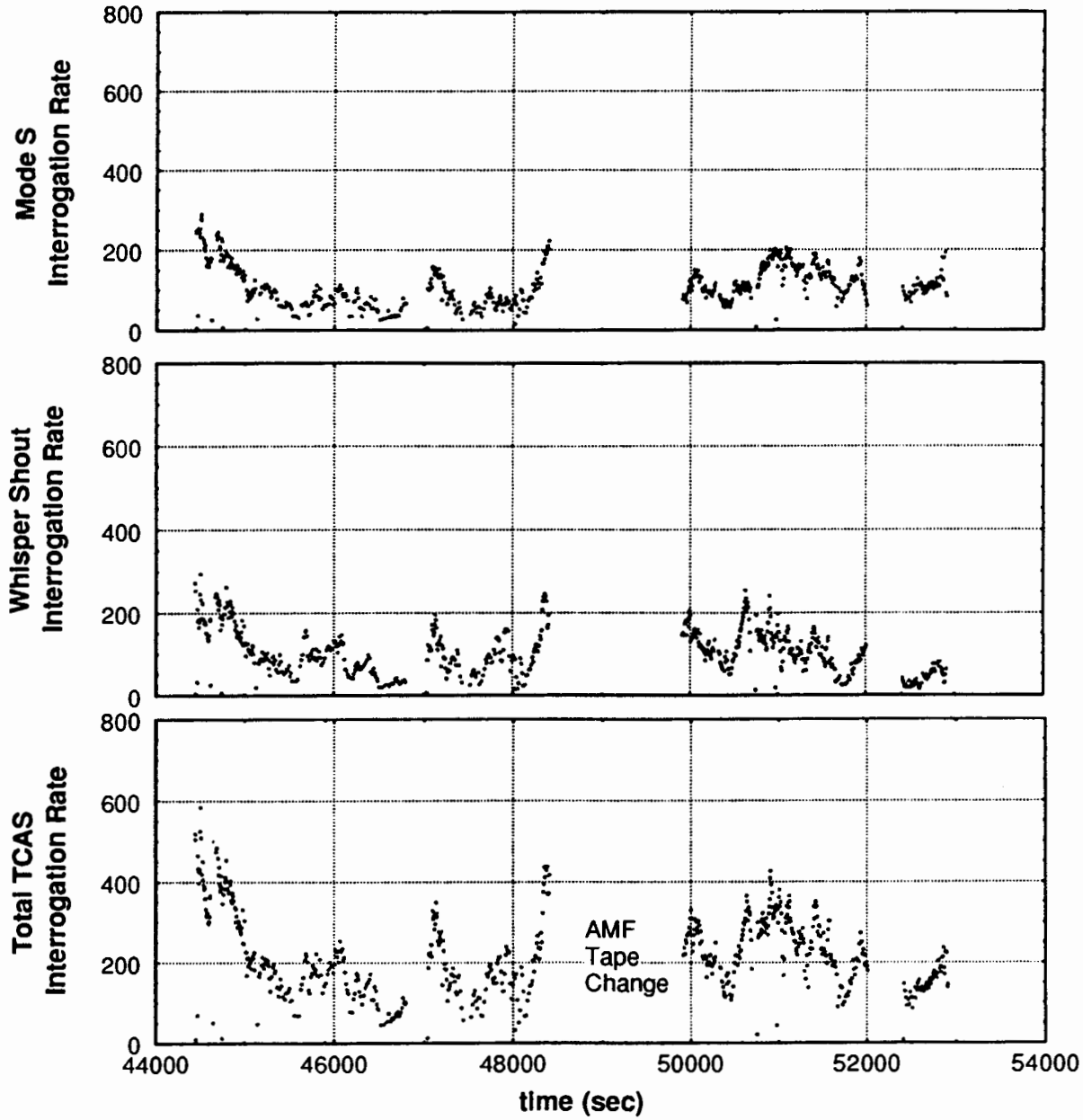

Figure 2b. O'Hare TCAS Interrogation Rate Activity — 22 October 1991.

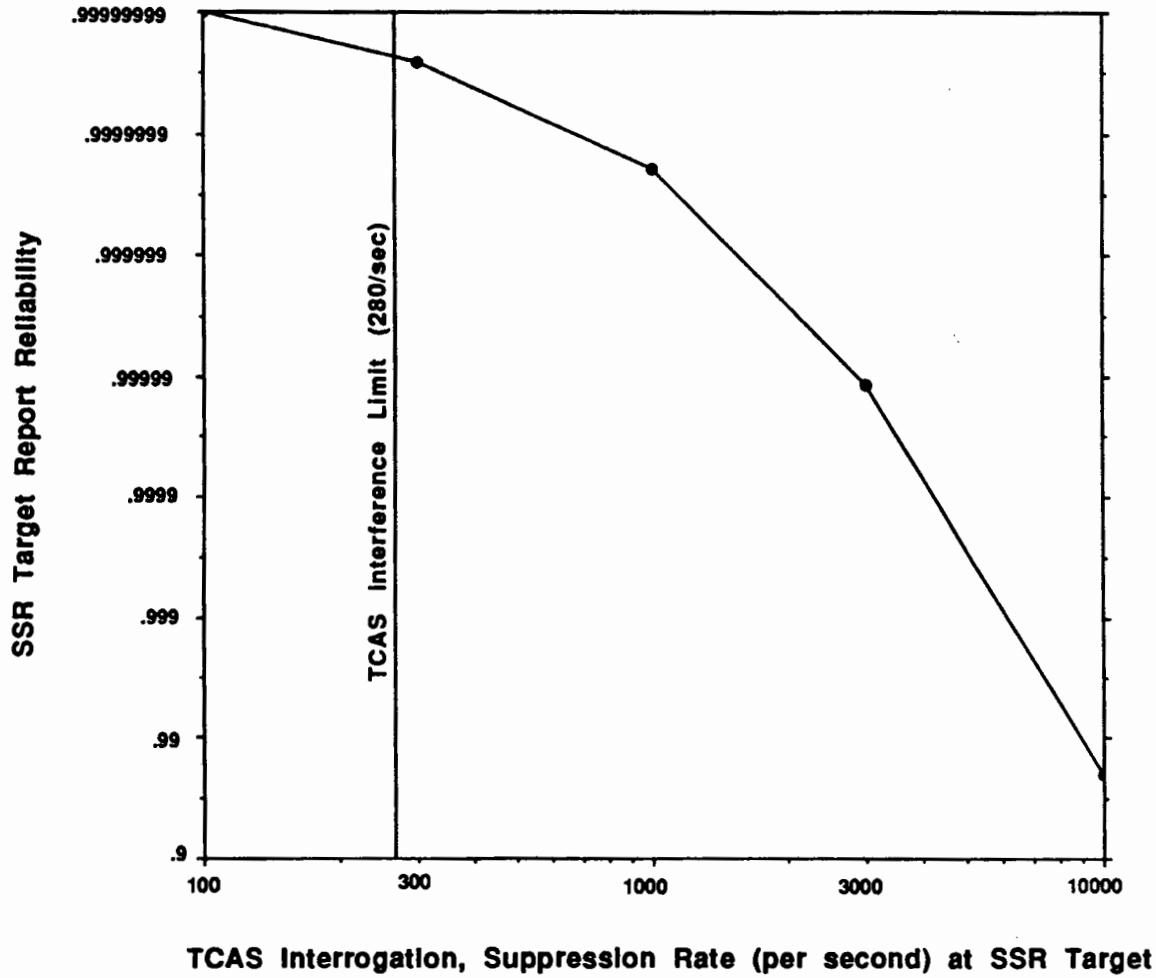

Figure 3. SSR Target Report Reliability vs TCAS Rate (Runlength = 20, Lead Edge = 5, Hits = 8).

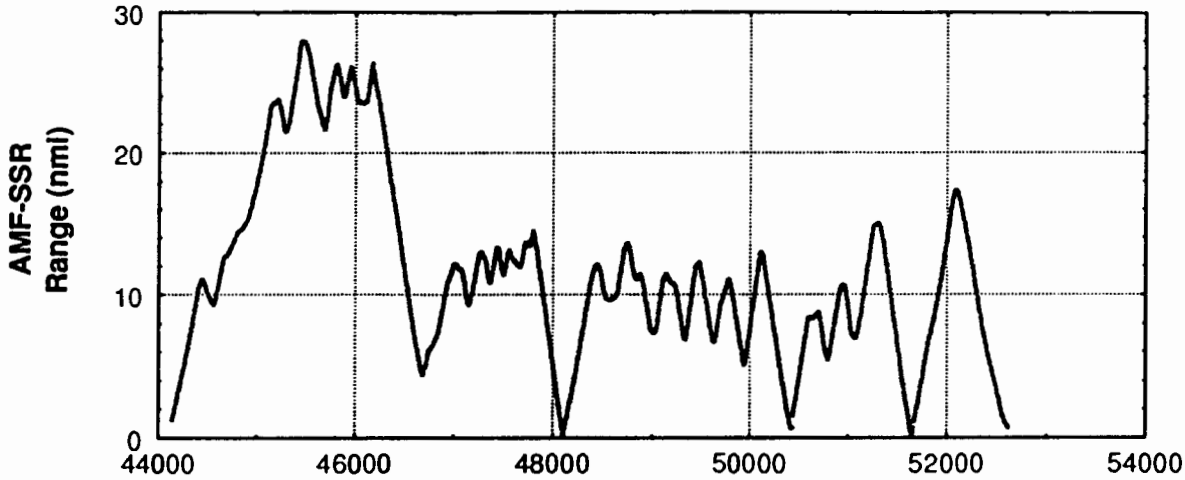

Figure 4a. AMF Range Track Relative to O'Hare Radar.

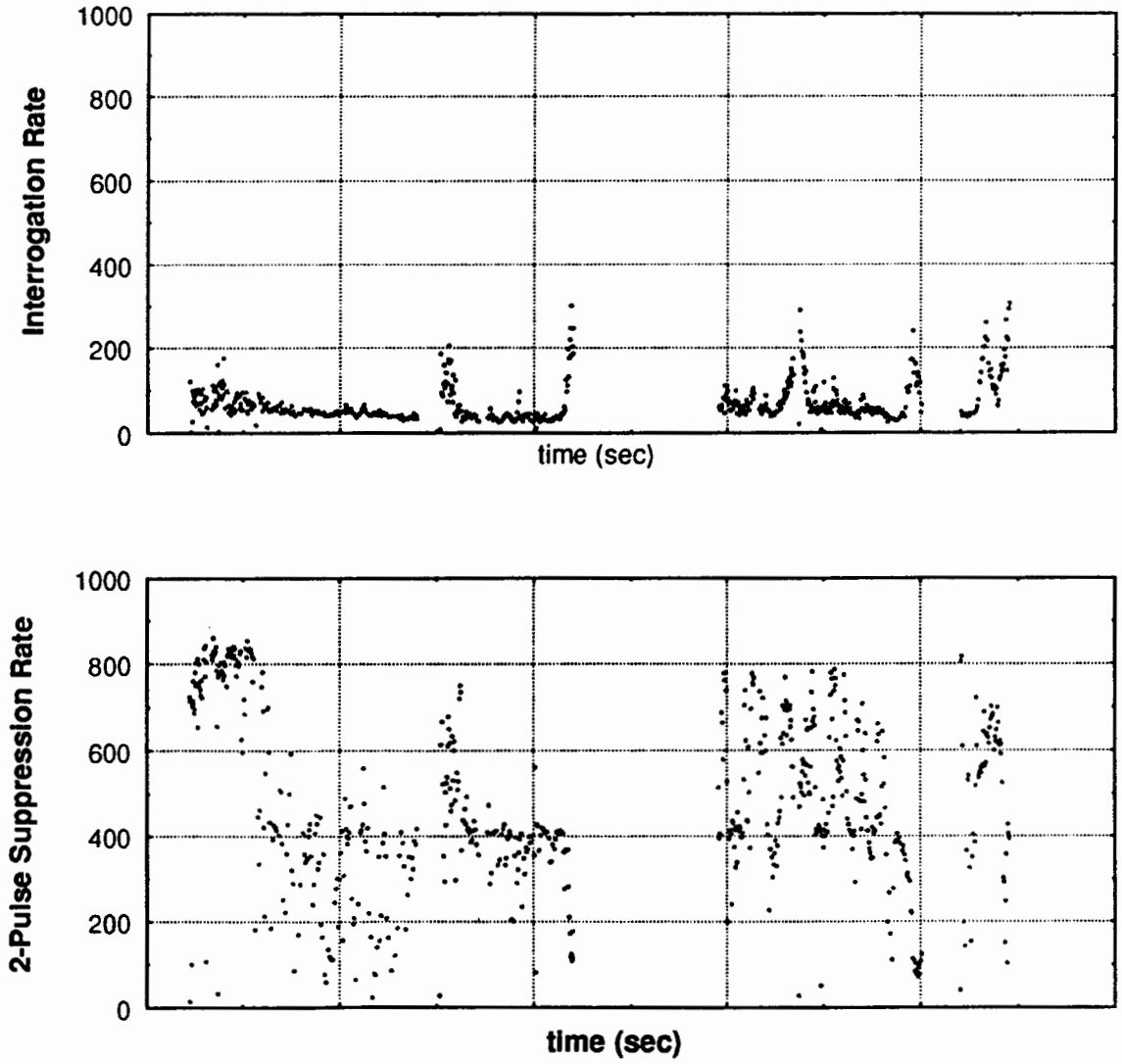

Figure 4b. O'Hare SSR Activity - 22 October 1991.

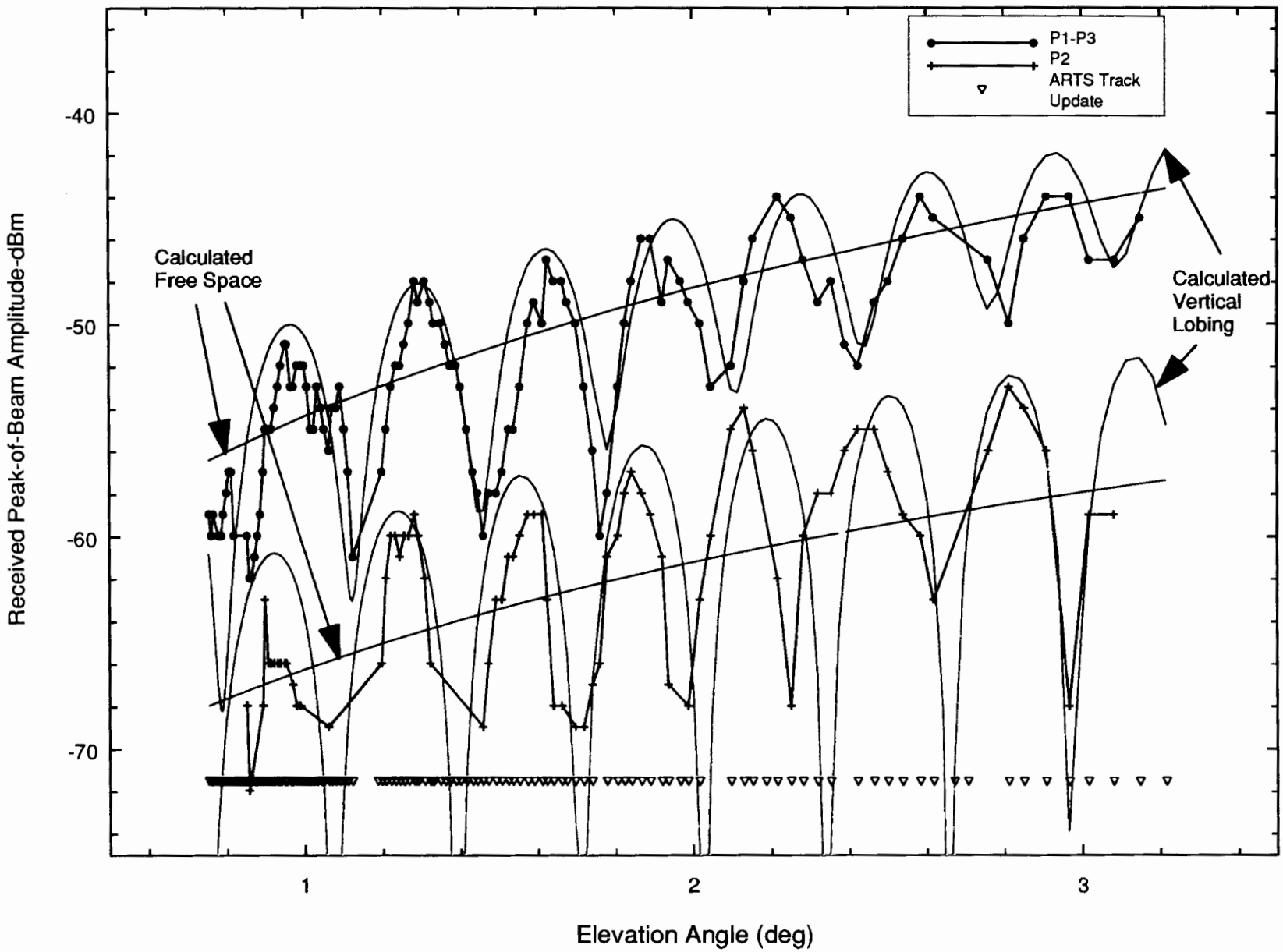

Figure 5. SSR Vertical Lobing Pattern — 65-Degree Radial / Altitude = 4000 feet / Bottom AMF Antenna.

Figure 5 indicates that serious multipath-induced vertical lobing is occurring along the 65-degree radial, and also that the displaced phase center between the main and omni SLS antennas is causing observable differential lobing between the two. The depth of the most severe P1-P3 elevation pattern null does not appear to be a problem in terms of adequate interrogation power at these ranges even for a minimum capability transponder with a threshold level of -69 dBm (the AMF transponder MTL is -74 dBm). The lowest null indicated is 7 dB above -69 dB which should still result in an acceptable azimuth run length of at least 20. The depth of the lobing nulls may be significant in situations where the free-space link power margin is small due to range, aircraft antenna, or degraded transponder effects.

The more serious concern is the impact of differential lobing. Differential lobing can cause shortened runlengths by suppressing transponders within the main beam. Examination of the terrain and building locations surrounding the O'Hare SSR indicate that differential lobing problems are a strong possibility in the 40- to 85-degree azimuth sector and possibly in the 120- to 150-degree sector. Figure 5 illustrates lobing at an azimuth of 65 degrees , and a P1-P3 null is seen to occur very close to a peak in the P2 lobing structure at 1.75 degrees elevation which suggests the possibility of main-beam transponder suppression and a shortened runlength. This situation is also accompanied by an ARTS coast of the AMF aircraft. Individual azimuth scans showing the SSR runlengths before, during and following the coasted AMF scan at 1.75 degrees are illustrated in Figures 6, 7, and 8. Figure 6 shows an acceptable runlength with P2 values approximately 11 dB below the peak of the main beam. Figure 7 illustrates the scan during which ARTS coasted the AMF aircraft. The runlength is considerably shortened with P2 amplitudes comparable to the P1 amplitudes. Figure 8 indicates that the P2 values are only 8 dB below the main beam peak, but the runlength was sufficient to cause an AMF target update. This is reasonable since the AMF transponder was measured to have a 100% suppression probability for a 3 dB P1/P2 ratio.

A similar situation is illustrated by Figures 9 through 12 which show the SSR runlengths during the time of the AMF coasted scan at 2.4-degrees elevation. This is in a region where the P2 elevation pattern peaks simultaneously with the occurrence of a P1-P3 pattern null. The runlengths are seen to successively shorten because of decreasing P1/P2 ratios until, as illustrated in Figure 11, AMF was coasted because of insufficient runlength.

The data presented in Figure 13 are another way of illustrating the potential of main beam suppression. They show the P1/P2 ratios at the azimuth peak-of-beam as a function of elevation angle for the 4000-ft altitude run. P1/P2 ratios between 9 dB and 0 dB are candidates for transponder suppression depending on the transponder. In four instances of AMF coast, the P1/P2 ratio was as low as 3 dB.

The SSR track degradation due to differential lobing can be further aggravated by the fact that low main-beam P1 amplitudes are susceptible to destructive interference from the P1 amplitude transmitted via the omni. This can either contribute to the low P1/P2-ratio suppressions within the main beam or can cause the transponder to reject the interrogation on the basis of the tolerance allowed for relative P1, P3 amplitudes. This phenomena is analyzed in greater detail in Section 3.2.

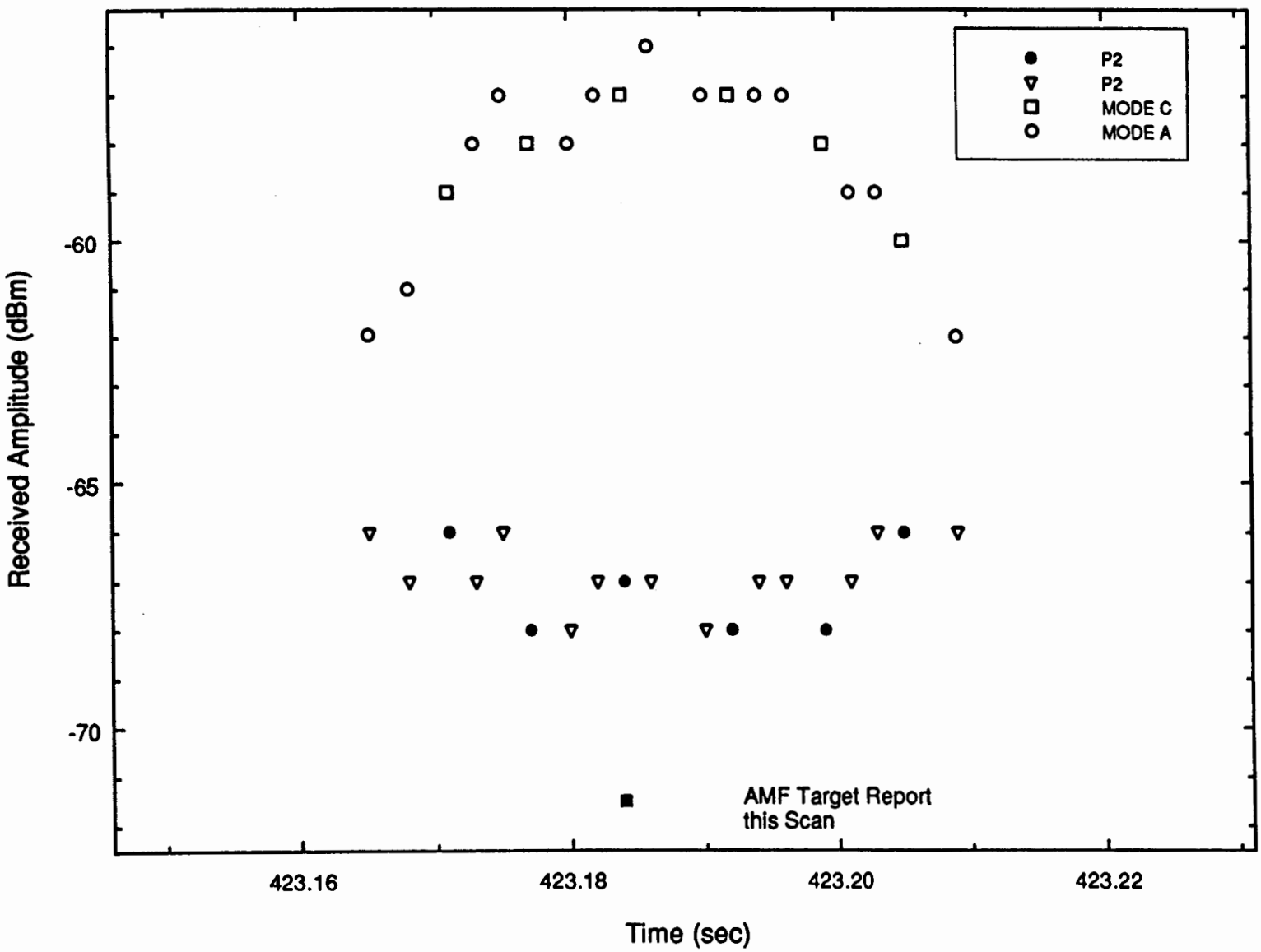

Figure 6. SSR Azimuth Pattern — 1.75-Degree Elevation / 65-Degree Radial / Altitude = 4000 feet.

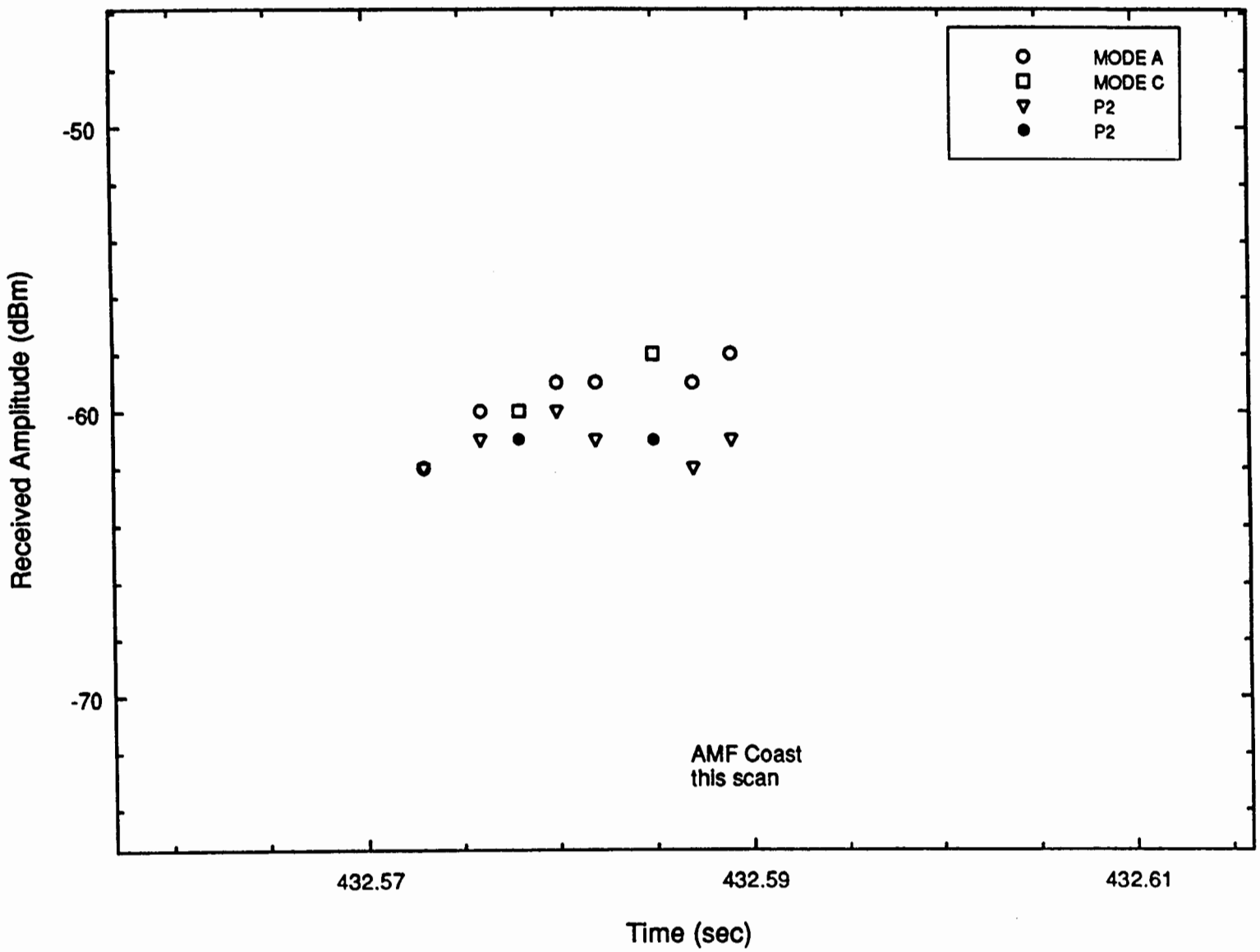

Figure 7. SSR Azimuth Pattern — 1.75-Degree Elevation / 65-Degree Radial / Altitude = 4000 feet.

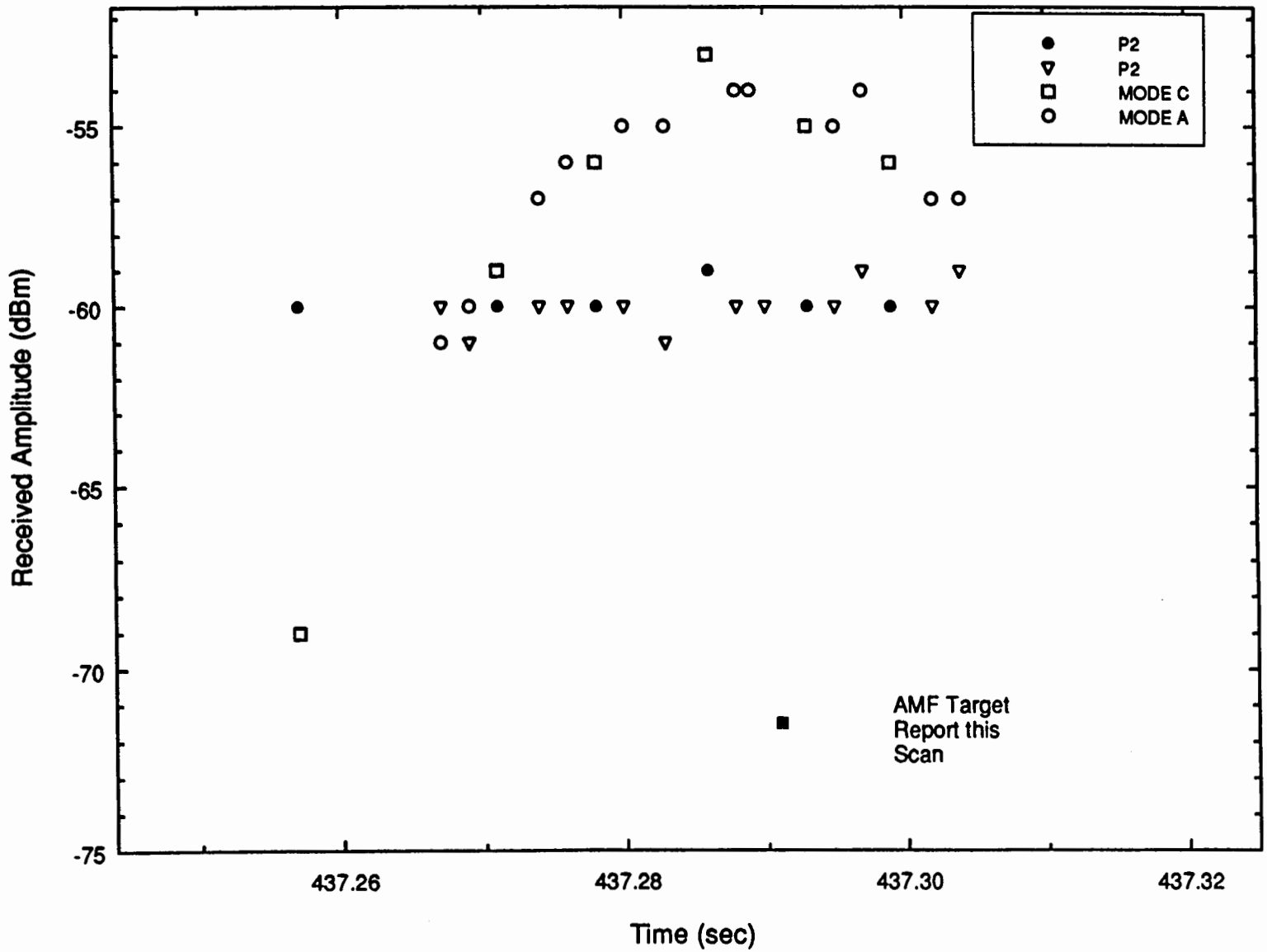

Figure 8. SSR Azimuth Pattern — 1.75-Degree Elevation / 65-Degree Radial / Altitude = 4000 feet.

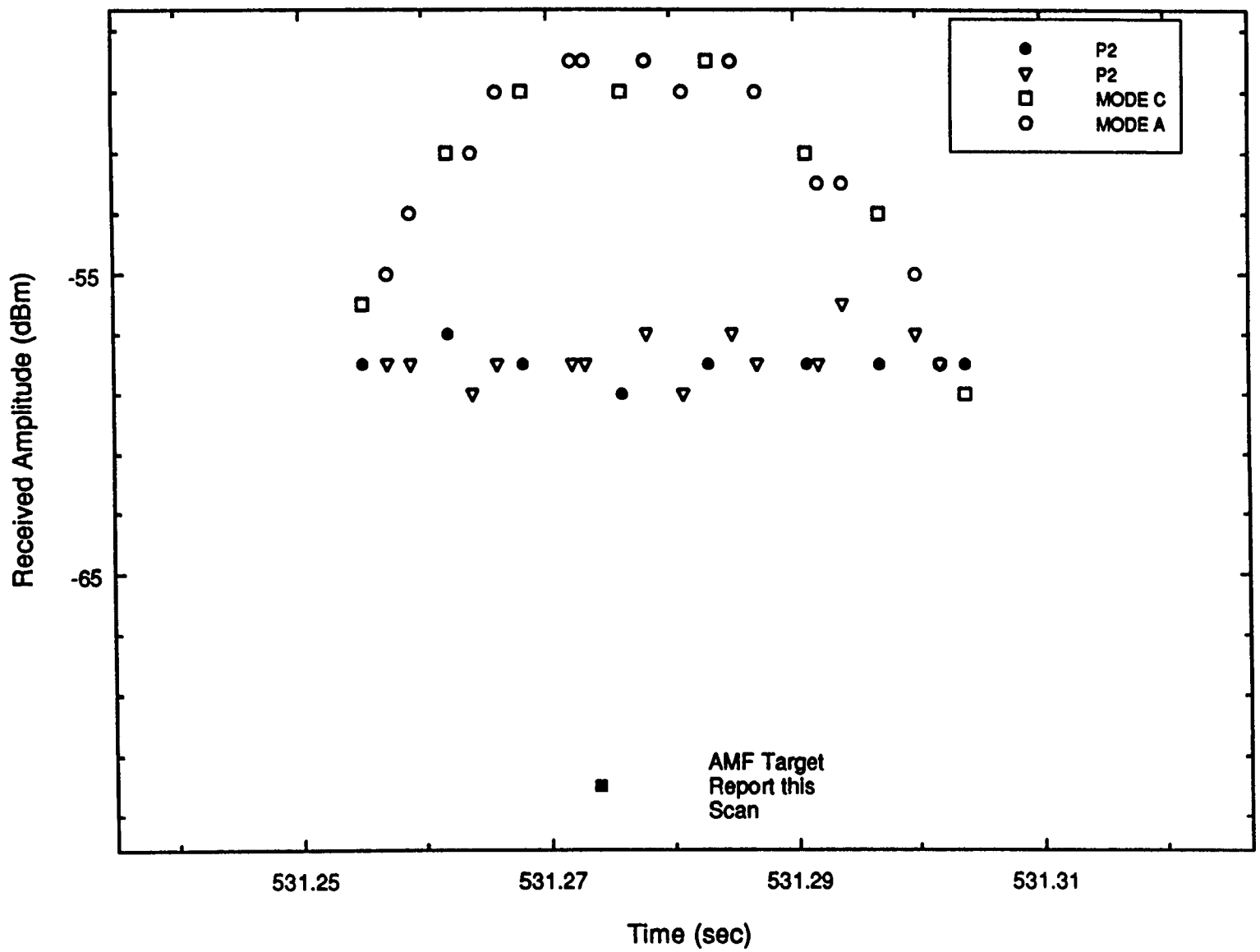

Figure 9. SSR Azimuth Pattern — 2.4-Degree Elevation / 65-Degree Radial / Altitude = 4000 feet.

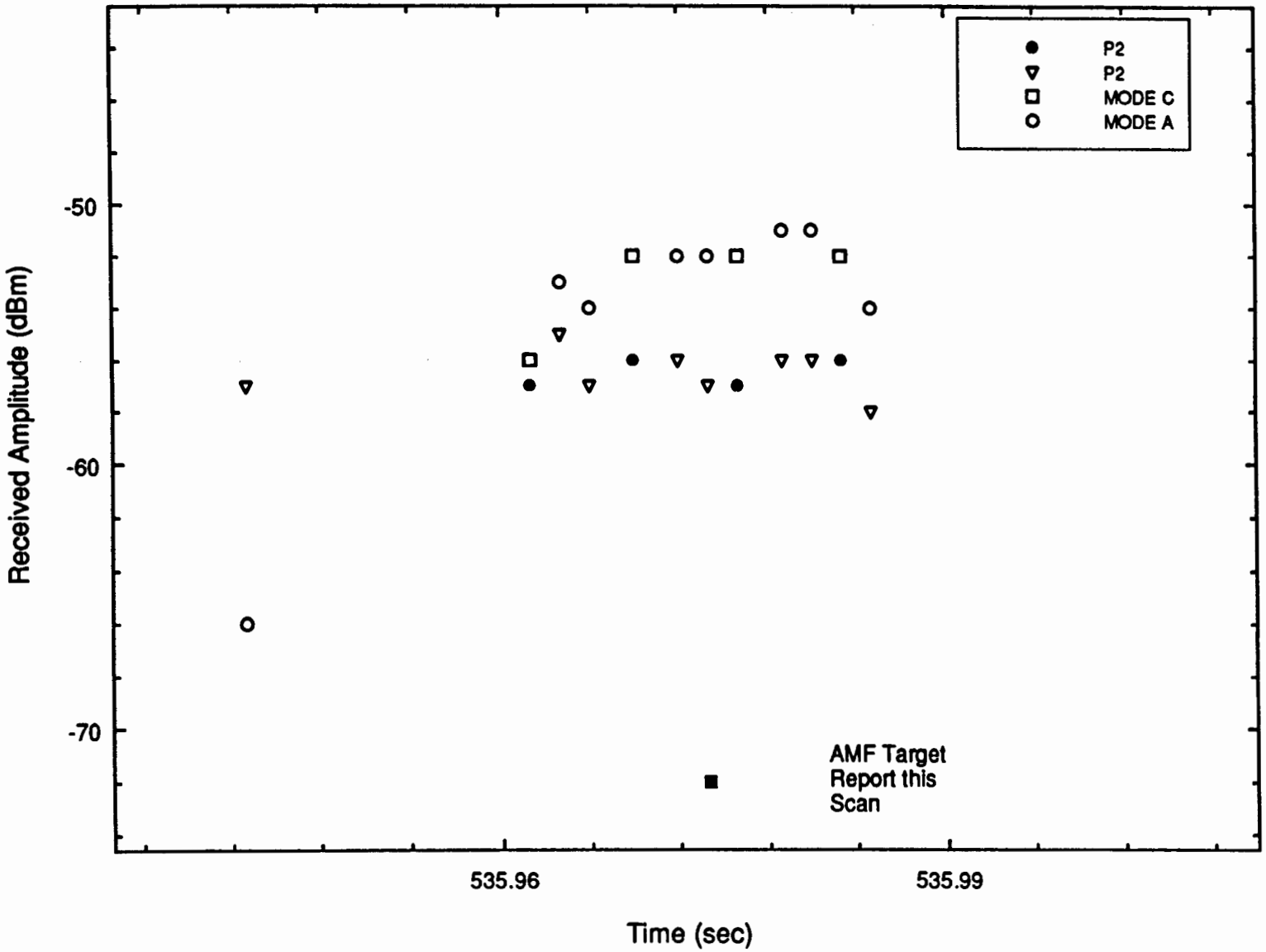

Figure 10. SSR Azimuth Pattern — 2.4-Degree Elevation / 65-Degree Radial / Altitude = 4000 feet.

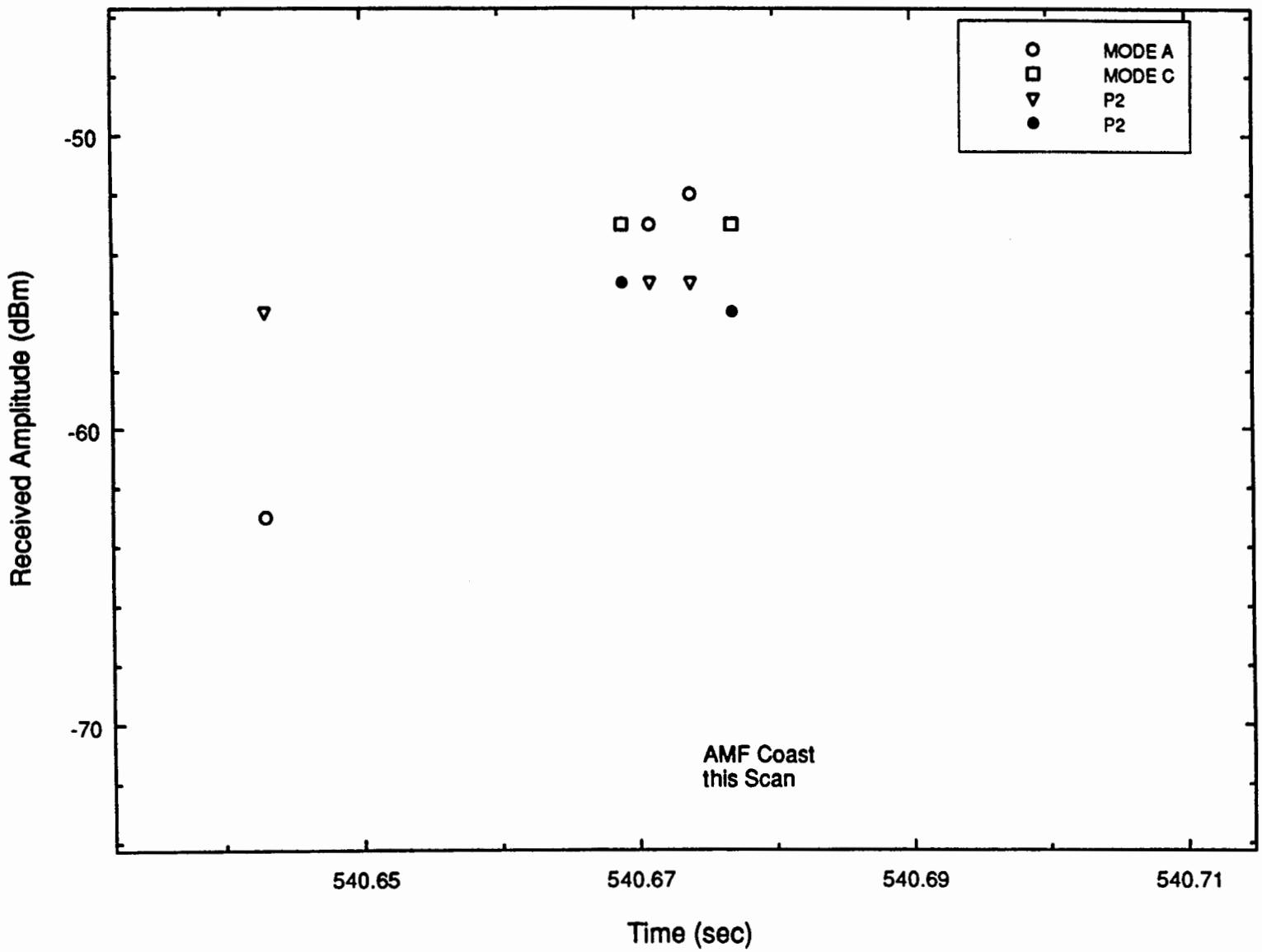

Figure 11. SSR Azimuth Pattern — 2.4-Degree Elevation / 65-Degree Radial / Altitude = 4000 feet.

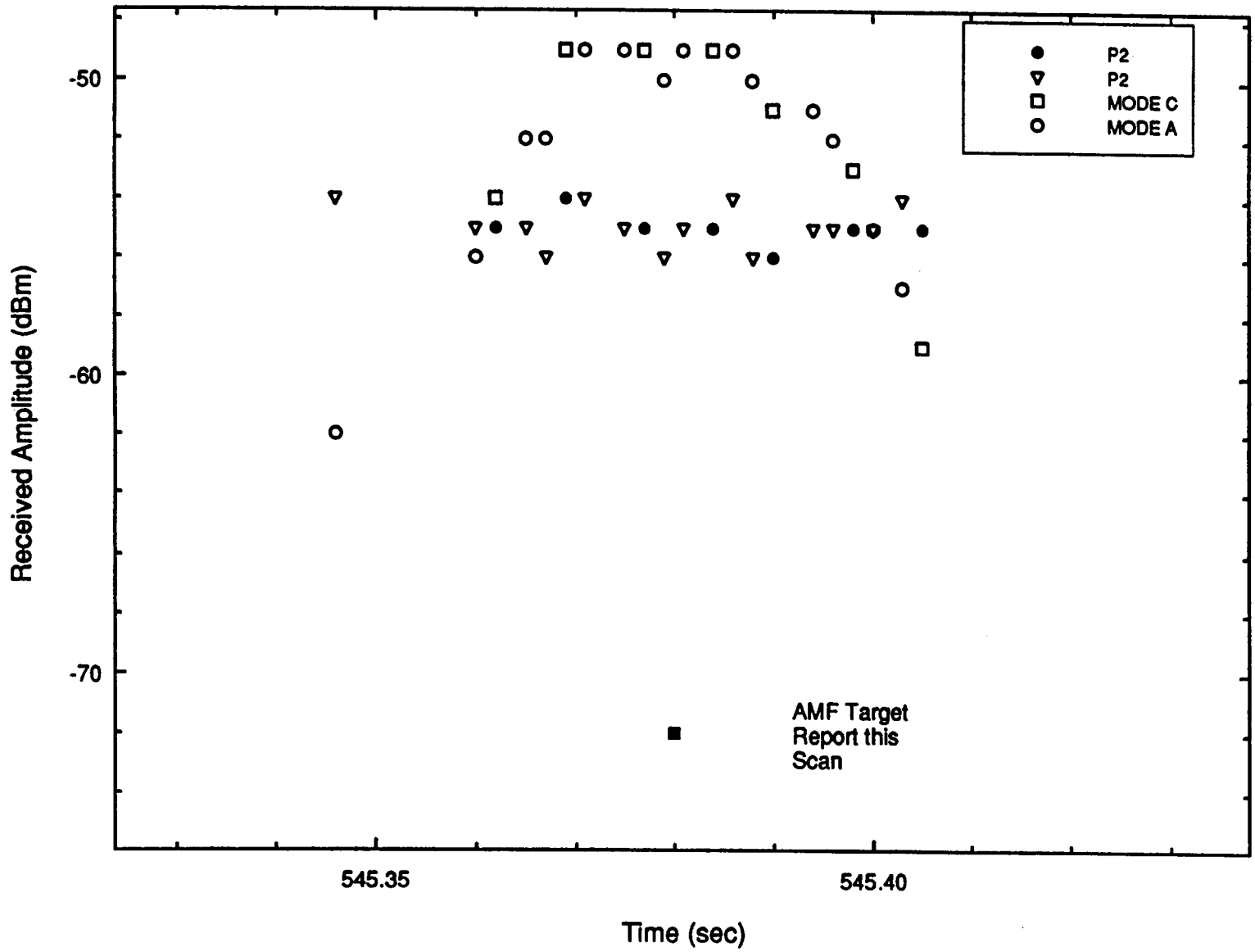

Figure 12. SSR Azimuth Pattern — 2.4-Degree Elevation / 65-Degree Radial / Altitude = 4000 feet.

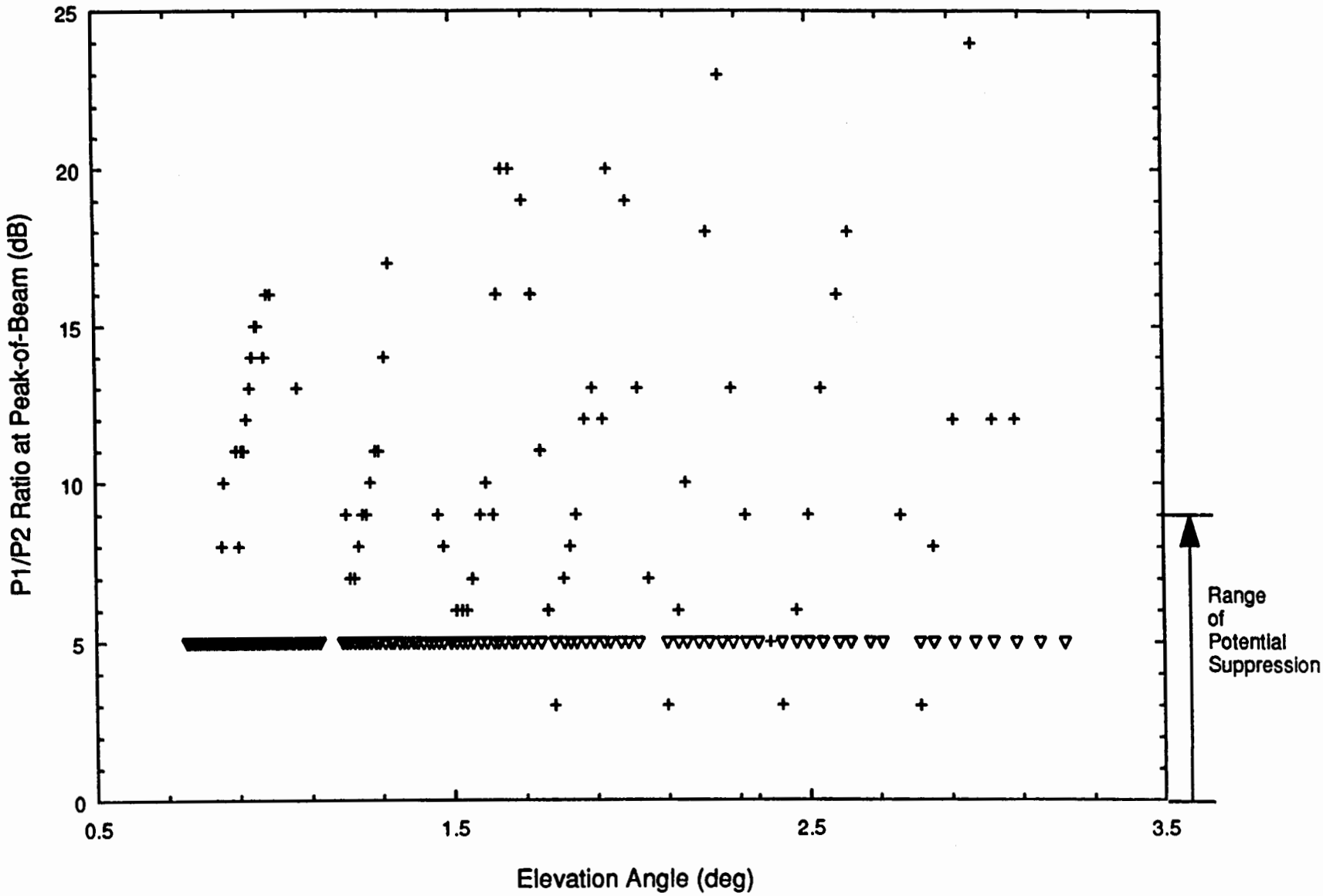

Figure 13. Peak-of-Beam P1/P2 Ratio at AMF vs Elevation Angle / 65-Degree Radial / Altitude = 4000 feet / Bottom AMF Antenna.

3.1.2 Results Of The 170-Degree Radial Flight

Measured SSR interrogation amplitudes verses elevation angle from the 170-degree radial flight is shown in Figures 14 and 15 for the 3000-ft and 5000-ft altitude flights, respectively. As expected, the data does not show appreciable vertical lobing since the terrain in this direction does not appear to support in-beam multipath.

Signal fading on the order of 8 to 12 dB is evident in both figures at the lower elevation angles. The cause of the fade is believed to be the standby ASR and beacon which is located at 170-degrees azimuth relative to the main SSR. Figure 16 shows the 155- to 175-degree azimuth portion of the panoramic photos taken from the main SSR tower. Although the photo shows the standby antennas, oriented orthogonal to the SSR, their actual orientation during the AMF flights is uncertain. The flight paths of the 3000-ft and 5000-ft runs are shown on the photo and illustrate the correlation of the signal fade with AMF aircraft position relative to the center of the obstruction.

The ARTS track of the AMF aircraft indicates numerous coast intervals during the time of the most severe fading. It is felt that the signal fade, coupled with the nominally low received power levels at these ranges is the primary reason for the coasting.

3.1.3 Results Of The 300-Degree Radial Flight

Vertical lobing was not expected on the 300-degree azimuth radial, and the data support this. What is observed from the plot of received SSR power versus elevation angle in Figure 17 is a signal-fade characteristic similar to that seen at 170-degrees azimuth. Examination of the panoramic photo (Figure 18) in the vicinity of 300 degrees shows a pole at 306-degrees azimuth.

3.2 EFFECT OF VERTICAL LOBING ON SSR RUNLENGTH

3.2.1 Runlength Analysis Using AMF Interrogator-Of-Opportunity Data

A runlength analysis was done by searching for pulse sequences having the P1, P3 spacings of Mode A/C/2, with or without the P2 pulse. Two-pulse suppressions (i.e., there was no P3 pulse) were ignored. The amplitudes of the pulses were as measured by the AMF receiver channel associated with the top antenna. The pulse-bearing measurements were not used during the combing process, although the bearing measured on the P1 pulse was saved. These ATCRBS interrogations were then plotted as shown in the example in Figure 19. The horizontal axis spans 100 milliseconds, and the vertical axis spans 360 degrees. Each interrogation is plotted using the symbol "A," "C," or "2," representing the three modes. The symbol is plotted at the interrogation's time and bearing with respect to the AMF. (Note that the AMF bearing is quantized to 6 degrees and is somewhat noisy, especially when the pulse amplitudes are low.) Underneath this symbol, a number from 1 to 8 is plotted, representing the elapsed time from the previous interrogation. The numbers represent the 8 values of the PRI stagger that is used by the Chicago SSR. If the elapsed time is not one of the 8 PRIs then a "_" is plotted. (Occasionally, the plotting program confuses PRIs 2 and 7, and sometimes fails to recognize a PRI.)

Underneath the stagger is plotted either an "I," "S," or "F," and below these a "P" is present. These symbols are explained as follows:

(a) An "I" (Interrogation) signifies that the P1 amplitude was greater than the P2 (if present) amplitude, and that the P3 amplitude was in the range from 1 dB below to 3 dB above P1.

(b) An "S" (Suppression) indicates that the P2 amplitude exceeds the P1 amplitude. Note that the ATCRBS National Standard permits transponders to suppress when the P2 is between the P1 amplitude and 9 dB below the P1 amplitude.

(c) An "F" (Failure) indicates that P2 (if present) is below P1, but P3 is outside the region from 1 dB below to 3 dB above P1.

(d) A "P" will be plotted below the symbols "I" or "F" if a P2 pulse was detected.

The amplitudes of the P1, P2, and P3 pulses (as seen via the top AMF antenna) are represented graphically. The P1 amplitude is indicated by a vertical line extending out the top of the Mode symbol. The height of the line indicates the P1 amplitude. The bottom of the line is -76 dBm. The scale factor is approximately 1 dBm per degree of the azimuth scale. The P2 amplitude is indicated by a tic mark ("---") along the axis of the P1 line. The P3 amplitude is indicated by a dashed ("- -") tick mark.

The P3 amplitudes reveal the antenna pattern of the main beam. The P2 amplitudes reveal the pattern of the omni control pattern, and the P1 amplitudes provide insight into operation of the I^2SLS function. Figure 20 reveals the following points:

(a) When the P1/P2 ratio is large (over 24 dB), the P1 and P3 amplitudes track each other closely. The runlength is quite long (about 30) because the beamwidth is not narrowed by either SLS or by differences between P1 and P3.

(b) When the P1/P2 ratio is moderate (around 11 dB), the P1 amplitude falls off more rapidly at the beam edges than the P3 amplitude. This is probably due to the I^2SLS function. Apparently, the phase difference between the P1 contribution from the array, and the P1 contribution from the stick omni causes a "fade" in the net P1 amplitude at the edge of the beam. The P3 pulse is transmitted solely over the array, so its falloff is affected only by the actual shape of the beam. Similarly, the P2 pulse is transmitted solely over the omni, so its amplitude is essentially constant over the beamwidth. But, since the net P1 power is a combination of the array and omni patterns and their relative phases, its shape depends on the elevation angle and ground reflection characteristics, both of which affect the amplitudes and phases of the two electric vectors which sum to form the resultant P1.

(c) When the P1/P2 ratio is small (around 6 dB), the P1 amplitude is less than P3 even at the center of the beam and falls off very rapidly toward the beam edges. The runlength is determined by the transponder's test of the relative P1/P3 amplitude, not by the SLS function. The runlength (about 10) is barely long enough to allow the generation of a target report. Since the mode interlace is AAC, it may be very difficult to get enough Mode C replies to provide the target report with an altitude.

The plots assume a transponder will reply if P2 is below P1. In fact, the ATCRBS National Standard allows a transponder to suppress when P2 is from just below P1 to 9 dB below P1. Therefore, the plots indicate upper bounds on the runlength. For example, when the P2 is only 6 dB below P1 throughout the beam dwell, it is possible that some transponders would not reply at all.

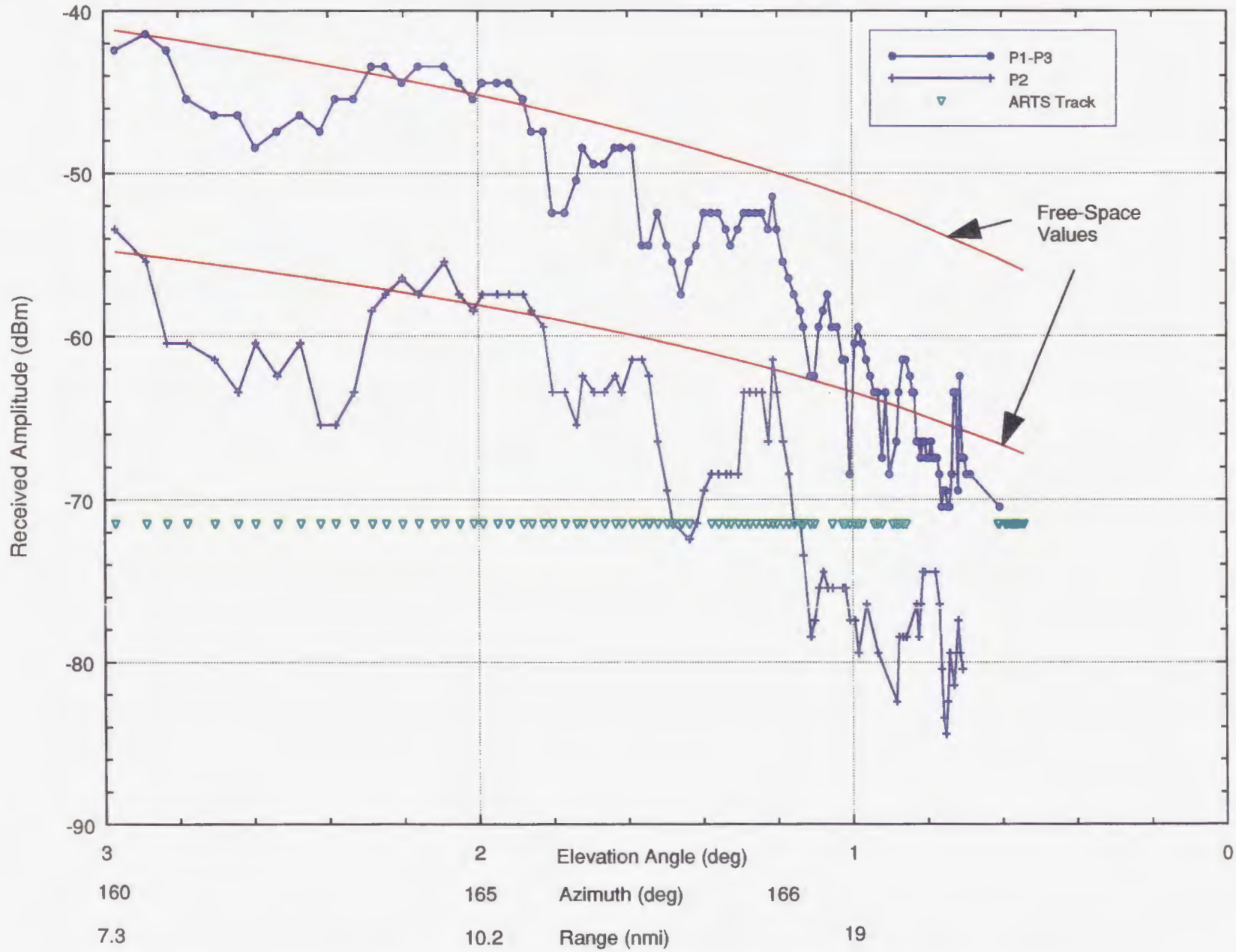

Figure 14. SSR Elevation Pattern — 170-Degree Radial / Altitude = 3000 feet / Bottom AMF Antenna.

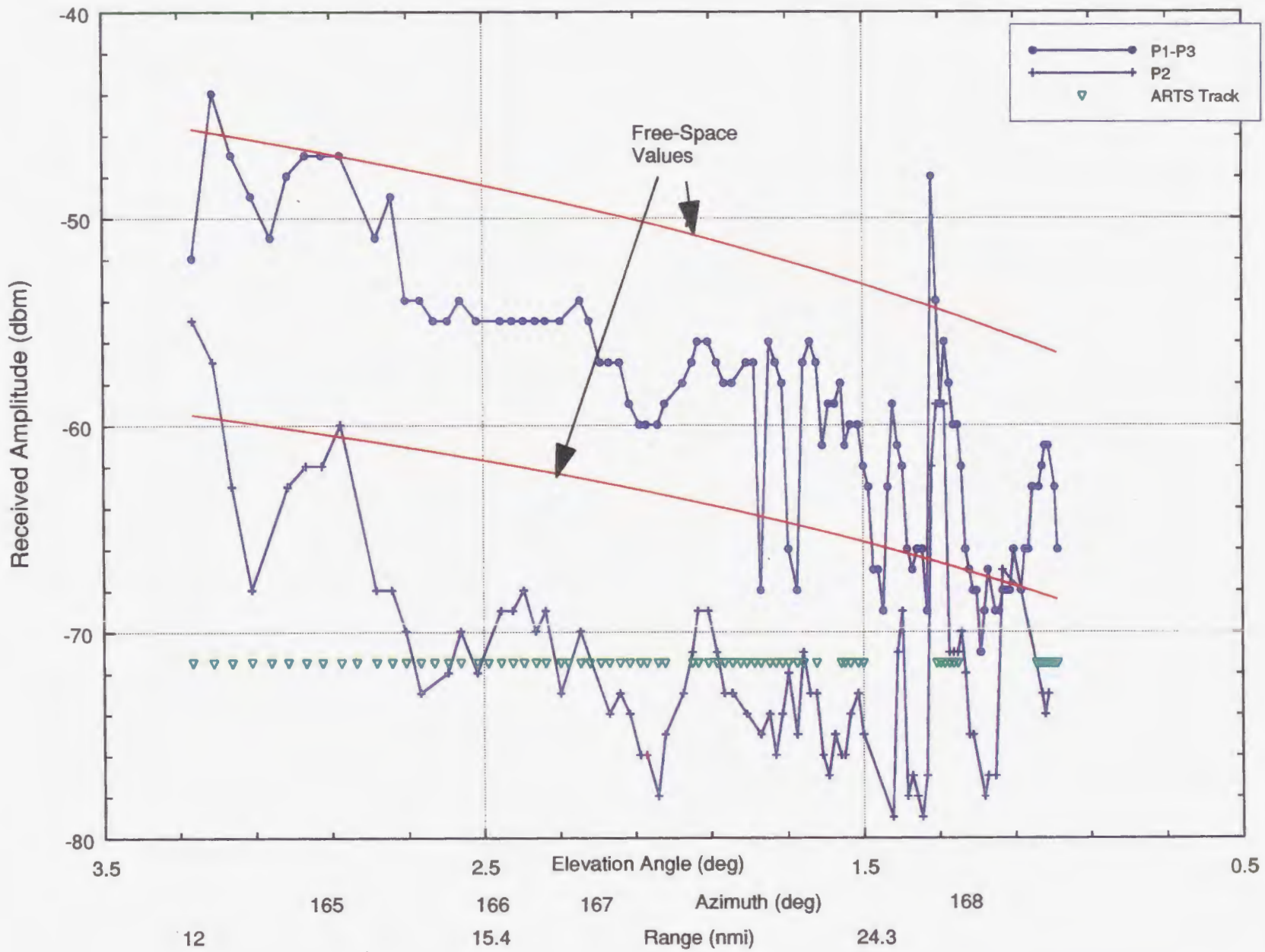

Figure 15. SSR Elevation Pattern — 170-Degree Radial / Altitude = 5000 feet / Bottom AMF Antenna.

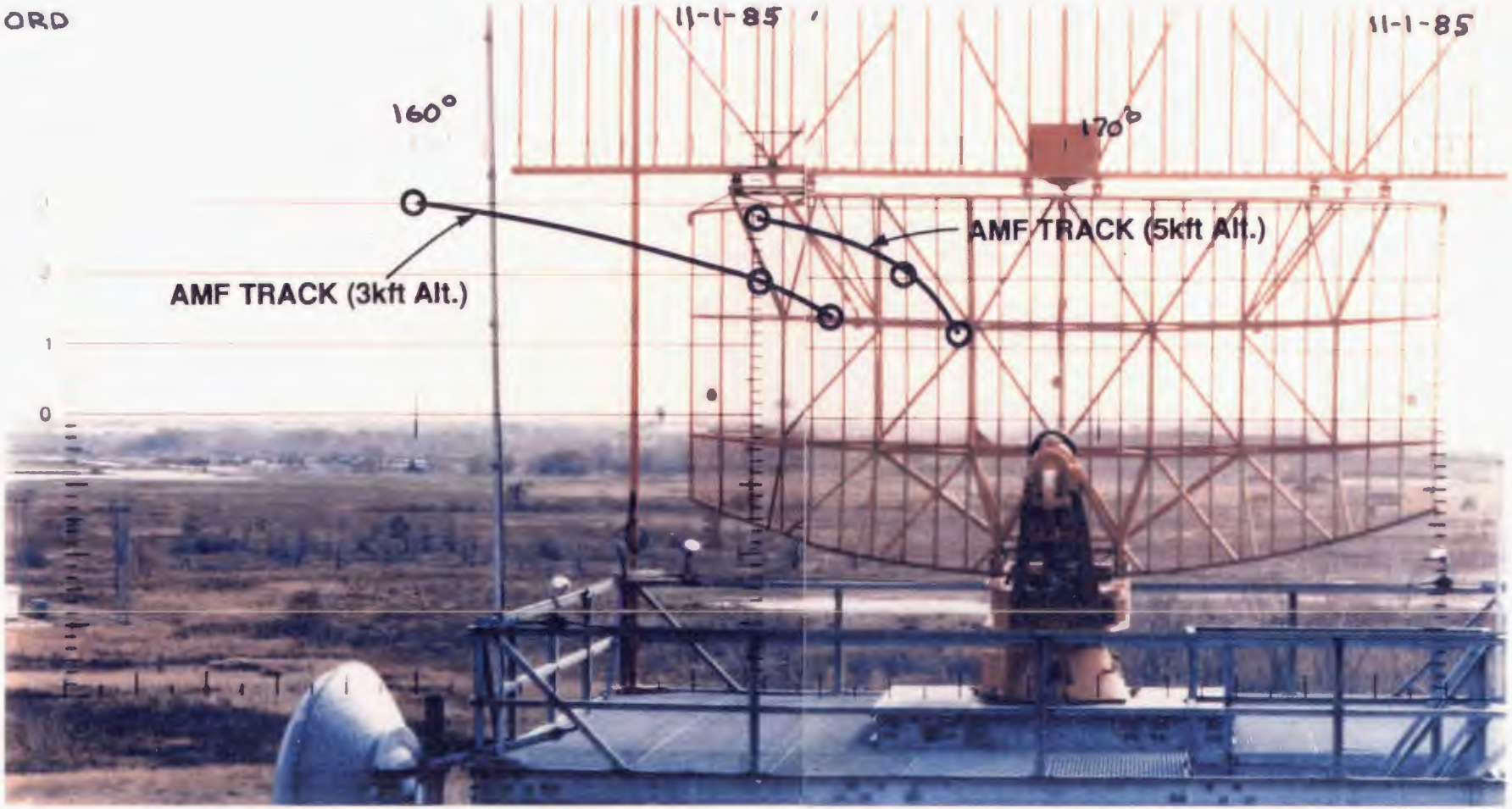

Figure 16. View from the main O'Hare SSR Antenna in the direction of 165-degrees azimuth.

201948-1

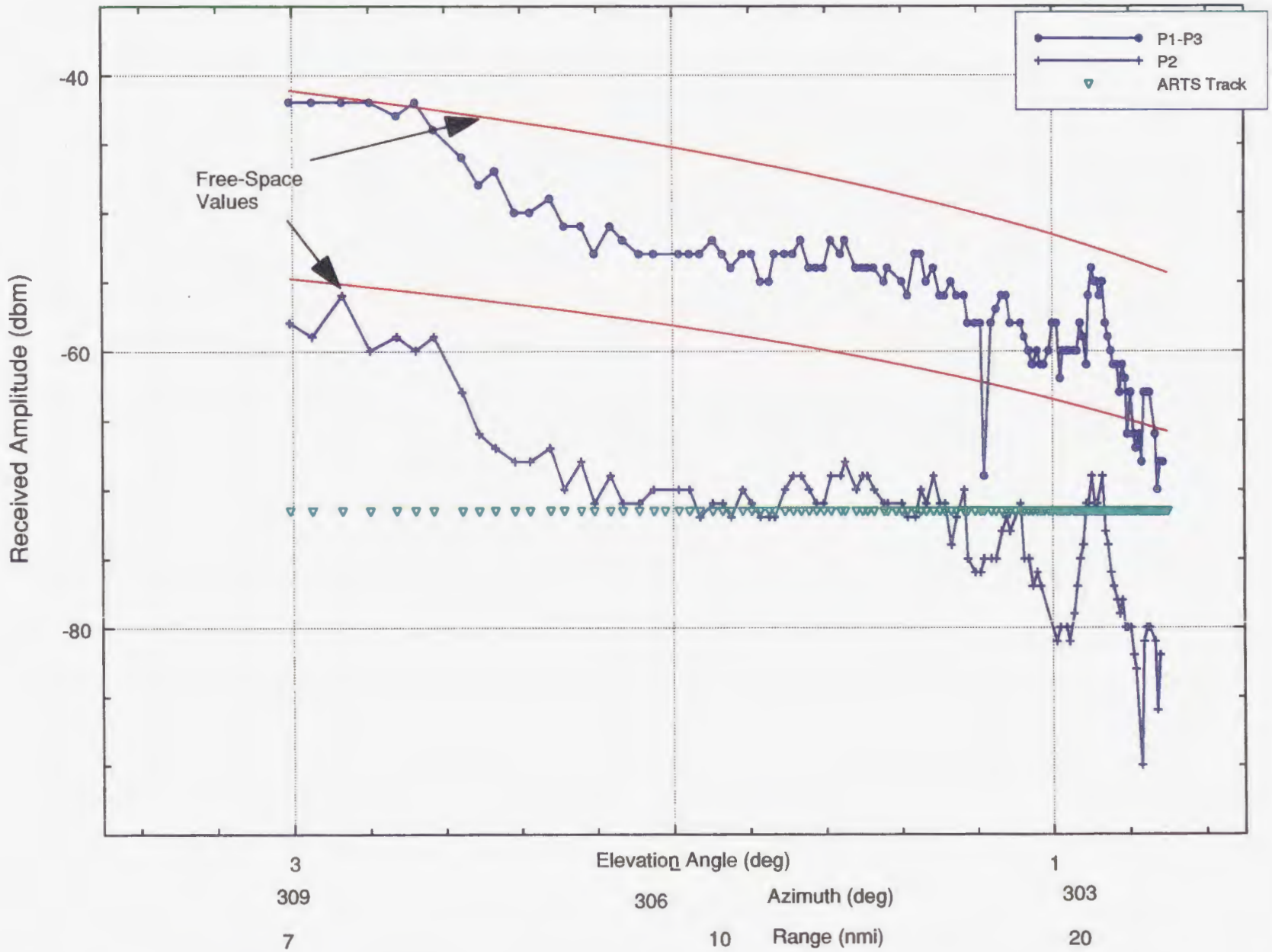

Figure 17. SSR Elevation Pattern — 300-Degree Radial / Altitude = 3000 feet / Bottom AMF Antenna.

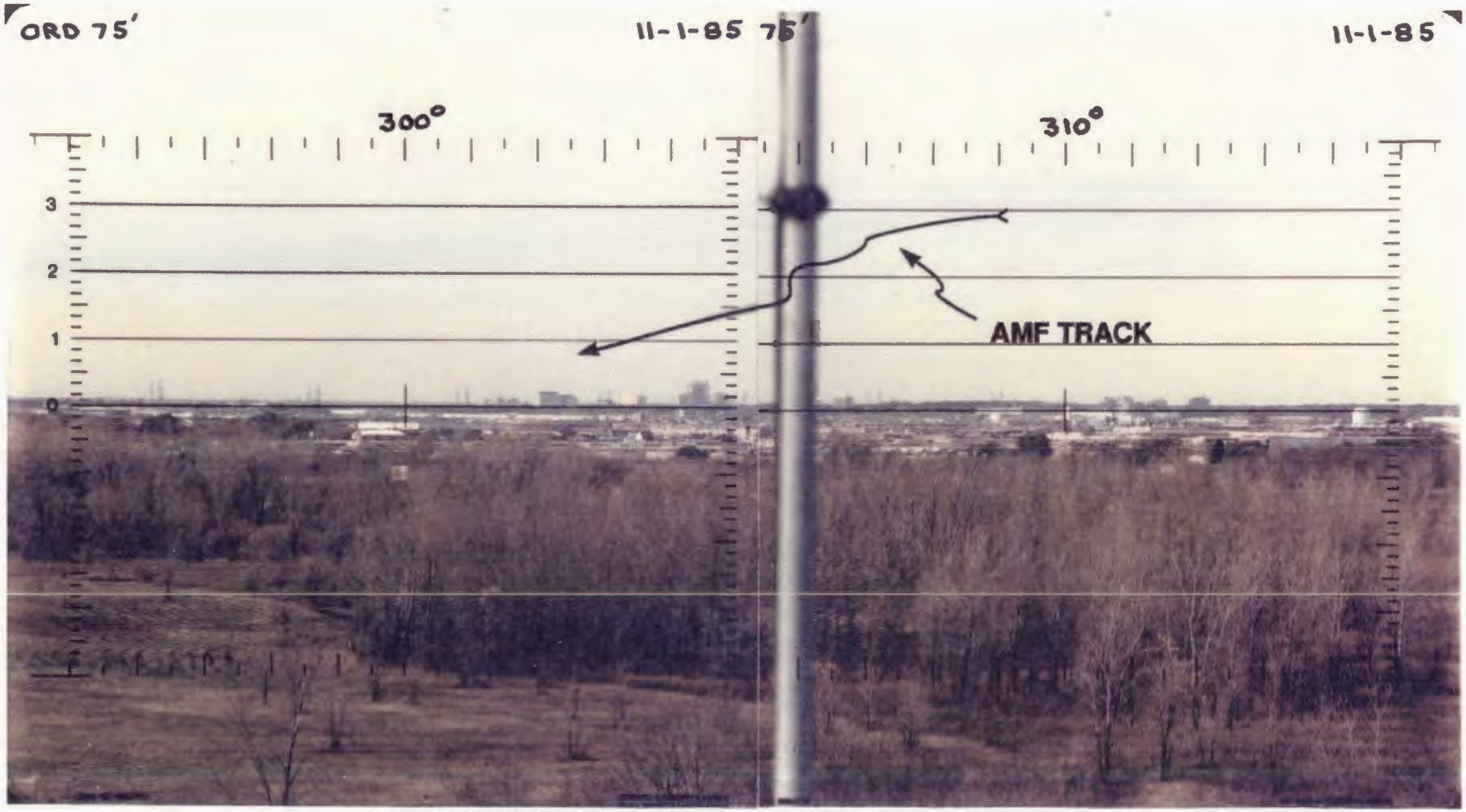

Figure 18. View from the main O'Hare SSR Antenna in the direction of 215-degrees azimuth.

203179-1

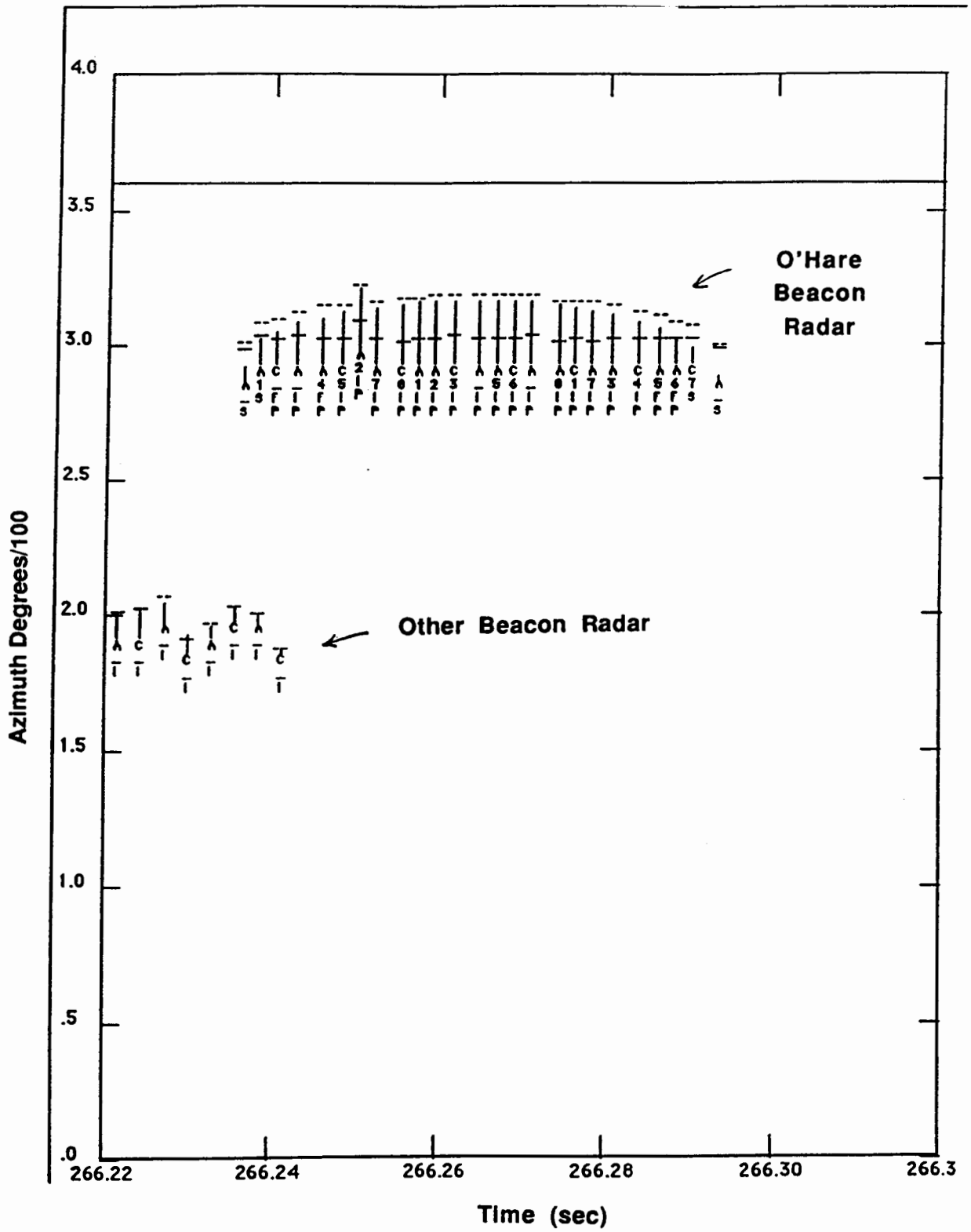

Figure 19. Chicago Runlength.

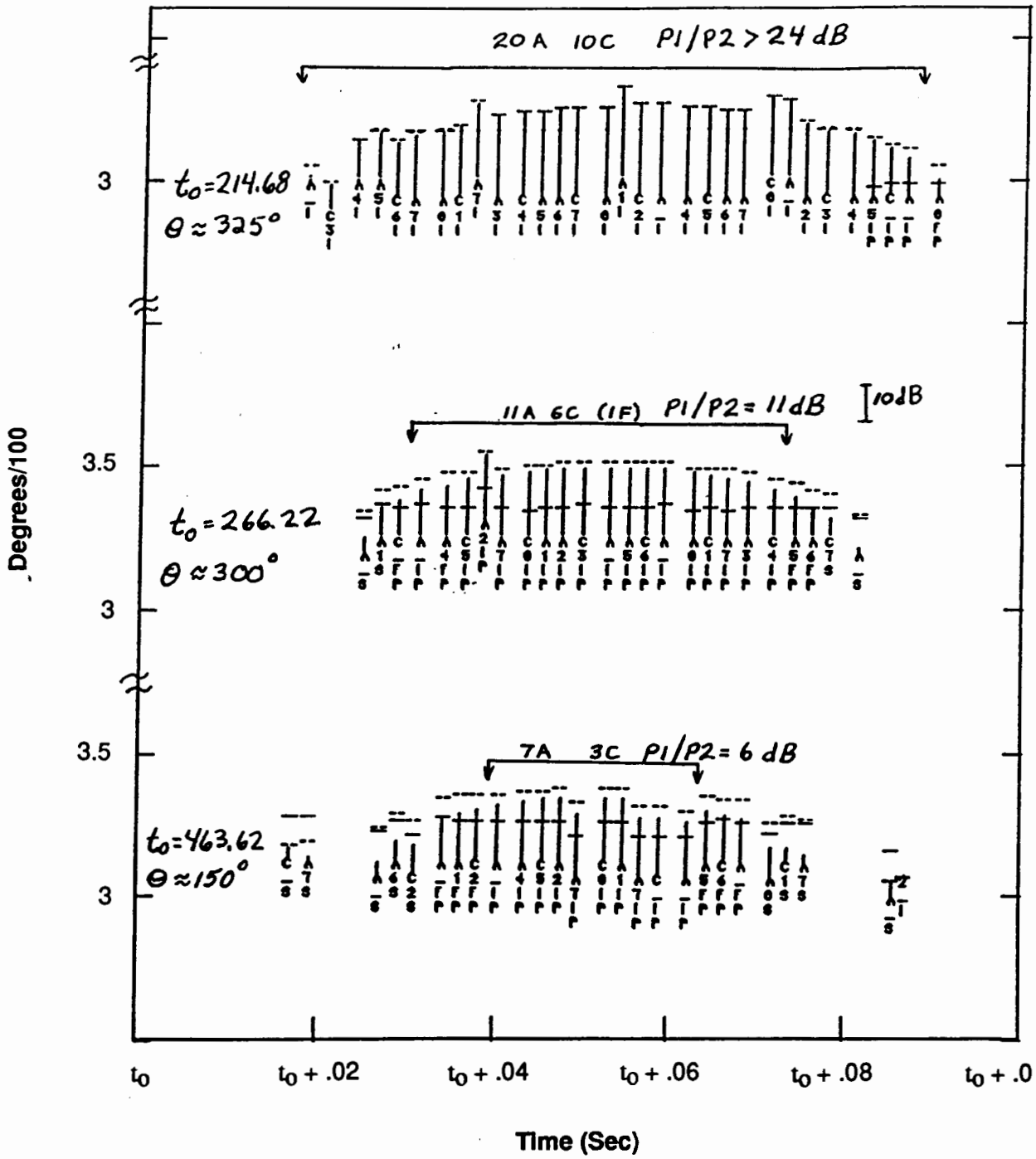

Figure 20. Chicago Runlength vs P1/P2 Ratio.

3.2.2 Theoretical Analysis of SSR Beam Runlength

Section 3.2.1 illustrated various measured SSR runlengths as viewed from a victim transponder onboard the AMF aircraft. It was noted that due to differential lobing, the P1/P2 and P1/P3 ratios vary widely as a function of aircraft location, or more specifically the aircraft elevation angle relative to the sensor.

As previously discussed, the 5-ft array transmits a P1-P3 pulse sequence and the omni transmits a P1-P2 pulse sequence. This is referred to as the I^2SLS pattern, and is done to prevent mainbeam reflections from interrogating aircraft. Consequently, the P1 pulse received at the transponder is a combination of the 5-ft array and the stick omni P1 signals. These pulses may add constructively or destructively depending on their phase difference. The P3 amplitude is indicative of the main beam antenna pattern, while the P2 amplitude reveals the omni pattern.

The phase difference between the two antennas is due to both a geometric phase difference and the phase difference at the antenna feed. The geometric phase difference is dependent on the vertical displacement between the antennas. The phase difference at the antenna feed is due to cable length differences.

A model was developed to assess the performance of a displaced 5-ft array/omni configuration in conjunction with an I^2SLS function. This model considered the appropriate contributing factors such as terrain characteristics, relative and absolute antenna heights, and differences in the phase of the antenna feeds.

The model used the following information:

(a) height of the stick omni and 5-ft array above the reflector surface,

(b) an assumption of -1 for the ground reflection coefficient,

(c) the general characteristics of the terrain (a sloping 30-ft vertical displacement over a 10,000-ft horizontal displacement), and

(d) relative input power to the two antennas.

As a result of the I^2SLS function and the presence of the SSR vertical lobing pattern, the following points were verified using the theoretical model:

(a) When the P1/P2 ratio is large (over 24 dB), the P1 and P3 amplitudes are very close. The additional P1 power in the omni is not sufficient to perturb the P1 mainbeam power regardless of phase difference between antennas, therefore, there is no impact on the P1/P3 ratio. The resulting antenna pattern is shown in Figure 21.

(b) When the P1/P2 ratio is moderate (around 11 dB) and small (around 6 dB), the net P1 power is sensitive to the elevation angle and the phase difference between antennas. For instance, even though the P1/P2 ratio may be the same for different elevation angles, P1 may be greater than P3 at one angle and less than P3 at another. In addition, feed phase differences can cause the omni and main P1 pulses to add constructively or destructively. As a result, the P1 amplitude may be greater or less than the P3 amplitude at any one elevation angle. In order to theoretically match the measured antenna beam of Figure 20, an adjustment to the relative omni and main P1 phases at the antenna feeds was necessary. With this adjustment, Figures 21 and 22 match the measured data represented in Figure 16.

When P1/P2 is 11 dB, the P1 amplitude falls off more rapidly at the beam edges than the P3 amplitude. (See Figure 20). This is due to the P1 omni electric field contribution in conjunction with a relatively low P1/P2 power. The azimuth pattern in Figure 22 is at a .922-degree elevation angle and required a phase difference of 93 degrees at the feed to match the data in Figure 20. All the pulses are considered interrogations because the P1/P3 ratio is at an acceptable level.

(c) When the P1/P2 ratio is small (around 6 dB), the electric field vectors from the mainbeam P1 pulse, and the omni P1 pulse are of the same order of magnitude. For this condition, the relative phase between the omni and main beam (physical displacement and feed) has a strong influence on the resultant field and causes the greatest variation in the P1 shape. Figure 23 corresponds to the measured data results, at an elevation angle of .838 degrees and 127-degree phase feed difference. At the center of the beam, the P1/P2 ratio is at an acceptable level. However, at the edge of the beam, the interrogation fails because P3 is outside the region from 1 dB below to 3 dB above P1. Consequently, the runlength decreases, making it difficult to generate a target report.

3.3 ANALYSIS OF LOBING USING ARTS TARGET-OF-OPPORTUNITY

About 380 scans of Chicago CDR data from 21 April 1991 and 128 scans from 22 October 1991 were analyzed to determine if coasts in the V84 region could be attributed to low P1/P2 ratio. In April 1991, the stick omni was mounted on a pole attached to the southeast corner of the SSR platform. Since that time, the stick omni was moved to a location on top of the support-bracket for the backfill SLS antenna. However, the vertical height between the 5-ft array and the omni remained the same for both configurations. Both mounting configurations can lead to differential lobing in areas where the ground reflectivity is conducive to large reflections. Differential lobing between the mainbeam and the omni can create situations where the P1/P2 power ratio is within the suppression regime of the transponder. This analysis was performed for the peak of mainbeam, where the P1 power transmitted by the open array is much greater than the P1 power transmitted by the omni for I^2SLS function.

3.3.1 Coasting in April CDR Data

Since measured data for the mounting configuration existing in April are not available, the theoretical P1/P2 ratio was computed assuming a ground reflection coefficient of -1, an antenna height of 86 ft above the ground level at the point of ground reflection, a 4/3-earth model to account for earth curvature and refraction, and 2.1 dB more power to the omni than the array. The omni pattern was assumed to have no elevation variation. The array was assumed to have the normal elevation cutoff and to be tilted down by 2 degrees.

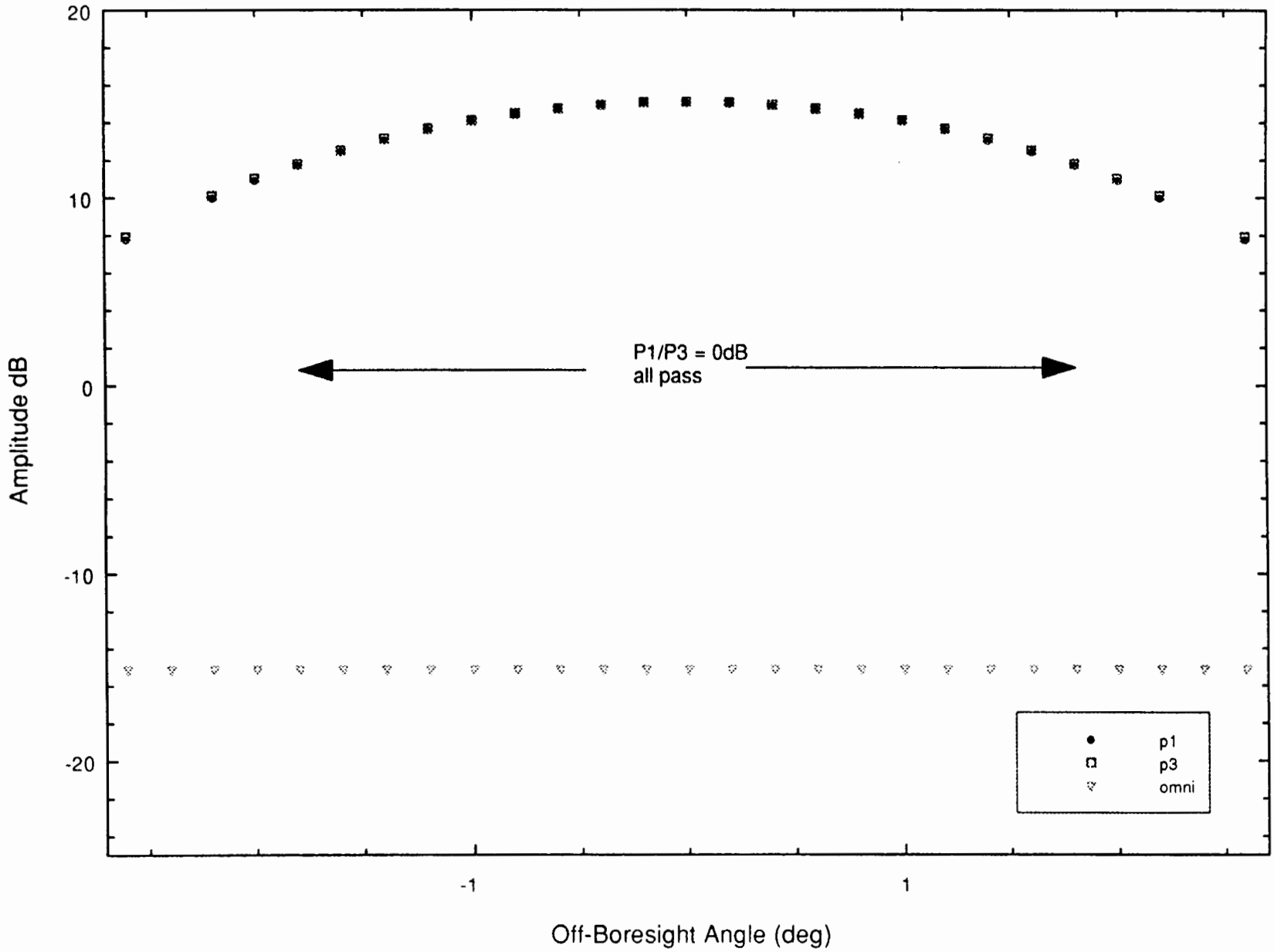

Figure 21. SSR Horizontal Pattern: P1/P2 > 24 dB — Azimuth Sweep at Elevation Angle = 1.08 degrees.

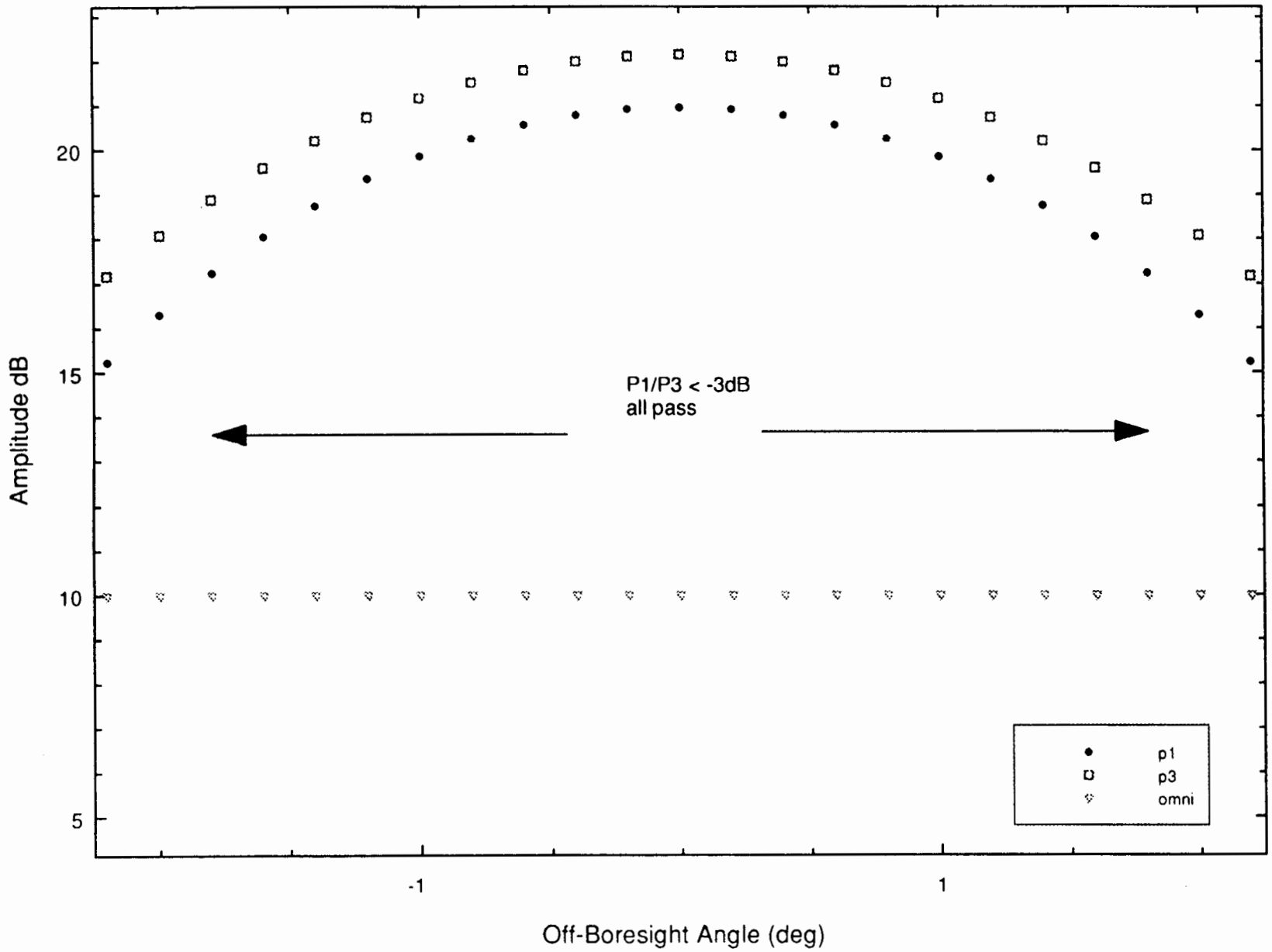

Figure 22. SSR Horizontal Pattern: P1/P2 = 11 dB — Azimuth Sweep at Elevation Angle = .922 degrees Adjusted Differential Feed Phase = 93 Degrees

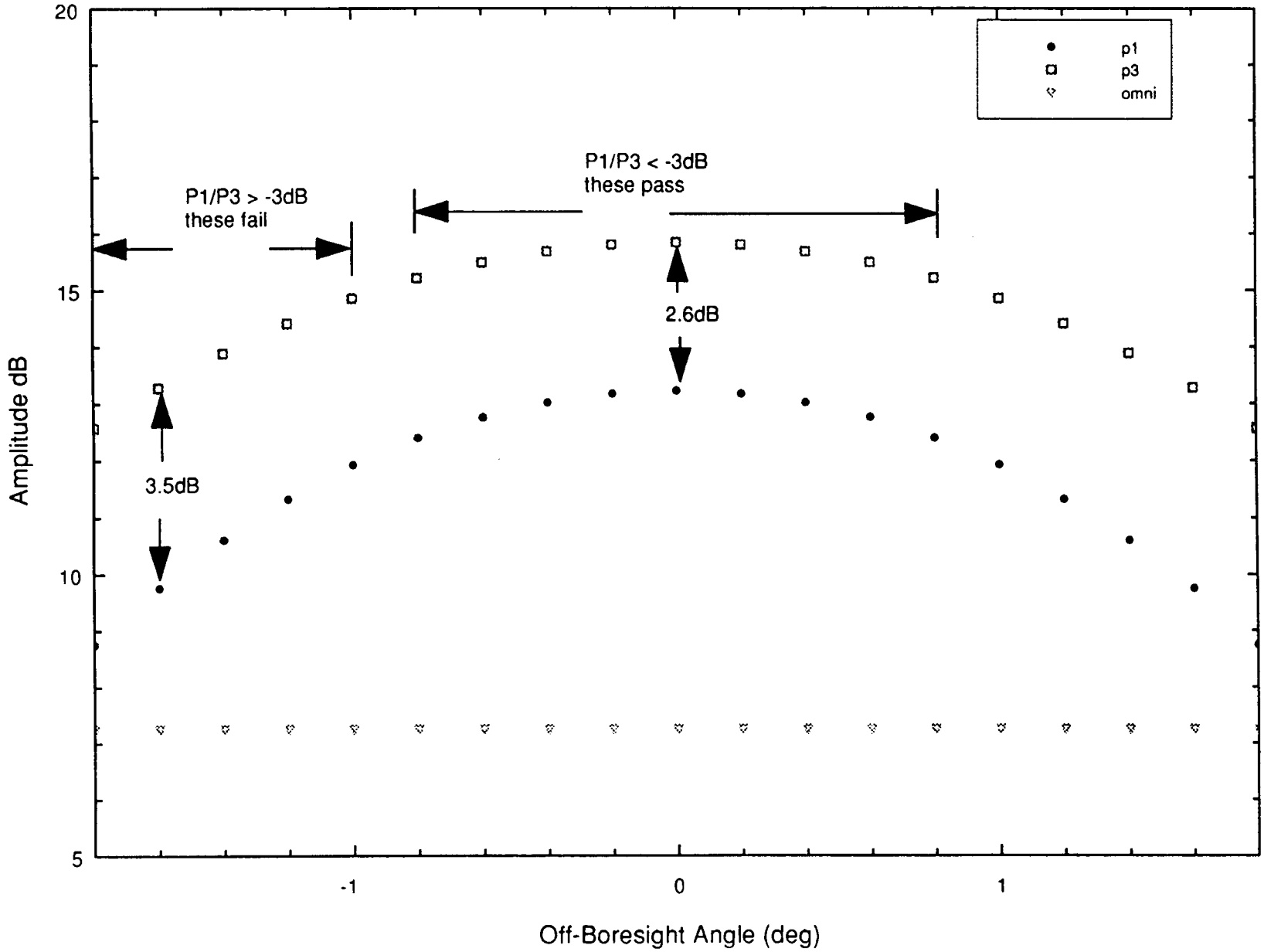

Figure 23. SSR Horizontal Pattern: P1/P2 = 6 dB — Azimuth Sweep at Elevation Angle = .838 degrees
Adjusted Differential Feed Phase = 127 Degrees

The locations of 1530 track updates and 50 coasts from the April CDR data are shown in the 50- by 50-nmi plot in Figure 24a. There are coasts at ranges from 44 to 52 nmi, and from 17 to 28 nmi. There are no coasts from 28 to 44 nmi. Table 3-1 lists the coasts from 17 to 28 nmi. The column labeled "P1/P2 dB" indicates the value of the P1/P2 ratio. Three elevation angles are computed for each coast, corresponding to the reported altitude and +/- 100 ft. The three elevation angles are used to determine three P1/P2 ratios using the relative main and omni gains at each elevation angles and taking into consideration a 2.1 db difference in P1 and P2 transmitter power levels. In all cases except coast index 318, at least one of the altitudes shows a low P1/P2 ratio. For case 318, other analysis shows that the actual altitude is about 8400 ft, which would result in a low P1/P2 ratio. Note that the last column, "PRCV dBm" shows that the P1 power received at the transponder would always be well above Minimum Threshold Level (MTL).

Figure 24B shows where on the airport surface the ground bounce reflection point would be for each update and coast. The grouping of coast reflection points at x=1200,y=1200 ft correspond to the coasts from 17 to 28 nmi. The grouping near the end of 9L correspond to the coasts from 44 to 52 nmi. In between these groups are the potential reflection points for the track ranges from 28 to 44 nmi. It appears that the characteristics of the ground in this region do not support a strong enough reflection to amplify the omni P2 and fade the mainbeam P1.

3.3.2 Coasting in October CDR Data

Measured data for the current SSR antenna mounting configuration was used to determine the P1/P2 ratio as a function of elevation angle. The resultant elevation antenna patterns for the 5-ft array and omni antenna are shown in Figure 25.

The track updates and coast reports for the same northeast quadrant as depicted in Figure 24a are shown in Figure 26a. Again, the data indicate coasting in two clusters along V84, at the 23-nmi intersection and farther out at approximately 40 nmi, with a region of no coasts from 25 to 38 nmi.

Figure 26b illustrates the point of reflection where the ground bounce energy would be concentrated for both the updates and coasts. Again the grouping of coasts at x=1200,y=1200 ft and near the end of 9L are evident.

In conclusion, this analysis indicates that the coasts along V84 are probably due to the differential lobing between the 5-ft array and the omni antenna. Since both 5-ft array and omni antenna configurations for April and October were equivalent in terms of vertical spacing, the elevation lobing patterns would remain relatively the same. Given that low P1/P2 ratios caused by differential lobing is occurring which results in reduced reply runlengths, their incidence will depend entirely on the reflectivity of the terrain. Both data sets indicate correlation with multipath from highly reflective terrain, essentially the airport concrete surfaces. Reflectivity from other surfaces such as the grass and soil between concrete will depend on their moisture content at any particular time. Therefore, variations in ground reflectivity may account for the fact that the coast rate of tracks along V84 varies with the track range.

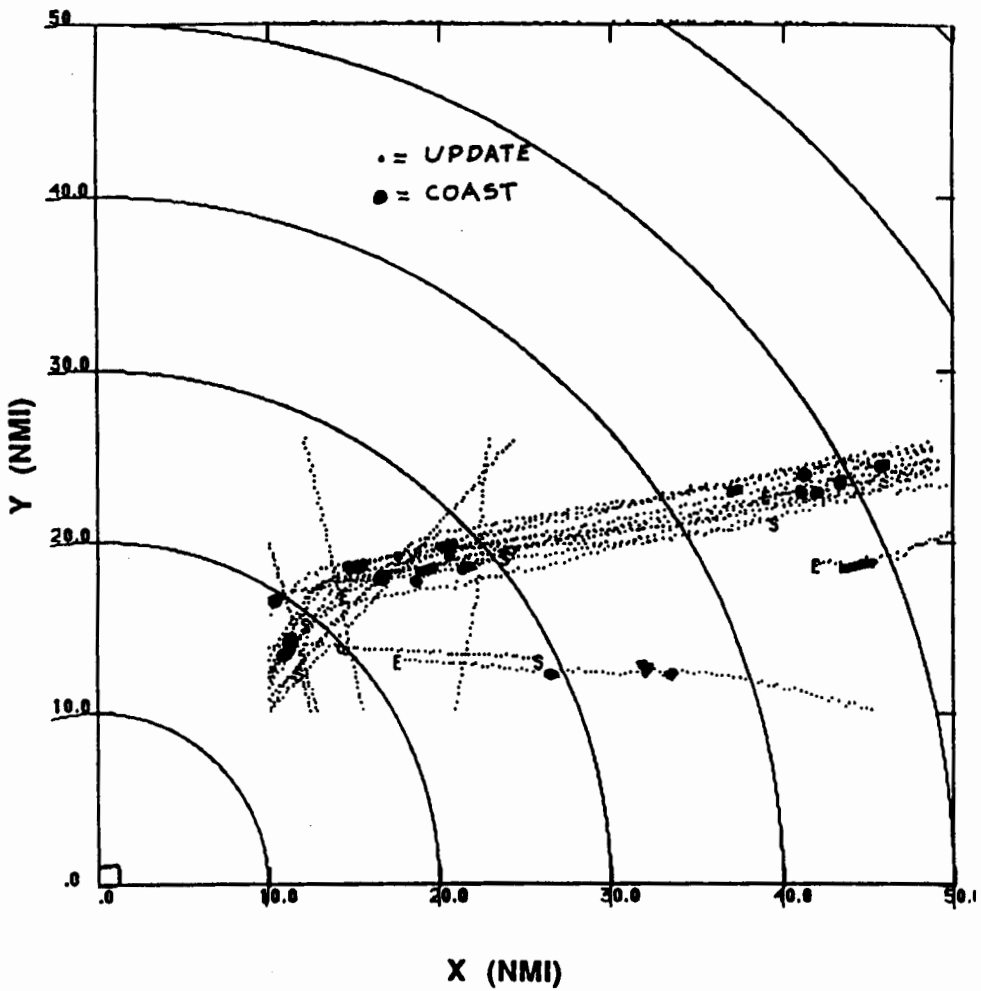

Figure 24a. Radar Tracks Along V84 (from 4/21/91 CDR data).

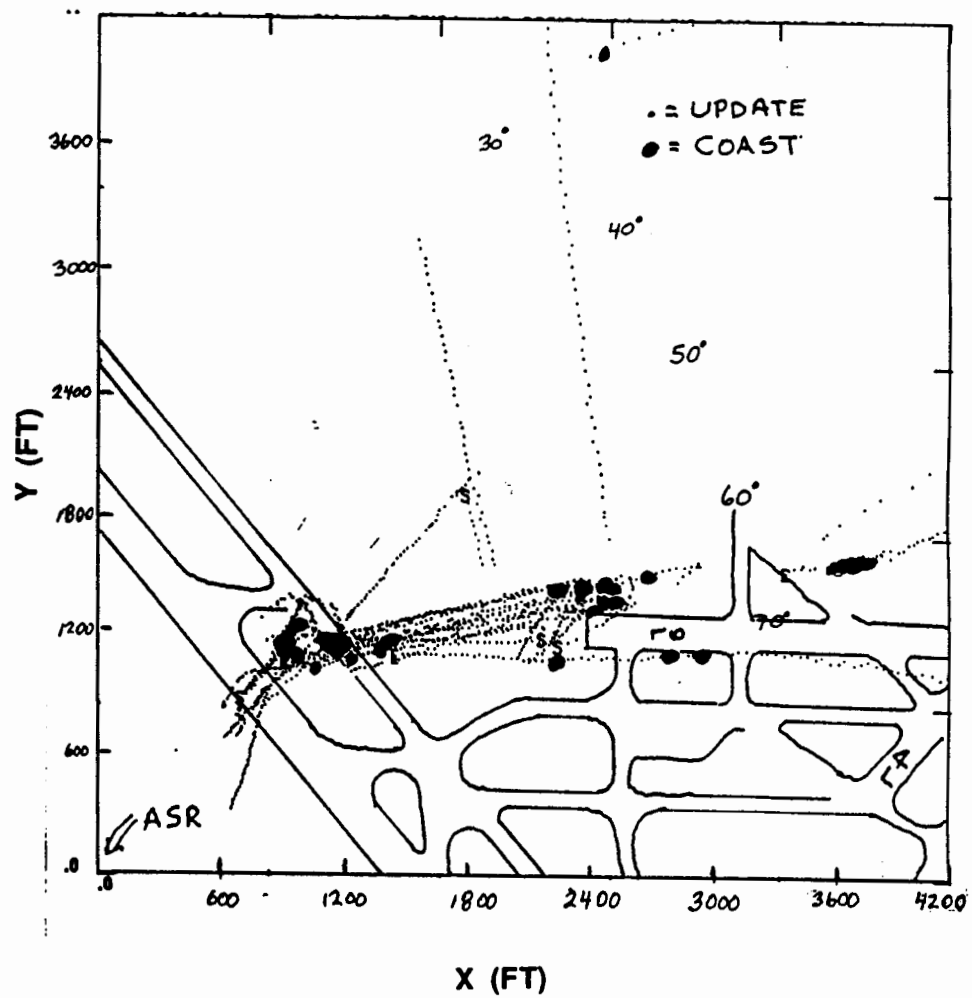

Figure 24b. Fresnal Zone Center Corresponding to Radar Tracks in Figure 24a.

TABLE 3-1

4/21/91 COASTS ON V84 (TILT = -2 DEG)

	TIME M SEC	RANGE NMI	AZ DEG	CODE	ALT FT	TRK	CST	ELEV DEG	MB GAIN dB	OMNI GAIN dB	P1/P2 dB	ANT FT	A/C HT FT	PRCV dBm
7	0 50 30.660	28.601	49.698	3034	9800.	147	1	2.846	17.026	5.781	9.145	86.0	8728.0	-59.1
7	0 50 30.660	28.601	49.698	3034	9900.	147	1	2.879	15.234	8.493	4.641	86.0	8828.0	-60.9
7	0 50 30.660	28.601	49.698	3034	10000.	147	1	2.912	17.166	9.816	5.250	86.0	8928.0	-59.0
8	0 50 35.400	28.276	49.303	3034	9800.	147	1	2.882	15.234	8.693	4.441	86.0	8737.2	-60.8
8	0 50 35.400	28.276	49.303	3034	9900.	147	1	2.915	17.516	9.816	5.600	86.0	8837.3	-58.5
8	0 50 35.400	28.276	49.303	3034	10000.	147	1	2.948	20.393	9.887	8.406	86.0	8937.3	-55.6
16	0 51 12.990	25.774	46.474	3034	9800.	147	1	3.186	15.721	8.549	5.072	86.0	8804.9	-59.5
16	0 51 12.990	25.774	46.474	3034	9900.	147	1	3.222	16.589	9.828	4.660	86.0	8904.9	-58.6
16	0 51 12.990	25.774	46.474	3034	10000.	147	1	3.259	19.621	9.808	7.713	86.0	9004.9	-55.6
36	0 52 47.090	20.028	46.644	5353	6800.	84	1	2.751	22.514	-5.899	26.313	86.0	5935.9	-50.5
36	0 52 47.090	20.028	46.644	5353	6900.	84	1	2.798	19.710	.108	17.502	86.0	6035.9	-53.3
36	0 52 47.090	20.028	46.644	5353	7000.	84	1	2.845	15.794	7.216	6.478	86.0	6135.9	-57.2
37	0 52 51.800	19.846	45.893	5353	6800.	84	1	2.778	21.273	-9.903	29.076	86.0	5939.5	-51.7
37	0 52 51.800	19.846	45.893	5353	6900.	84	1	2.825	17.725	4.372	11.254	86.0	6039.5	-55.2
37	0 52 51.800	19.846	45.893	5353	7000.	84	1	2.873	15.456	8.876	4.480	86.0	6139.6	-57.5
46	0 53 33.930	17.999	38.939	5353	6800.	84	1	3.080	22.173	-12.497	32.569	86.0	5974.5	-49.9
46	0 53 33.930	17.999	38.939	5353	6900.	84	1	3.133	18.658	5.476	11.083	86.0	6074.5	-53.4
46	0 53 33.930	17.999	38.939	5353	7000.	84	1	3.185	15.218	9.233	3.885	86.0	6174.5	-56.9
48	0 53 43.520	28.475	46.779	3431	9800.	420	1	2.860	15.567	7.216	6.251	86.0	8731.6	-60.5
48	0 53 43.520	28.475	46.779	3431	9900.	420	1	2.893	15.898	9.044	4.754	86.0	8831.6	-60.2
48	0 53 43.520	28.475	46.779	3431	10000.	420	1	2.926	18.558	9.971	6.487	86.0	8931.6	-57.5
79	0 56 9.310	28.676	49.331	1742	9800.	227	1	2.838	18.076	4.880	11.096	86.0	8725.9	-58.1
79	0 56 9.310	28.676	49.331	1742	9900.	227	1	2.871	15.567	7.787	5.681	86.0	8825.9	-60.6
79	0 56 9.310	28.676	49.331	1742	10000.	227	1	2.903	16.491	9.457	4.934	86.0	8925.9	-59.7
87	0 56 46.960	26.254	45.772	1742	9900.	227	1	3.159	17.620	6.652	8.867	86.0	8892.4	-57.8
87	0 56 46.960	26.254	45.772	1742	10000.	227	1	3.195	15.251	8.922	4.230	86.0	8992.4	-60.1
87	0 56 46.960	26.254	45.772	1742	10100.	227	1	3.230	17.621	9.923	5.599	86.0	9092.5	-57.8

TABLE 3-1 (cont.)

4/21/91 COASTS ON V84 (TILT = -2 DEG)

	TIME M	TIME SEC	RANGE NMI	AZ DEG	CODE	ALT FT	TRK	CST	ELEV DEG	MB GAIN dB	OMNI GAIN dB	P1/P2 dB	ANT FT	A/C HT FT	PRCV dBm
146	1	1 24.340	37.578	43.517	6274	7900.	278	1	1.616	14.054	7.172	4.781	86.0	6530.5	-64.4
146	1	1 24.340	37.578	43.517	6274	8000.	278	1	1.641	17.351	8.673	6.578	86.0	6630.5	-61.1
146	1	1 24.340	37.578	43.517	6274	8100.	278	1	1.666	20.545	9.749	8.695	86.0	6730.5	-58.0
158	1	2 20.750	26.058	42.375	1116	9900.	61	1	3.184	15.509	8.743	4.665	86.0	8897.5	-59.8
158	1	2 20.750	26.058	42.375	1116	10000.	61	1	3.220	16.271	9.762	4.409	86.0	8997.6	-59.0
158	1	2 20.750	26.058	42.375	1116	10100.	61	1	3.257	19.621	9.911	7.610	86.0	9097.6	-55.7
202	1	5 47.710	37.111	38.916	6631	14200.	262	1	3.239	17.271	9.828	5.343	86.0	12849.6	-61.1
202	1	5 47.710	37.111	38.916	6631	14300.	262	1	3.264	19.312	9.911	7.301	86.0	12949.6	-59.1
202	1	5 47.710	37.111	38.916	6631	14400.	262	1	3.290	20.976	9.448	9.427	86.0	13049.7	-57.4
203	1	5 52.410	37.443	38.630	6631	14200.	262	1	3.207	15.251	9.232	3.919	86.0	12837.2	-63.2
203	1	5 52.410	37.443	38.630	6631	14300.	262	1	3.232	16.589	9.828	4.661	86.0	12937.2	-61.9
203	1	5 52.410	37.443	38.630	6631	14400.	262	1	3.257	18.660	9.911	6.649	86.0	13037.3	-59.8
292	1	12 51.080	17.521	38.628	3446	6800.	198	1	3.169	15.509	8.549	4.860	86.0	5983.0	-56.4
292	1	12 51.080	17.521	38.628	3446	6900.	198	1	3.223	17.972	9.968	5.904	86.0	6083.0	-53.9
292	1	12 51.080	17.521	38.628	3446	7000.	198	1	3.276	21.824	8.867	10.857	86.0	6183.0	-50.0
301	1	13 33.530	28.472	46.601	2713	9900.	12	1	2.893	15.653	9.196	4.357	86.0	8831.7	-60.4
301	1	13 33.530	28.472	46.601	2713	10000.	12	1	2.926	18.558	9.951	6.508	86.0	8931.7	-57.5
301	1	13 33.530	28.472	46.601	2713	10100.	12	1	2.959	21.139	9.688	9.352	86.0	9031.8	-54.9
316	1	14 43.970	24.287	39.466	2713	8600.	12	1	2.930	19.217	9.971	7.146	86.0	7641.8	-55.5
316	1	14 43.970	24.287	39.466	2713	8700.	12	1	2.969	21.768	9.370	10.298	86.0	7741.9	-52.9
316	1	14 43.970	24.287	39.466	2713	8800.	12	1	3.007	23.150	6.654	14.396	86.0	7841.9	-51.6
317	1	14 48.680	24.041	38.986	2713	8600.	12	1	2.962	21.362	9.370	9.891	86.0	7647.8	-53.3
317	1	14 48.680	24.041	38.986	2713	8700.	12	1	3.001	23.080	7.303	13.677	86.0	7747.8	-51.5
317	1	14 48.680	24.041	38.986	2713	8800.	12	1	3.040	23.328	2.044	19.185	86.0	7847.8	-51.3
318	1	14 53.330	23.758	38.377	2713	8600.	12	1	3.000	23.000	7.861	13.038	86.0	7654.6	-51.5
318	1	14 53.330	23.758	38.377	2713	8700.	12	1	3.040	23.328	3.395	17.833	86.0	7754.6	-51.2
318	1	14 53.330	23.758	38.377	2713	8800.	12	1	3.079	22.606	-12.516	33.022	86.0	7854.6	-51.9
335	1	16 13.430	28.730	45.881	3443	9800.	404	1	2.832	18.759	3.819	12.840	86.0	8724.3	-57.4
335	1	16 13.430	28.730	45.881	3443	9900.	404	1	2.865	15.794	7.216	6.478	86.0	8824.3	-60.4
335	1	16 13.430	28.730	45.881	3443	10000.	404	1	2.897	15.456	9.043	4.312	86.0	8924.4	-60.7

TABLE 3-1 (cont.)

4/21/91 COASTS ON V84 (TILT = -2 DEG)

	TIME M SEC	RANGE NMI	AZ DEG	CODE	ALT FT	TRK	CST	ELEV DEG	MB GAIN dB	OMNI GAIN dB	P1/P2 dB	ANT FT	A/C HT FT	PRCV dBm
336	1 16 18.140	28.374	45.535	3443	9800.	404	1	2.871	15.221	8.276	4.844	86.0	8734.5	-60.8
336	1 16 18.140	28.374	45.535	3443	9900.	404	1	2.904	16.822	9.567	5.155	86.0	8834.5	-59.2
336	1 16 18.140	28.374	45.535	3443	10000.	404	1	2.937	19.530	9.974	7.455	86.0	8934.5	-56.5
361	1 18 15.700	28.164	46.709	2666	9800.	60	1	2.894	15.653	9.334	4.220	86.0	8740.4	-60.3
361	1 18 15.700	28.164	46.709	2666	9900.	60	1	2.928	18.558	9.979	6.480	86.0	8840.4	-57.4
361	1 18 15.700	28.164	46.709	2666	10000.	60	1	2.961	21.139	9.595	9.444	86.0	8940.5	-54.9
367	1 18 43.770	18.402	37.687	3443	7100.	404	1	3.163	15.978	7.859	6.019	86.0	6267.2	-56.3
367	1 18 43.770	18.402	37.687	3443	7200.	404	1	3.214	16.924	9.882	4.942	86.0	6367.2	-55.4
367	1 18 43.770	18.402	37.687	3443	7300.	404	1	3.265	20.976	9.325	9.551	86.0	6467.2	-51.3
372	1 19 7.280	24.500	42.932	2666	9400.	60	1	3.210	15.722	9.591	4.031	86.0	8436.8	-59.1
372	1 19 7.280	24.500	42.932	2666	9500.	60	1	3.248	18.660	9.944	6.616	86.0	8536.8	-56.1
372	1 19 7.280	24.500	42.932	2666	9600.	60	1	3.286	21.824	8.867	10.858	86.0	8636.9	-53.0
373	1 19 12.000	24.196	42.592	2666	9400.	60	1	3.253	19.312	9.911	7.301	86.0	8444.2	-55.4
373	1 19 12.000	24.196	42.592	2666	9500.	60	1	3.292	22.005	8.867	11.038	86.0	8544.2	-52.7
373	1 19 12.000	24.196	42.592	2666	9600.	60	1	3.330	23.168	6.170	14.899	86.0	8644.3	-51.5

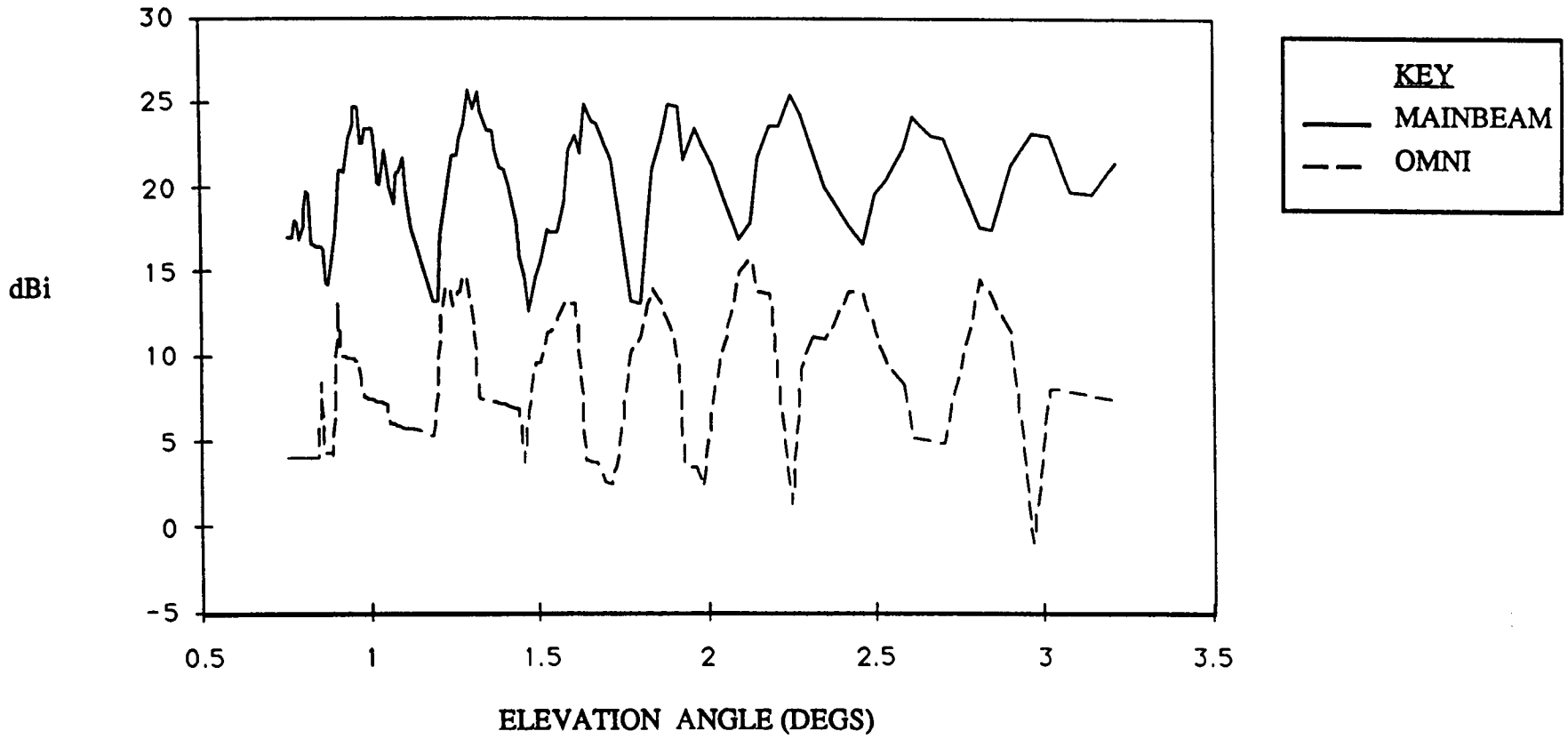

Figure 25. Mainbeam and Omni Antenna Elevation Patterns from AMF Measurements.

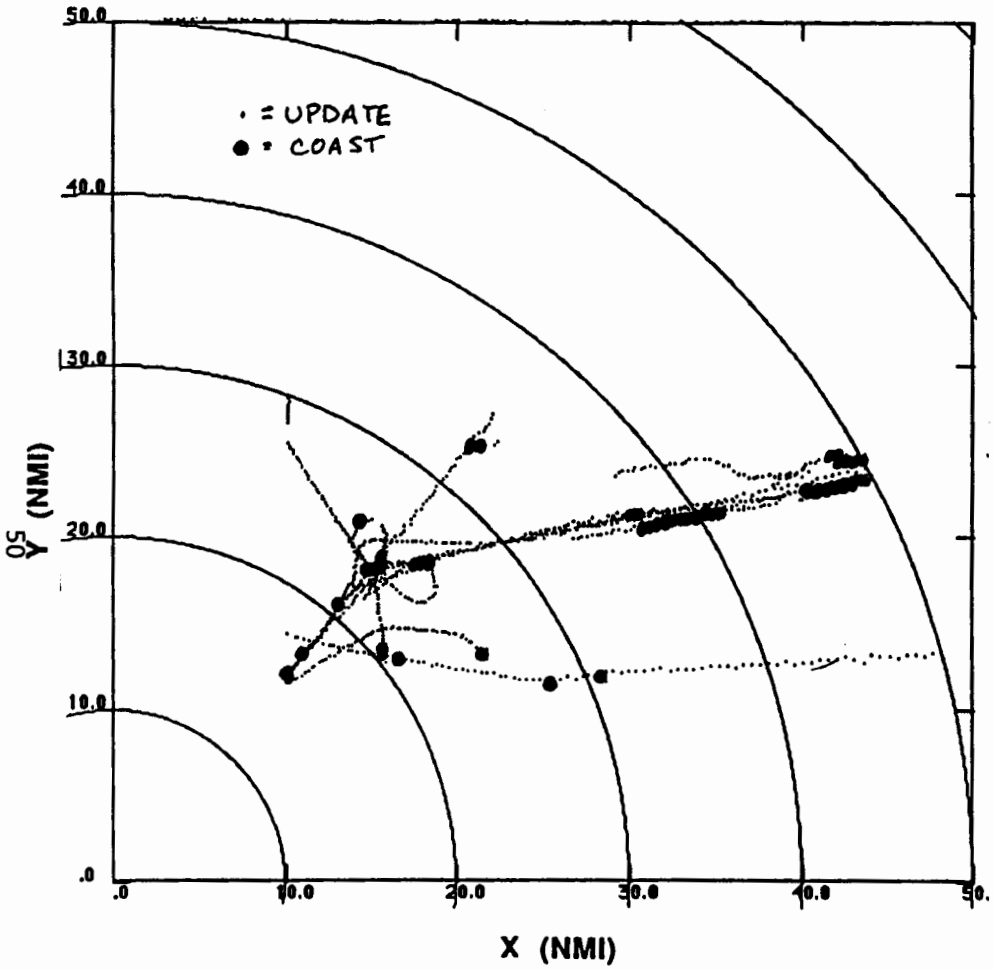

Figure 26a. Radar Tracks Along V84 (from 10/22/91 CDR data).

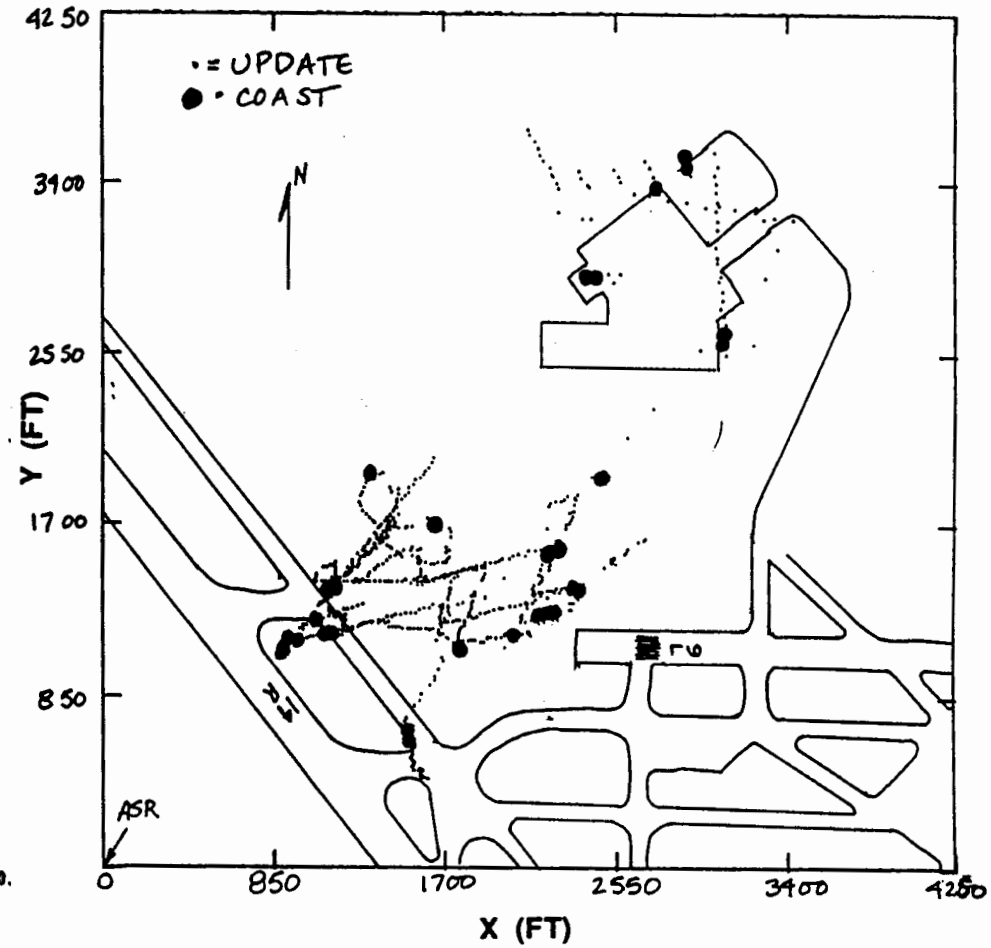

Figure 26b. Fresnal Zone Centers Corresponding to Radar Tracks in Figure 26a.

4. EVALUATION OF ARTS TRACK PERFORMANCE

4.1 GENERAL

Coincident with the AMF pulse data analyses, a study was performed of the ORD ARTS III/A surveillance data extracted from Continuous Data Recordings (CDR) of 22 October 1991. The primary focus of this study was to gather statistics of the ORD ground sensor performance under various traffic densities within the ORD terminal area. The ground sensor performance was analyzed with two objectives in mind:

(a) Obtain SSR Blip/scan ratios under various conditions.

(b) Explain why particular radar tracks coasted.

The first objective was obtained through direct analysis of the CDR data stream during any particular time frame of interest under an assortment of conditions. Blip/scan ratios were calculated as functions of time, airline, track, and other factors. This analysis and the associated results are presented in Section 4.3.

Associating the coasts with plausible causes is more difficult. The list of possible coast causes include: outside of ORD surveillance area (beyond range filter limits or below minimum elevation angle), uncorrelated target report, code garble, low P1-P3 power on the interrogation uplink, low P1-P2 power ratio, aircraft maneuvering causing shadowing, and airline and/or aircraft specific factors. This analysis and the associated results are presented in Section 4.4.

Initially, two samples of CDR data were examined encompassing both high and low traffic densities to assess differences in blip/scan ratios and causes of coasting. The specific samples selected for the initial detailed analysis are:

"High-Density Sample": 22 October 1991, 8:03 am to 9:37 am(local time)

"Low-Density Sample": 2 October 1991, 11:44pm to 23 October 1991, 7:13 am (local time)

The complete October CDR sample comprised 9 data sets, giving continuously recorded values over a 36-hour, 31-minute period, from 21 October 1991, 6:42pm through 23 October 1991, 7:13am (local time). The two samples (high density, low density) initially examined were two of these data sets. For correlations of coasting with aircraft body type, all the separate data sets were used and combined, in effect, as one large sample.

In the following sections, the CDR data analysis results are discussed in detail after a brief outline explaining the content and extraction process for obtaining surveillance data.

4.2 CDR DATA CONTENT AND EXTRACTION

The ARTS III/A radar system continuously stores all system inputs (Sensor Receiver and Processor (SRAP) outputs, controller keyboard inputs, ARTCC flight plans, etc.) and outputs (aircraft tracking data) to magnetic media. The primary purpose for data storage is to provide an ability to replay in case of an accident or incident. The recordings also serve to provide the technical community with surveillance data upon which the radar performance can be judged. Although the type of messages available in the CDR data are extensive, only four messages were relevant to this

investigation – target reports, track reports, flight plans, and (primary) radar reports. A brief definition of each is provided below:

(a **Target Report (Message Code 7)**: Referred to as the beacon report, it is the reported position (Range, Azimuth) and transponder code based upon the detection of several replies within one radar scan. Target report data is stored on the CDR disk as received from the SRAP.

(b) **Track Report (Message Code 10)**: Based upon the target report position and transponder code, a track is initiated and updated according to the correlation parameters set within the tracking function. The track report contains the target position data (in *X,Y,* Altitude), the predicted range and azimuth for the next scan, and the associated airline flight identification (Flight ID) based upon the transponder code/flight plan match. It also contains the track status (i.e., active or coasting) which is a primary focus of this analysis. The track status data is further discussed in Section 4.3.

(c) **Interfacility Messages (Message Code 13)**: Interfacility data messages are transmitted between Air Route Traffic Control Centers and ARTS IIIA facilities in order to transmit and update flight plans, interchange positional data, and transfer radar control of flights from one facility to another. These messages can also be transmitted between two ARTS IIIA facilities.

There are 18 different types of interfacility messages, identified by a type code within the message, and each type has a different specific format. Most of the message fields are coded in EBCDIC and translation to ASCII is necessary. The length of an interfacility message is variable and depends not only on the type of message, but on other factors within the message. For our purposes, only the flight plan messages were used; related messages (amendments, cancellations, etc.) were not examined.

Information provided in the flight plan message includes flight ID, aircraft type, beacon code, and entry/exit fix. The flight ID and aircraft type were used in this analysis.

(d) **Primary Radar Report (Message Code 20)**: Uncorrelated primary-report position data from the SRAP are recorded as received. Emphasis is placed on the fact that these are uncorrelated reports; correlated radar reports, i.e., an accompanying SSR or beacon report exists at the same range and azimuth, are not passed to the IOP but rather the beacon target report is said to be radar reinforced.

Figure 27 illustrates a simplified view of the process for developing the inputs to the controller display and the CDR.

At this time, it is necessary to define the term "coast" from both the CDR data and controller display points of view. Although the true meaning is equivalent for both viewpoints, a coast as defined for the CDR data implies that a target report was either unavailable or did not correlate during that particular scan. Therefore, the position data contained in the track update are the predicted positions based on previous track history. The display logic will post the aircraft position to the coasted position and replace the altitude field within the data tag with the label "CST." An aircraft can coast up to 9 times consecutively before being dropped from the display.

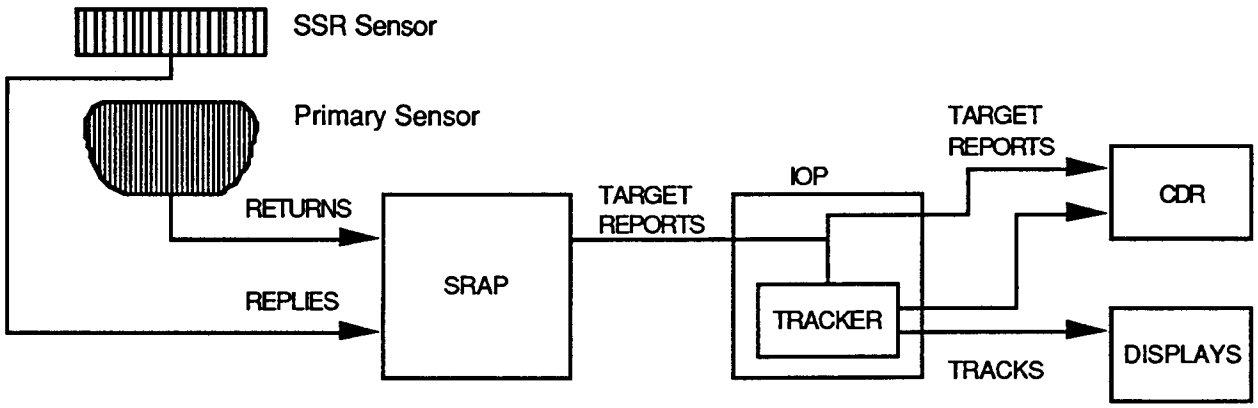

Figure 27. Simple Block Diagram of Radar Data Processing and Storage.

4.3 CHICAGO ARTS III/A RADAR PERFORMANCE ASSESSMENT

To enable analysis of ARTS blip/scan ratios, the ARTS CDR data for the high- and low-density periods were processed to provide the following information from the Sector Time (message code 6) and Tracking Data (message code 10):

- Time of report (in seconds, UTC or Zulu time)
- Track Status - a code value of 0 for an active normal report, or 1 for an active coast. Additional report status codes are 2 (illegal) and 3 (active hand-off).
- Reported Beacon Code
- Altitude in feet above mean sea level
- Displayed x-track in nautical miles; obtained by ARTS from the measured range and bearing.
- Displayed y-track in nautical miles (also from measured range and bearing)
- ARTS track number
- Aircraft identification (ARTCC flight number)

Examination of the extracted messages provide the following raw (unfiltered) results (i.e., total counts of track reports) for both samples:

		High Density	Low Density
Tracks Status	= 0 (normal)	116,473	84,891
	= 1 (coast)	7596	4058
	= 2 (illegal)	85	111
	= 3 (handoff)	8	2

Excluding the illegal and hand-off coasts, the track report counts gave the following overall blip/scan ratios for the high and low-density samples:

Overall blip/scan ratio	93.88%	95.44%

These ratios include all tracks (long and short), and reports at all ranges and elevation angles.

4.3.1 Aircraft Track Identification

The CDR data from each sample was processed to associate beacon code, track number, and aircraft flight number in order to identify unique aircraft tracks. The number of reports contained in each unique aircraft track was counted and used as a measure of track length. Track segments for aircraft, in which the flight number was not present, or the beacon or track numbers changed, were not used.

The two data samples were found to contain the following number of tracks that could be associated with a flight number, tail number or beacon code:

	High Density	Low Density
Tracks of 9 or fewer reports	2598	1730
Tracks of 10 or more reports	1136	779
Total	3734	2509

Only tracks with 10 or more reports were used for subsequent analysis. The high-density sample covered 94 minutes, and the low-density sample covered 449 minutes.

4.3.2 Track Specific Performance

Blip/scan ratios were calculated for the identified aircraft tracks as the number of active normal reports divided by the total of the normal and coasted reports. Figures 28 through 31 show the variation, throughout the high- and low-density periods, of the track specific blip/scan ratios for both major airlines only and for all airlines (general aviation excluded). In addition, the distributions of the number of tracks, for each sample period, by blip/scan ratio are illustrated in Figures 32 and 33.

In general, these results (prior to surveillance screening) show that the blip/scan ratios for most tracks are clustered in the upper 90% region and that over 50% of the tracks in the high-density sample indicate a blip/scan ratio of at least 95%.

4.3.3 Effect of Surveillance Screening

Additional criteria were used to exclude all track reports which indicated elevation angles below 0.5 degrees or above 40 degrees and ranges less than 2 nmi or greater than 45 nmi. The target altitude and x,y position coordinates in the track report message were used as the basis for the range and elevation angle rejection criteria. Equations to determine the aircraft position relative to a horizontal surface passing through the antenna were developed. The effect of the earth's curvature was included, and antenna height and aircraft altitudes were computed with respect to MSL.

The surveillance screening process provided the following results:

	High Density	Low Density
Normal reports	70,793	55,854
Coast reports	1737	1158
Total reports	74,530	57,012
Overall blip/scan ratio	97.61%	97.97%

The track reports were further analyzed to produce a series of graphs, for both the high-density and the low-density periods, showing the variation of blip/scan ratios with azimuth, elevation angle, range, and time of day. The number of reports was also plotted against azimuth, elevation angle, and range so that blip/scan variations could be compared to changes or patterns in traffic. These are presented in Figures 34 through 37. It is interesting to note that SSR performance is independent of number of TCAS aircraft as represented by the results for the high-density period (~15 TCAS) and the low-density period (~0 TCAS).

The blip/scan ratios measured in Chicago compare very favorably with measurements conducted by Lincoln Laboratory at a number of terminal areas in the United States in the mid-to-late 1970s (Report No. FAA-RD-77-113). These earlier measurements yielded the following results:

Location	Overall Blip/Scan Ratio (%)
Boston, MA	97.8
Washington, DC	96.0
Philadelphia, PA	91.9
Los Angeles, CA	91.7
Salt Lake City, UT	93.0
Las Vegas, NV	94.3

The above blip/scan ratio was computed using tracks that :

- are associated with 10 or more reports,
- occur at an elevation angle between 0.5 and 40 degrees,
- are at a range between 2 and 45 nmi, and
- correspond to an aircraft with an encoding altimeter.

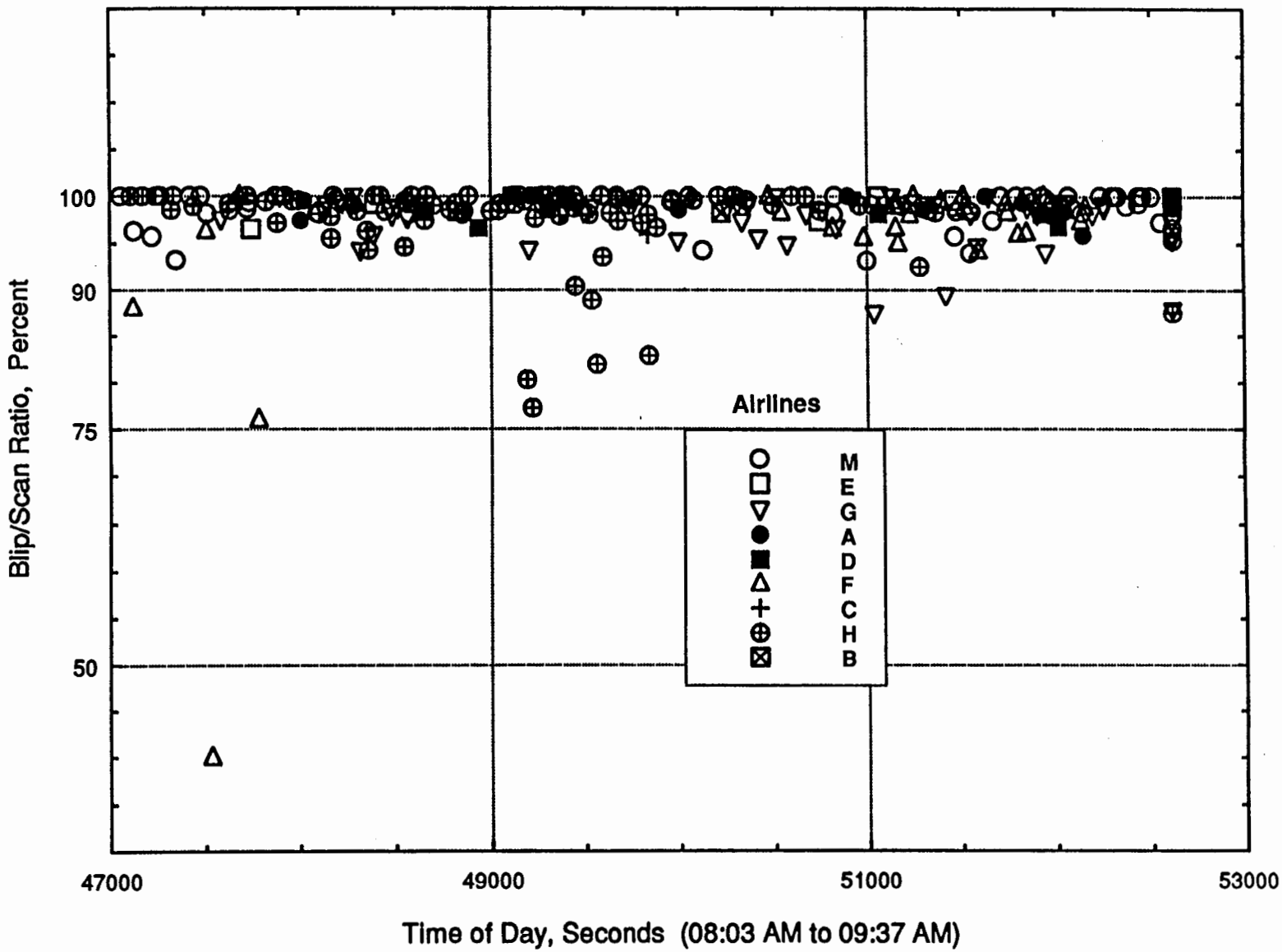

Figure 28. Single Track Blip/Scan Ratios by Major Airlines - High-Density CDR Sample. Short Tracks Eliminated; No Surveillance Screening Applied

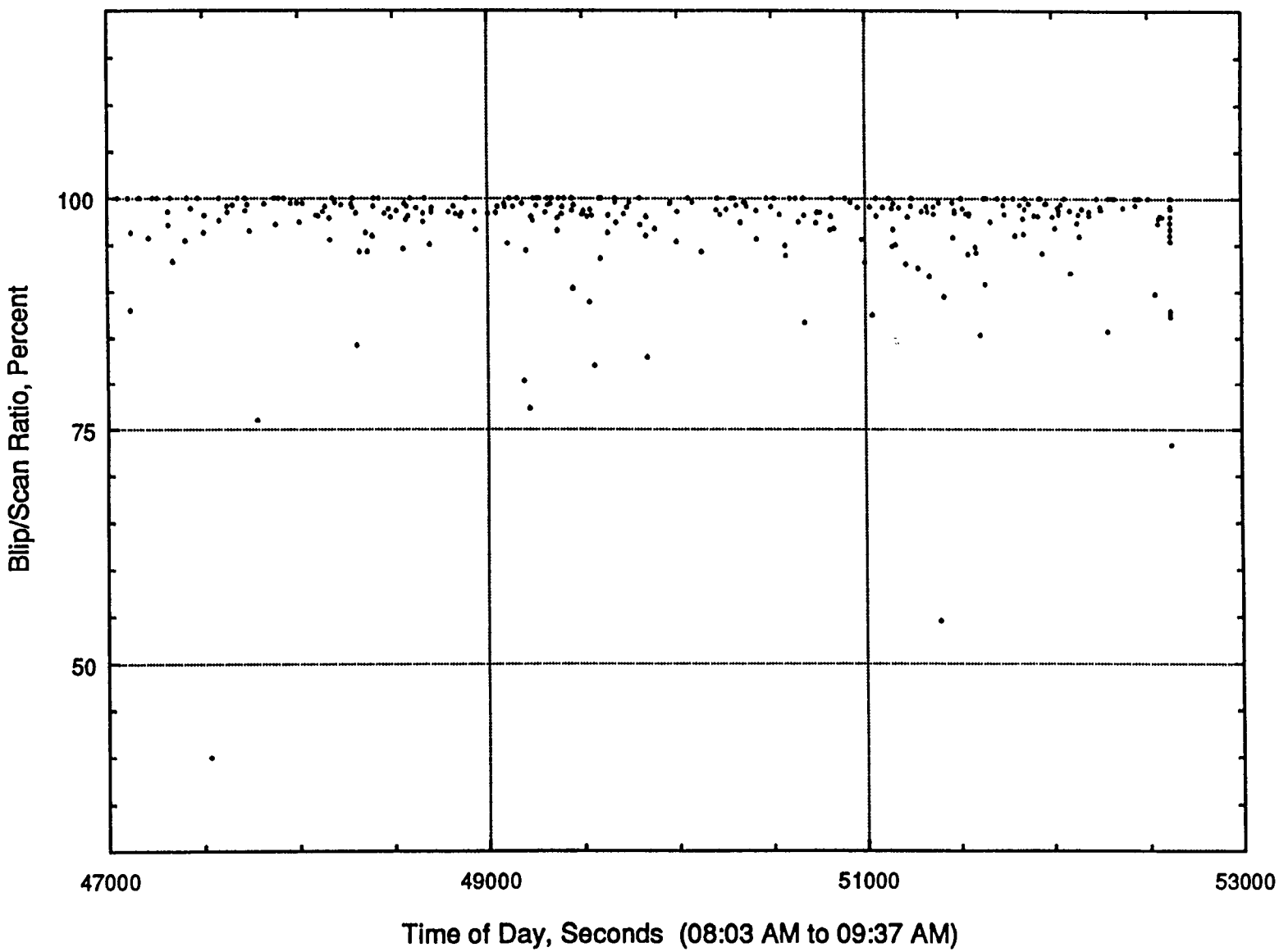

Figure 29. Single Track Blip/Scan Ratios by Airlines - High-Density CDR Sample. Short Tracks Eliminated; No Surveillance Screening Applied

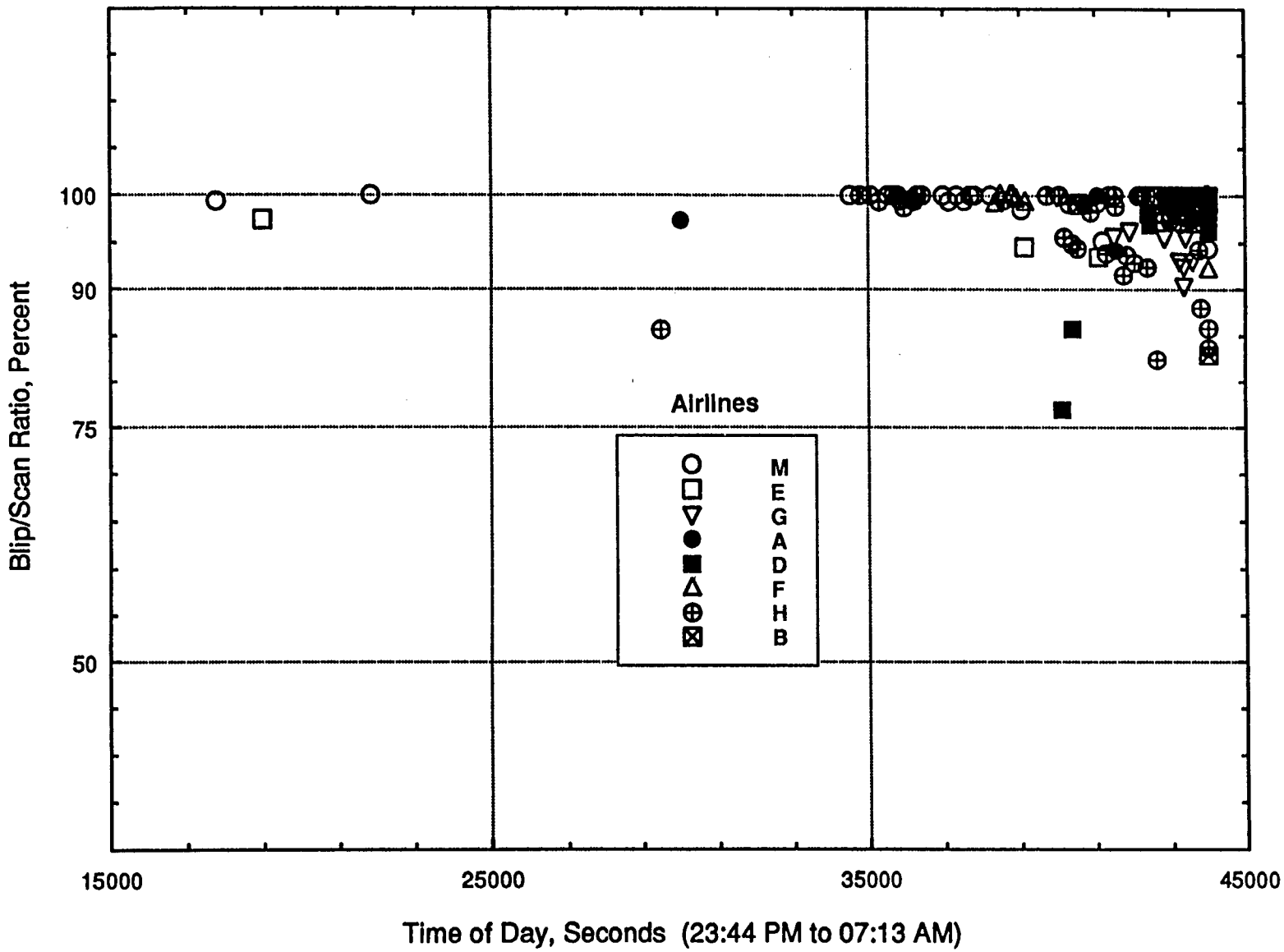

Figure 30. Single Track Blip/Scan Ratios by Major Airlines - Low-Density CDR Sample. Short Tracks Eliminated; No Surveillance Screening Applied

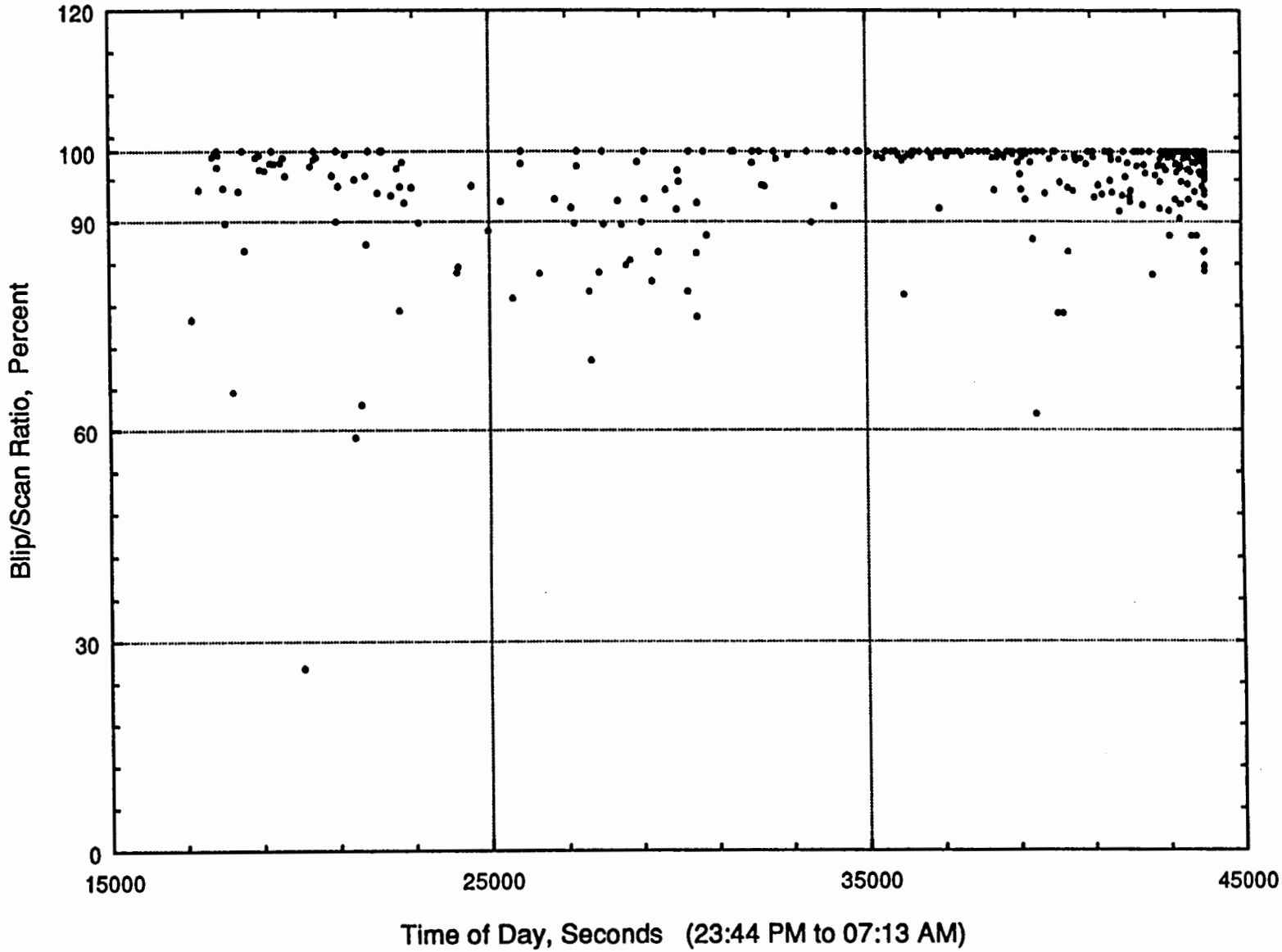

Figure 31. Single Track Blip/Scan Ratios by Airlines - Low-Density CDR Sample. Short Tracks Eliminated; No Surveillance Screening Applied

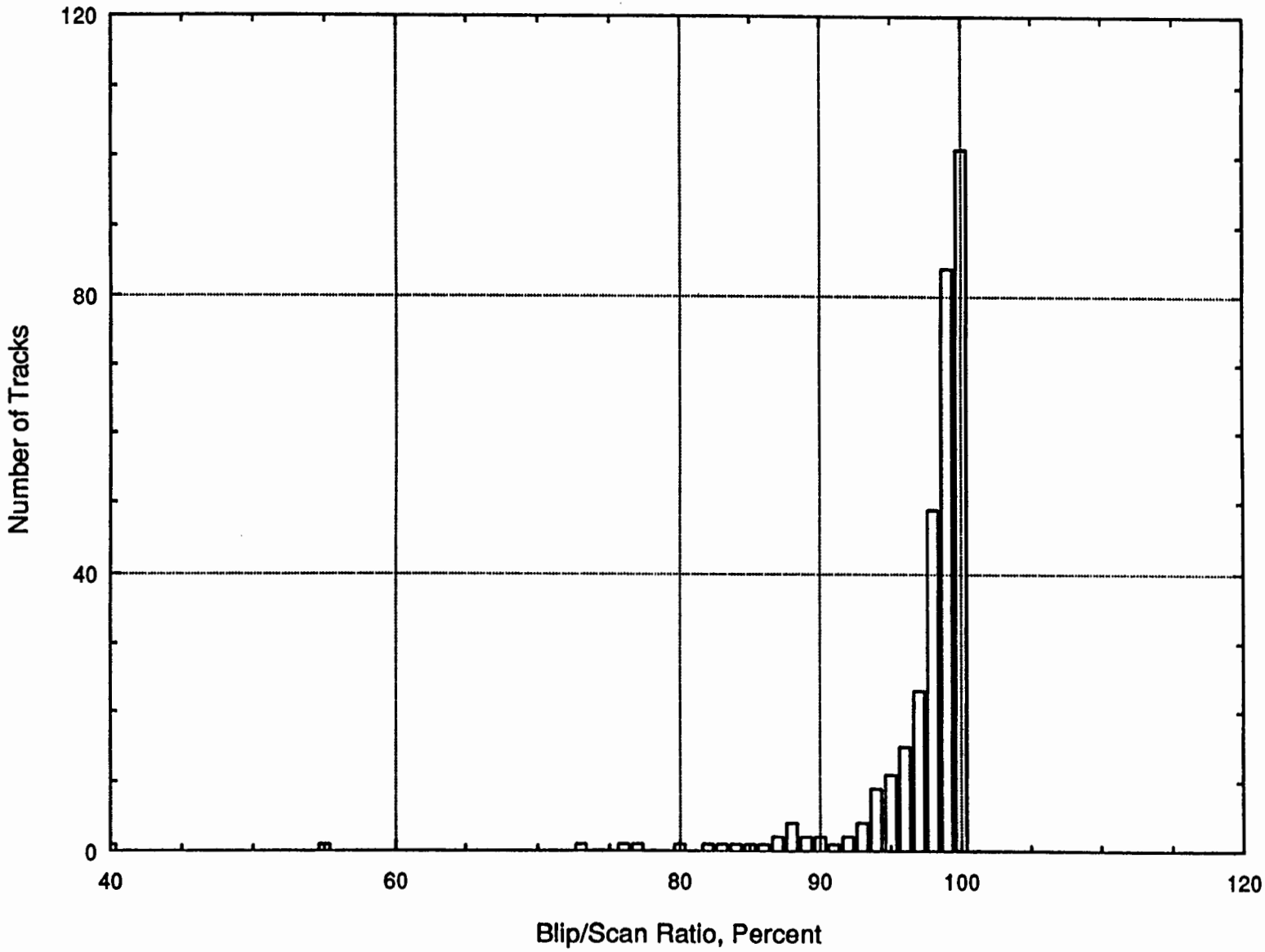

Figure 32. Single Track Blip/Scan Ratios by Major Airlines Histogram - High-Density CDR Sample. Short Tracks Eliminated; No Surveillance Screening Applied

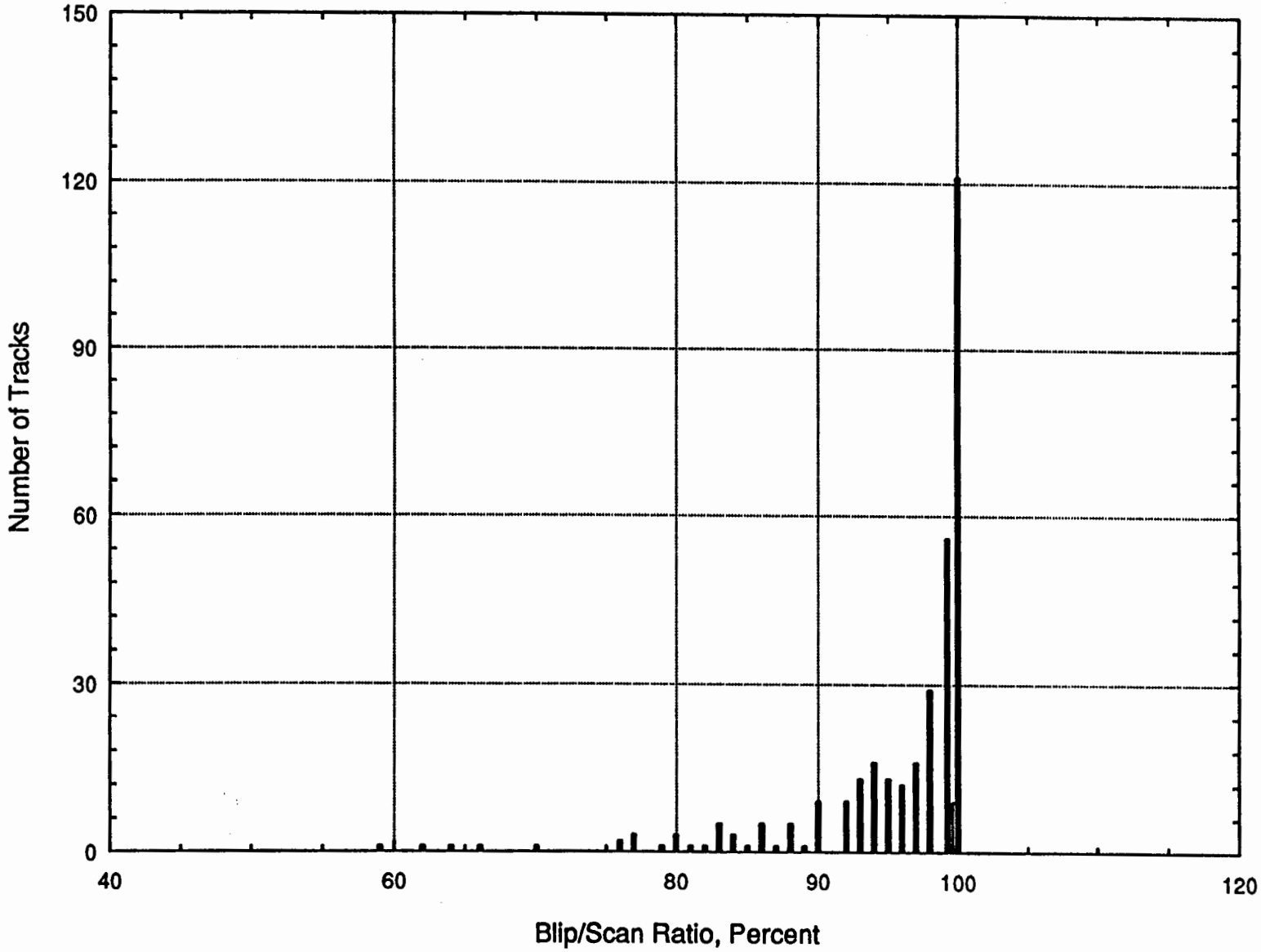

Figure 33. Single Track Blip/Scan Ratios by Airlines Histogram - Low-Density CDR Sample. Short Tracks Eliminated; No Surveillance Screening Applied

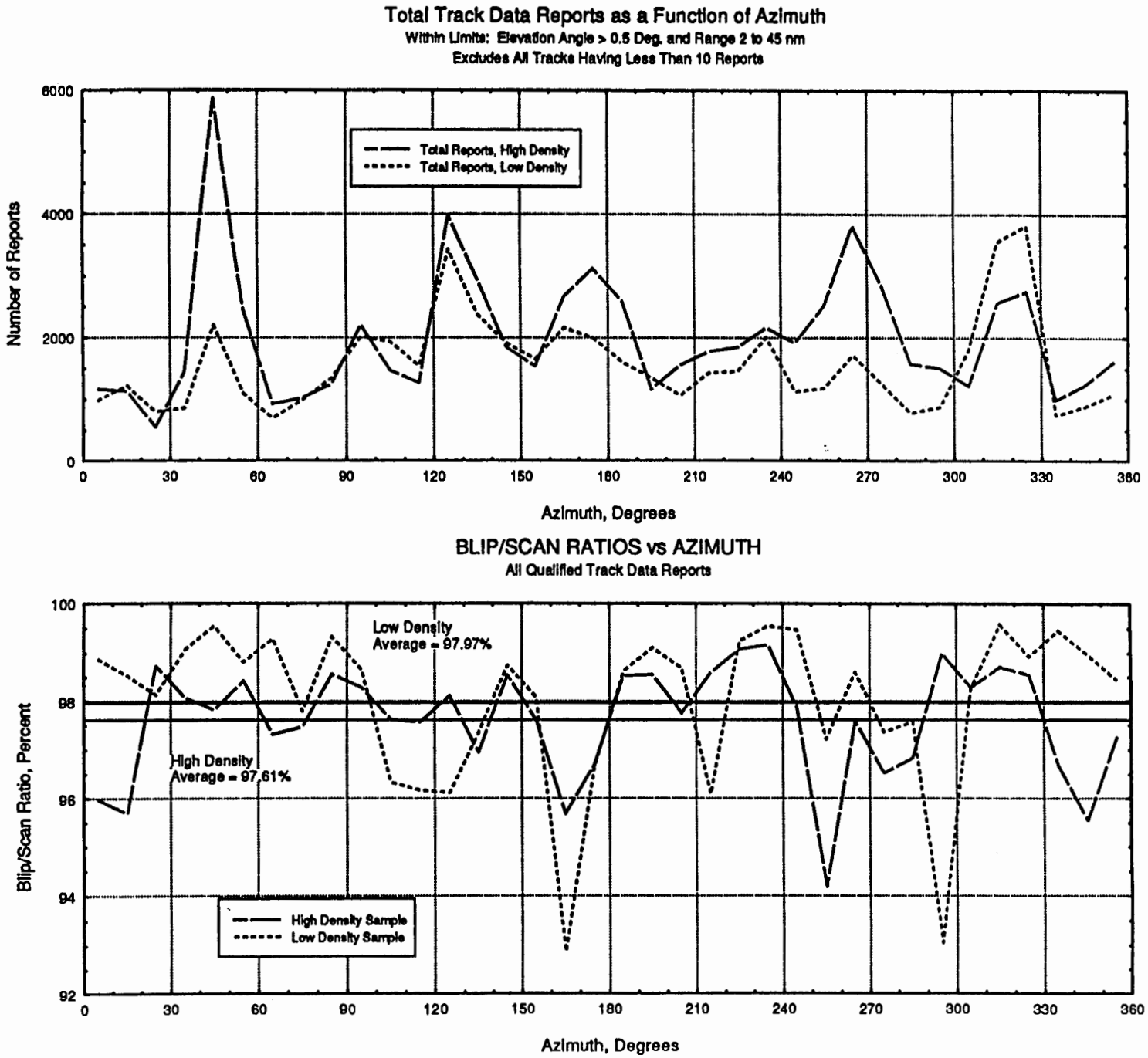

Figure 34. Total Track Reports and Blip/Scan Ratio vs. Azimuth - Both Data Samples.

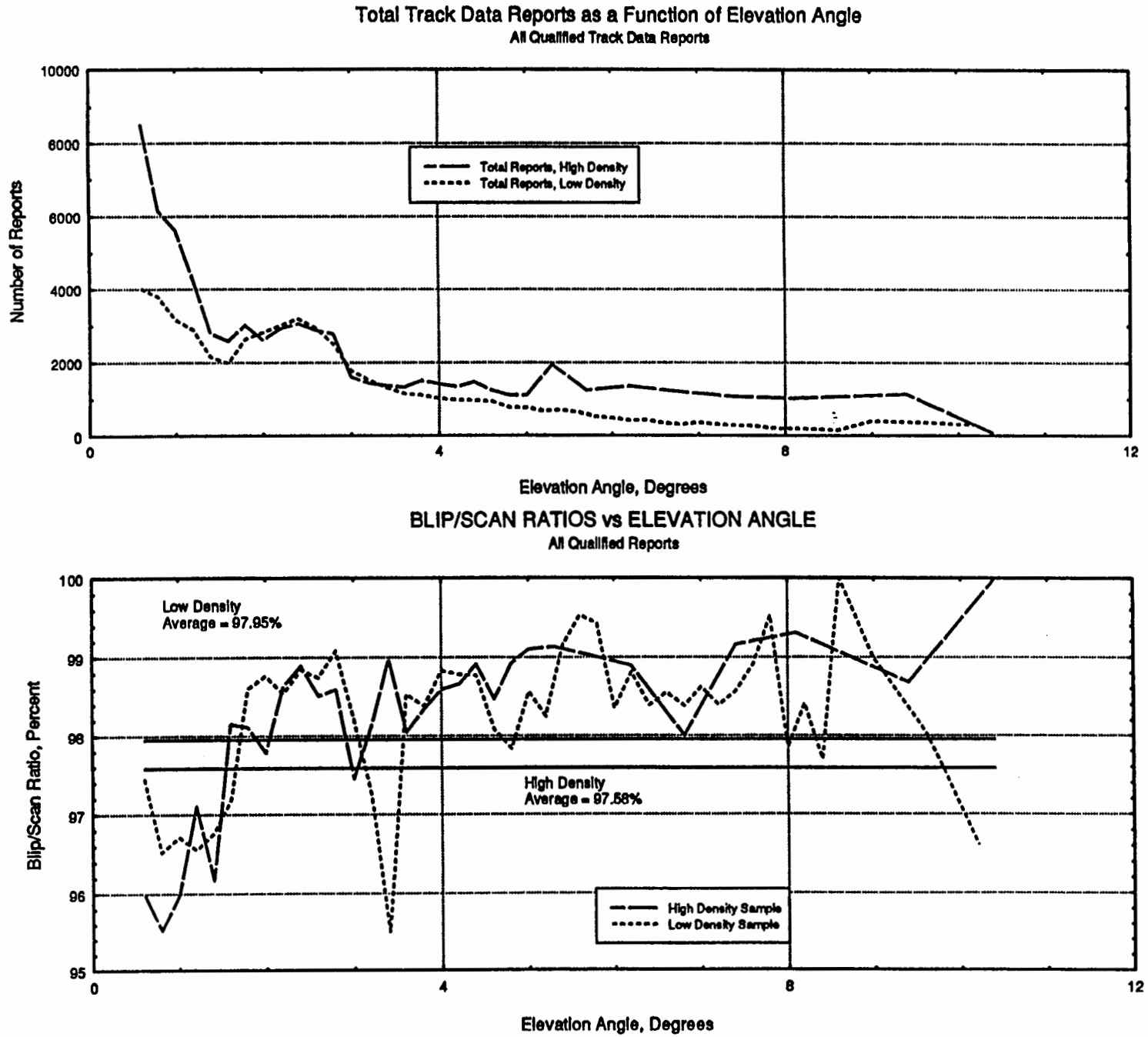

Figure 35. Total Track Reports and Blip/Scan Ratio vs. Elevation Azimuth - Both Data Samples.

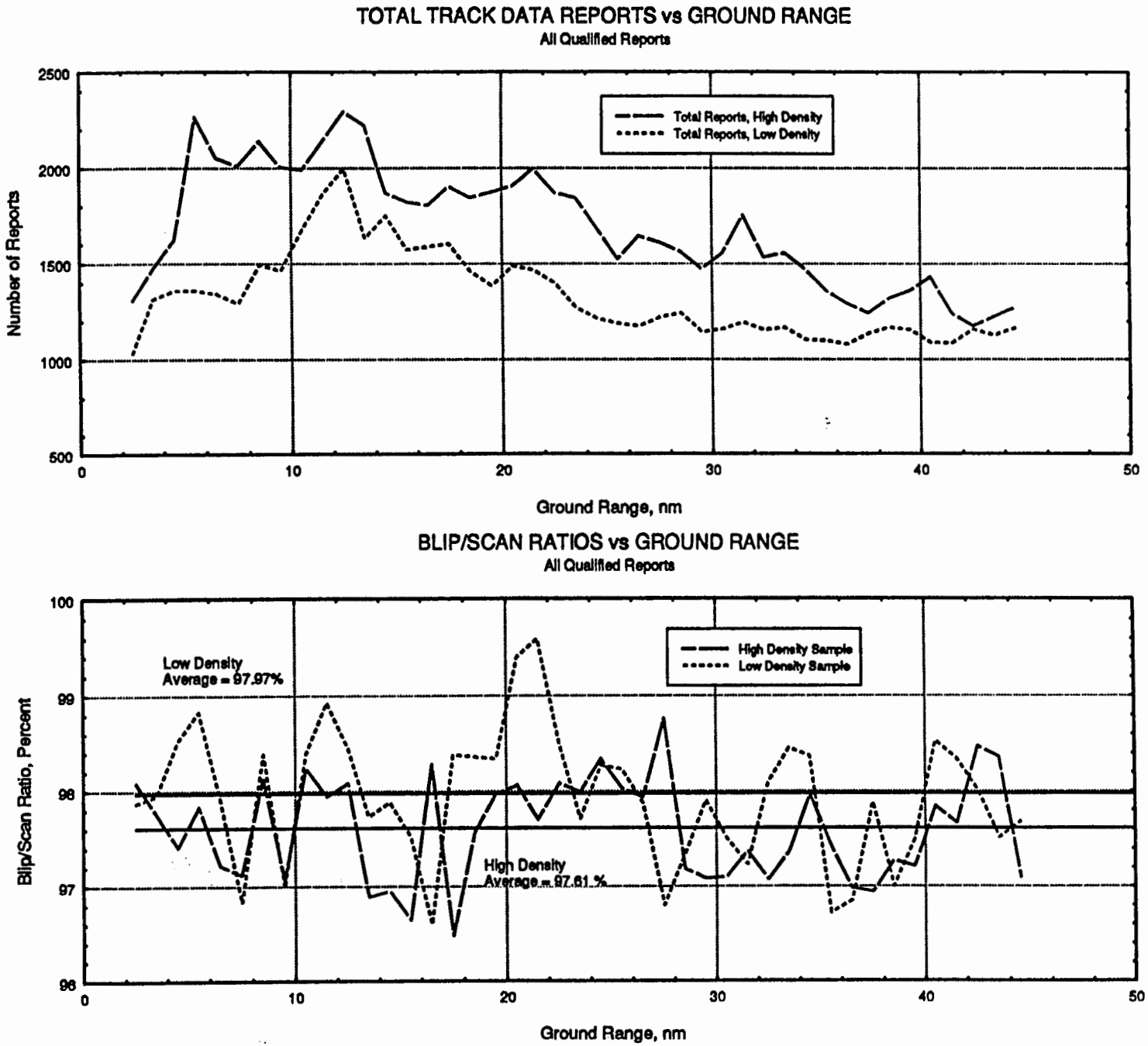

Figure 36. Total Track Reports and Blip/Scan Ratio vs. Ground Range - Both Data Samples.

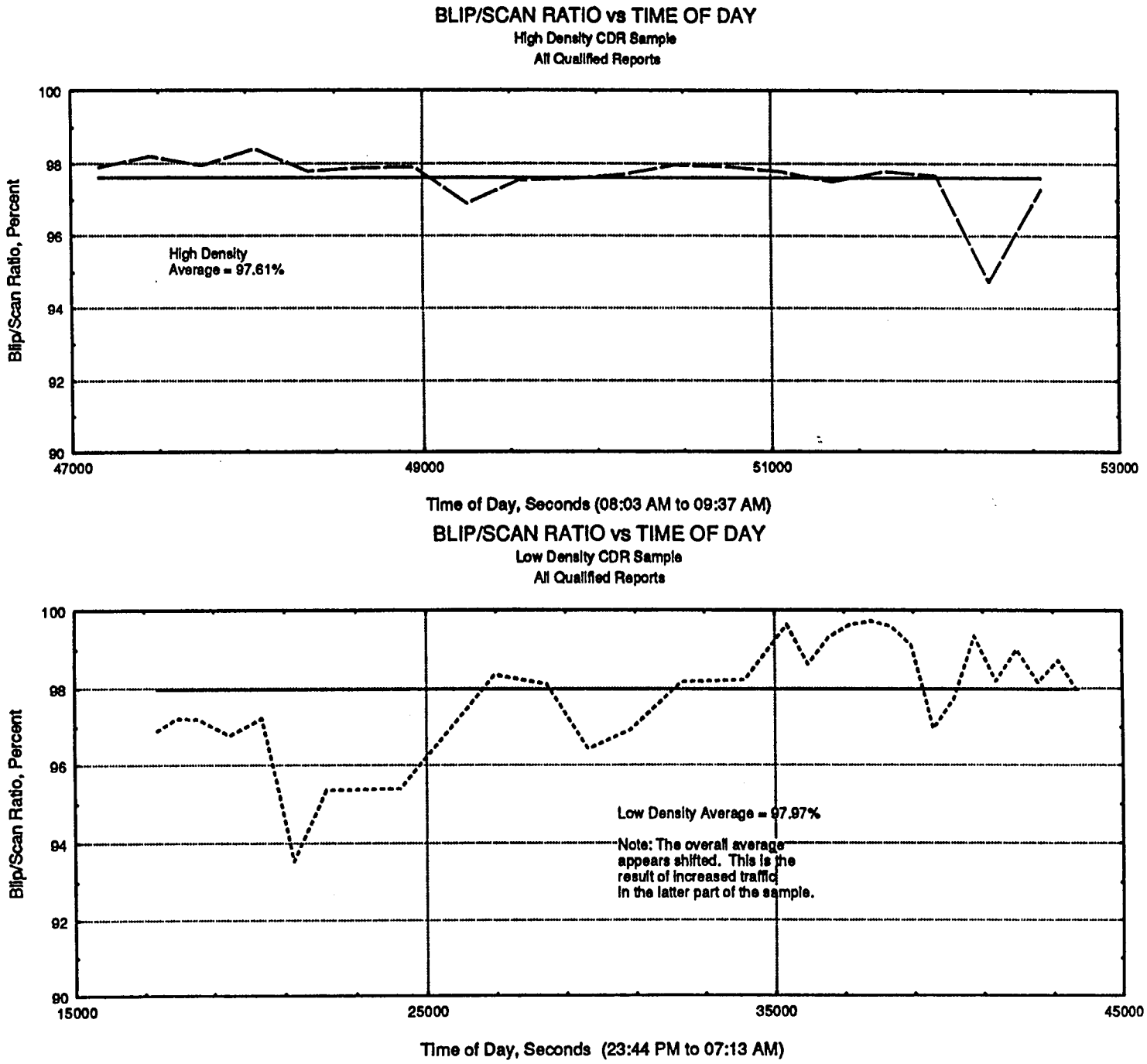

Figure 37. Blip/Scan Ratio vs. Time of Day - Both Data Samples.

4.3.4 Airline and Aircraft Specific Performance

While the overall blip/scan ratios, after surveillance limits were applied, were close to 98% for the high-density and the low-density samples, the analyses indicated that the performance for certain airlines and/or aircraft might be much poorer. (See Figures 21 and 23). To evaluate whether airline or aircraft specific factors might be causal, CDR flight plan records were linked to target report data and coast reports were correlated with flight ID, airline, and aircraft type.

4.3.4.1 CDR Flight Plan Extraction

The CDR data samples were processed to extract and decode the interfacility messages. Only those flight plans associated with airlines of interest were used. Files of paired flight ID and body type were produced to index track reports using the flight ID. Combined indices were used to associate body types with track reports that occurred in different CDR samples than the corresponding flight plan message.

4.3.4.2 Association of Flight Plans and Track Reports

A filtering program was written to read the track reports in the CDR data, select the reports of interest, look up the associated aircraft body type by cross-referencing the flight plan data, and accumulate track summary information. A processing method was devised to combine track segments that were split at CDR data sample boundaries.

Track report selection criteria were type of track report, airline and slant range. Interim analyses indicated that much of the extended coasting beyond 40 nmi was due to aircraft maneuvering in holding patterns. To exclude this mechanism from aircraft specific causes, only track reports for ranges from 2 to 40 nmi were selected. Airline-specific data were selected for all Airline-M and all Airline-H* flights from the CDR data covering the 36+ hour period from 6:42pm on 21 October 1991 through 7:13am on 23 October 1991.

In this 36-hour sample, Airlines -H and Airlines-M had the most flights of the major carriers, with totals of 1031 and 770, respectively. The distribution of the number of flight segments by aircraft type for each of these airlines was:

Airlines-M		Airlines-H	
Body Type	Number of Flights	Body Type	Number of Flights
ALL	770	ALL	1031
UNKN	26	UNKN	21
A300	4	B727	368
B727	205	B737	187
B757	49	B73S	262
B767	20	B747	3
DC10	46	B74F	2
FK10	40	B74S	2
MD80	380	B757	87
		B767	6
		DC10	80
		DC87	13

* Airlines will be referred to by a random letter assignment.

4.3.4.3 Aircraft Specific Coast Analysis

Track reports for Airline-H aircraft were analyzed in groups of 10 scans. Track coast data were accumulated for aircraft that had 2 or more 10 scan periods of 2 or more coasts per period to avoid single and isolated coast events due to turning, blockage, differential lobing, garble, etc. For each selected "high-coast" period, the aircraft body type was identified and the range, azimuth and elevation angle at the beginning of the 10-scan period was calculated. Figures 38 and 39 show the distribution of these high coast periods by range and elevation angle, respectively.

4.3.4.4 Summary of Analyses

Airline-H and Airline-M had the largest airline activity during the October CDR sample, and this analysis compares different measures of coast performance between these two airlines. Various plots of coast characteristics, given in Figures 40 to 47 show that coasting of Airline-H B73S and DC10 aircraft is significantly greater than coasting associated with other Airline-H aircraft and significantly greater than coasting associated with all Airline-M aircraft.

During the 36-hour October sample, the largest number of Airline-M flights used B727 and MD80 aircraft. For each of these tracks, the probability of coasting was calculated as the number of coast reports divided by total number of track reports. These track-specific values were then arranged in ascending order to give maximum coast probability as a function of the number of tracks (flights) as shown in Figure 40. Ninety-two percent of Airline-M B727 aircraft had coast probabilities not exceeding 5%, while 98% of Airline-M MD80 aircraft had coast probabilities below 5%.

By comparison, Figure 41 gives results for Airline-H aircraft from the same sample. Airline-H B737, and B757 aircraft showed coast probabilities similar to those for Airline-M. The results for Airline-H DC10 and B73S aircraft, however, are quite different. Twenty-five percent of the DC10 aircraft had coast probabilities greater than 5%, with values up to 27%. Only 66% of the B73S aircraft had coast probabilities below 5%; the remaining 34% had coast probabilities more or less evenly ranging up to 38%, with one outlier at 51%.

Figure 42 summarizes the above by comparing maximum coast probabilities for Airline-H B73S flights to all Airline-M flights (combined).

Figures 43 through 45 compare coast probabilities among Airline-M and Airline-H flights as a function of slant range, from 2 to 40 nmi. Figure 43 shows that the level of coast among Airline-M aircraft is generally below 2% and appears not to be range dependent. Figure 44 compares the three largest groups of Airline-H aircraft in the October sample, and shows the range dependency of coasting among B73S aircraft. Performance among the Airline-H B727 and B737 aircraft is not range sensitive and is comparable to the Airline-M flights.

Figure 45 summarizes these range dependency results by comparing the distribution of coast probabilities over slant range for Airline-H B73S flights to the same for all Airline-M flights (combined).

Tracking performance is clearly degraded for Airline-H B73S and DC10 flights. Figures 46 and 47 illustrate an approximate empirical estimation of the severity of this degradation. The maximum coast probabilities derived from the CDR data for all Airline-M flights (770 flights combined) were fit to an estimation equation, as shown in Figure 46. The observed performance results are quite well represented by this equation.

In Figure 47, the estimation equation derived from Airline-M performance results is plotted along with curves giving maximum coast probabilities for the different significant Airline-H aircraft groups. The combined Airline-H B727, B737 and B757 group shows slightly better performance than the Airline-M equation. For all aircraft in the Airline-H DC10 group, and all in the Airline-H B73S group, the estimation equation was applied to calculate the expected number of coasts for each track, and the distributions of these expected values were compared to the values actually observed. The comparison indicates that 69% of the total DC10 coasts, and 66% of the total B73S coasts, appear to be attributable to aircraft specific factors.

4.4 ASSOCIATION OF COASTS WITH KNOWN PHENOMENA

The previous section calculated blip/scan ratios for the Chicago sensor under a variety of traffic densities and conditions. The results show that while the blip/scans are quite good (>94%), there are still some tracks that have occasional coasts. Coasts are caused by a long list of reasons, some more easily explained than others. For instance, aircraft that are outside the active surveillance region have a higher probability of coast due to range filter limits and rapidly decreasing mainbeam power. Other well known phenomena causing coasts are aircraft antenna shadowing during maneuvers (turning) and synchronous garble. Synchronous garble occurs when two or more aircraft are within approximately 1.7 nmi of each other in range. Their replies overlap at the ground sensor receiver and therefore increase the possibility of missing replies and coasting. Other phenomena such as antenna pattern anomalies and transponder code garbling will also cause reply and coasting. Occasionally a target report is available, but is not correlated with a track causing the track to be coasted.

In this section, the ORD coasting data are examined and an attempt is made to associate all of the coast events with one or more plausible reasons by using position data obtained from the CDR recordings. The method of associating a reason(s) for each coast is discussed followed by an illustration of their application to the CDR database.

The following two causes of a coast are determined by the active surveillance region of the ground sensor system.

(a) Range Filter Limits: The beacon detection system has range filter limits which exclude generating target report data on aircraft which are too close (< 2 nmi) or too far (> 50 nmi). Tracks extending into these regions will coast since target report data are not available. The range data are obtained directly in the CDR messages.

(b) Low-Elevation Angle: Targets below a certain elevation angle cannot be accurately tracked due to the sharp gain cutoff in the mainbeam antenna pattern at low-elevation angles. The available power at these low angles is significantly reduced, and therefore replies cannot be guaranteed. A lower limit of 0.5 degrees is used.

To calculate the target elevation angle, a 4/3-earth radius is assumed and both target and antenna height are referenced to mean sea level. For example, at ORD (antenna height = 745.8-ft MSL) an aircraft at 30 nmi and 8000-ft altitude is at an elevation angle of 2.1 degrees, whereas a target at 20 nmi at 2000 ft is at an angle of 0.4 degrees.

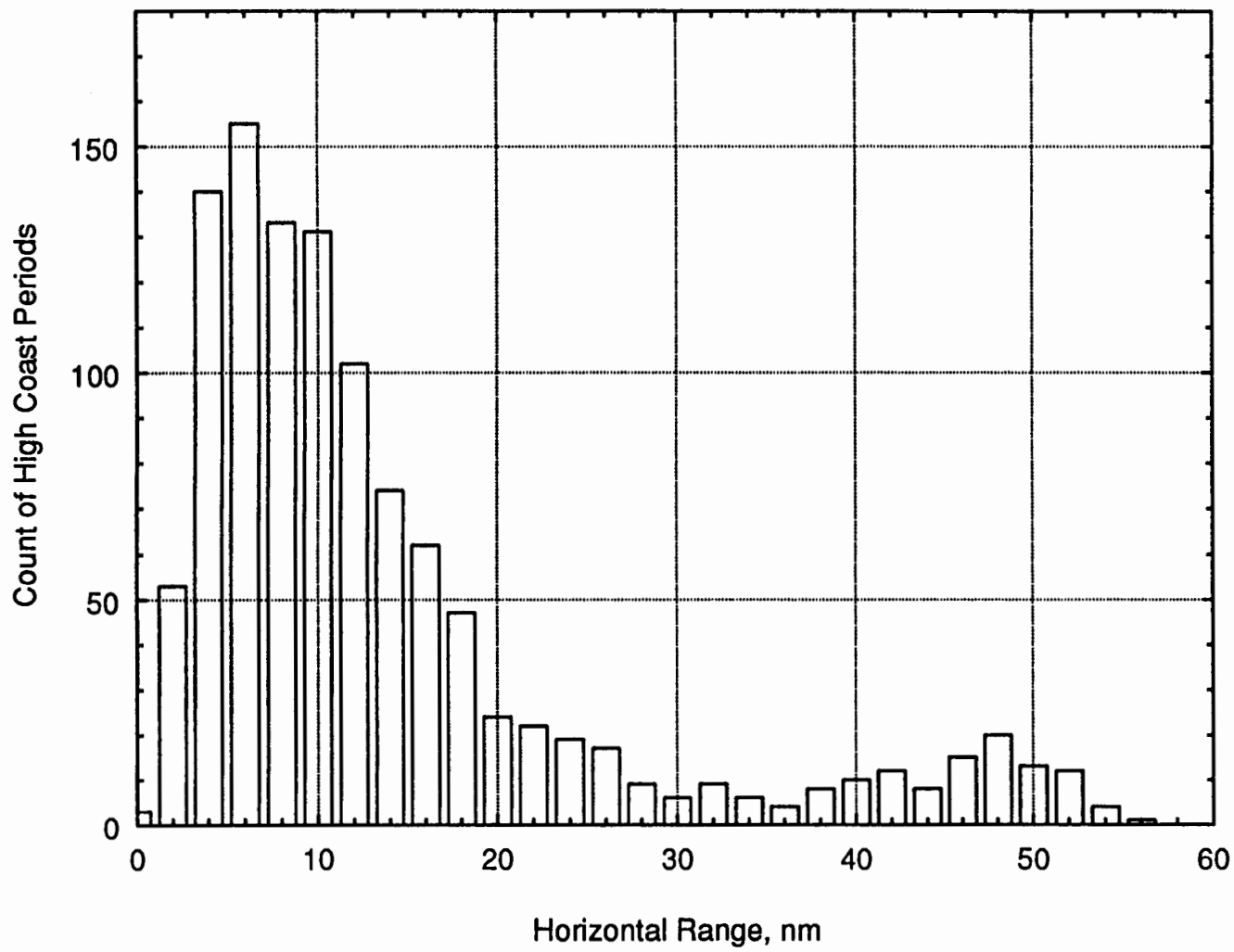

Figure 38. Distribution of High Coast Periods by Range. All High Coast Periods - No Surveillance Limits Applied / April to December 1991 CDR Extracts from Chicago.

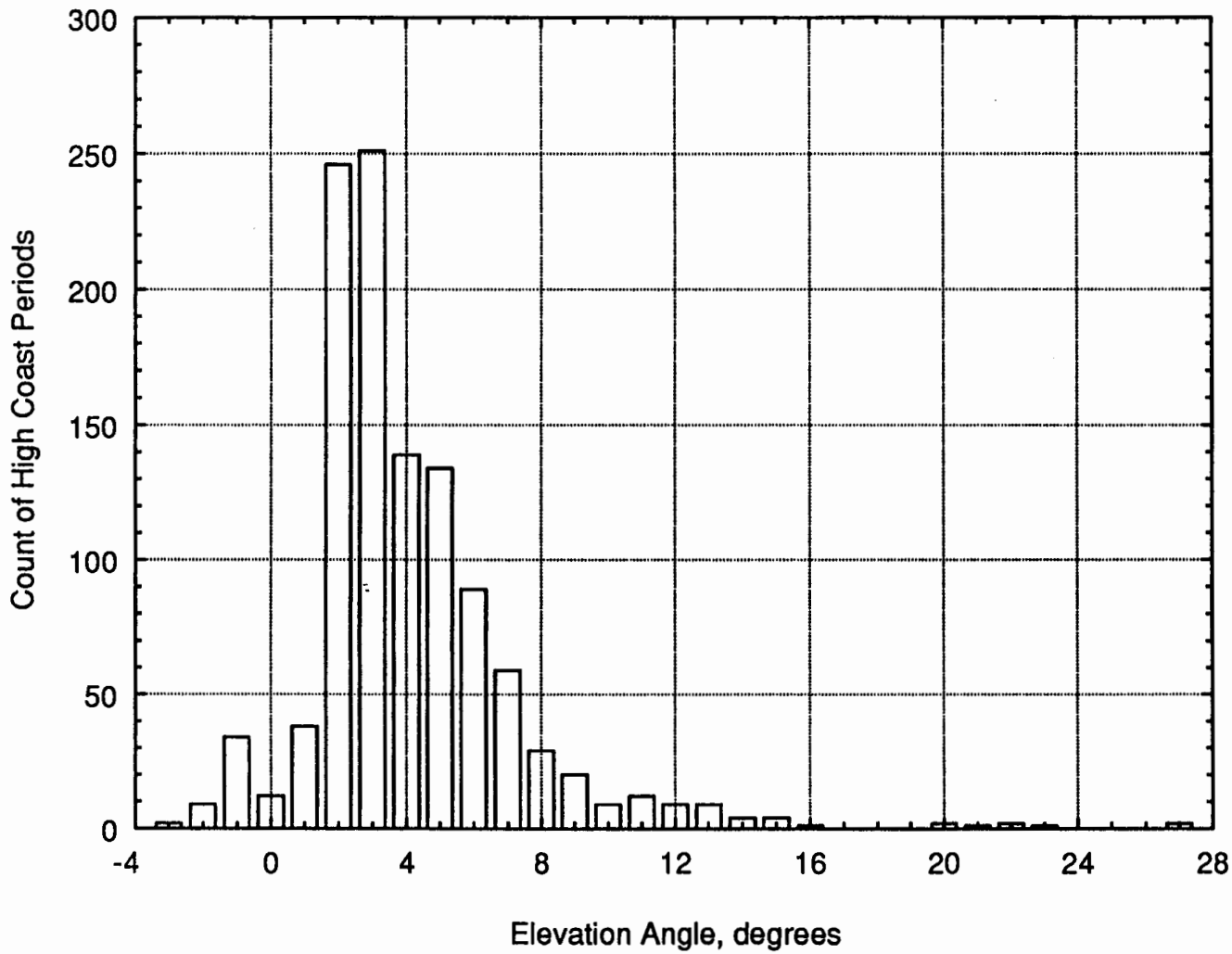

Figure 39. Distribution of High Coast Periods by Elevation Angle. All High Coast Periods - No Surveillance Limits Applied / April to December 1991 CDR Extracts from Chicago.

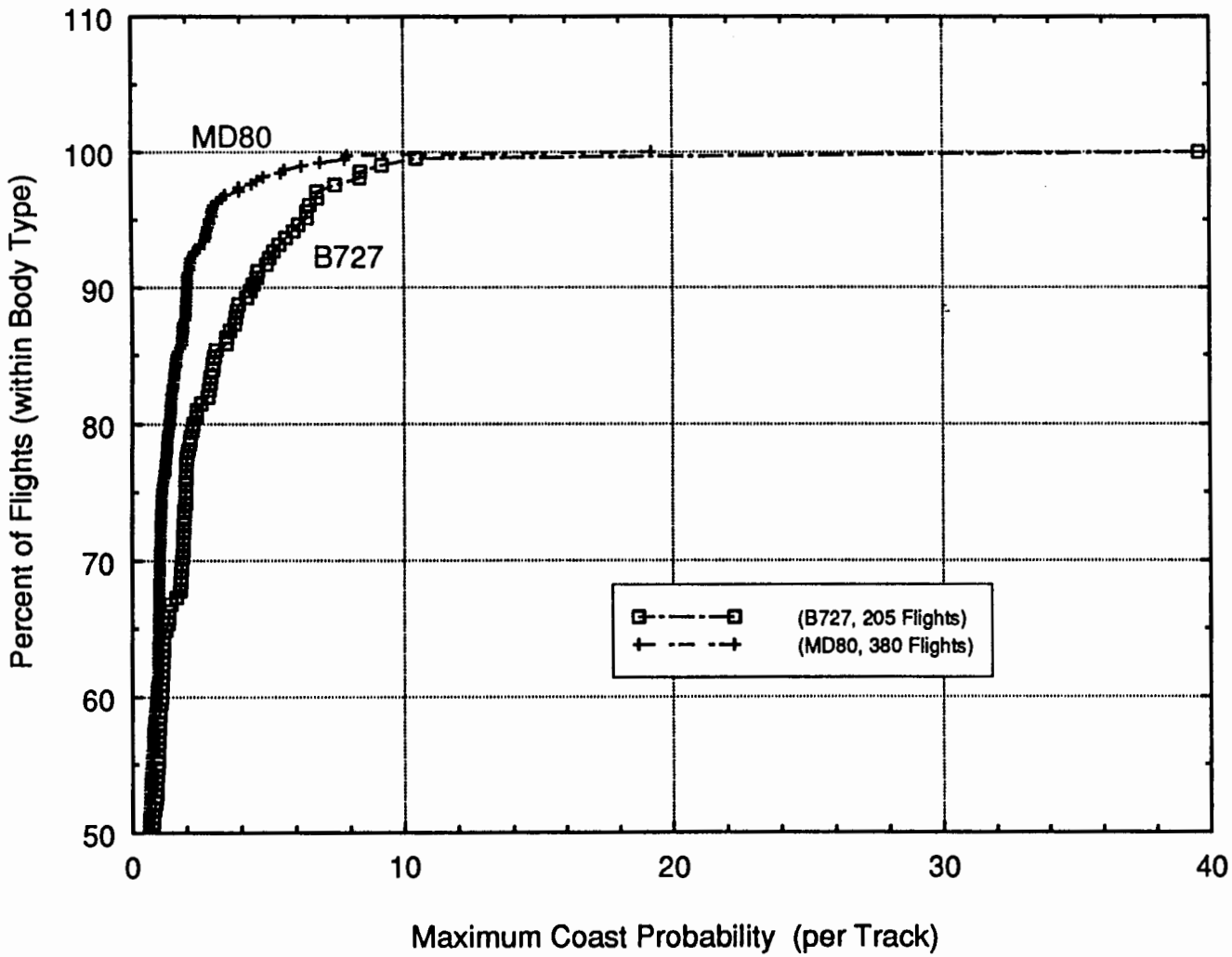

Figure 40. Maximum Single Track Coast Probabilities for Airlines. Coast Probabilities Among Principal Aircraft Types / Chicago CDR Data Sample - 6:42 pm 10/21/91 to Noon 10/23/91.

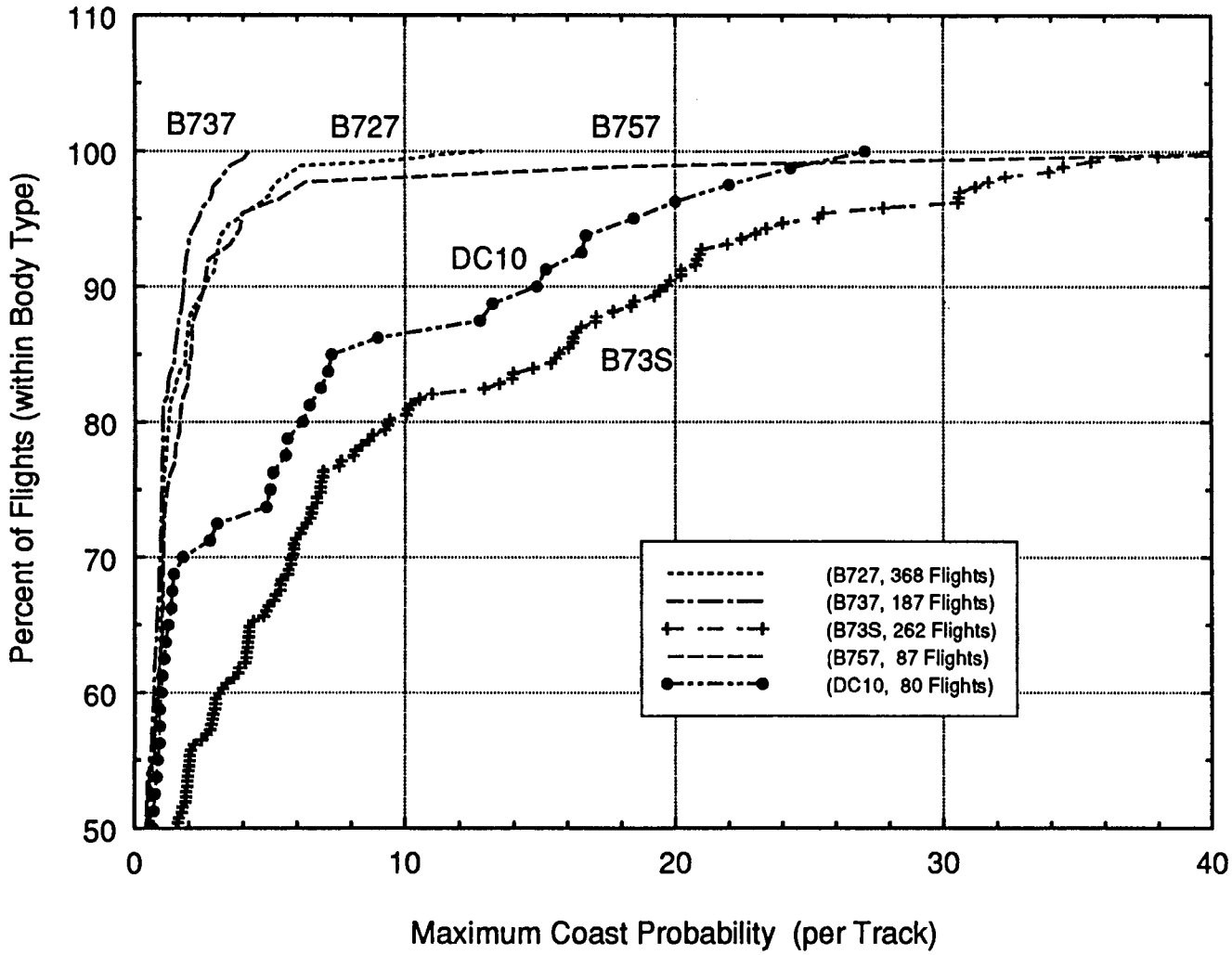

Figure 41. Maximum Single Track Coast Probabilities for Airlines. Coast Probabilities Among Principal Aircraft Types / Chicago CDR Data Sample - 6:42 pm 10/21/91 to Noon 10/23/91.

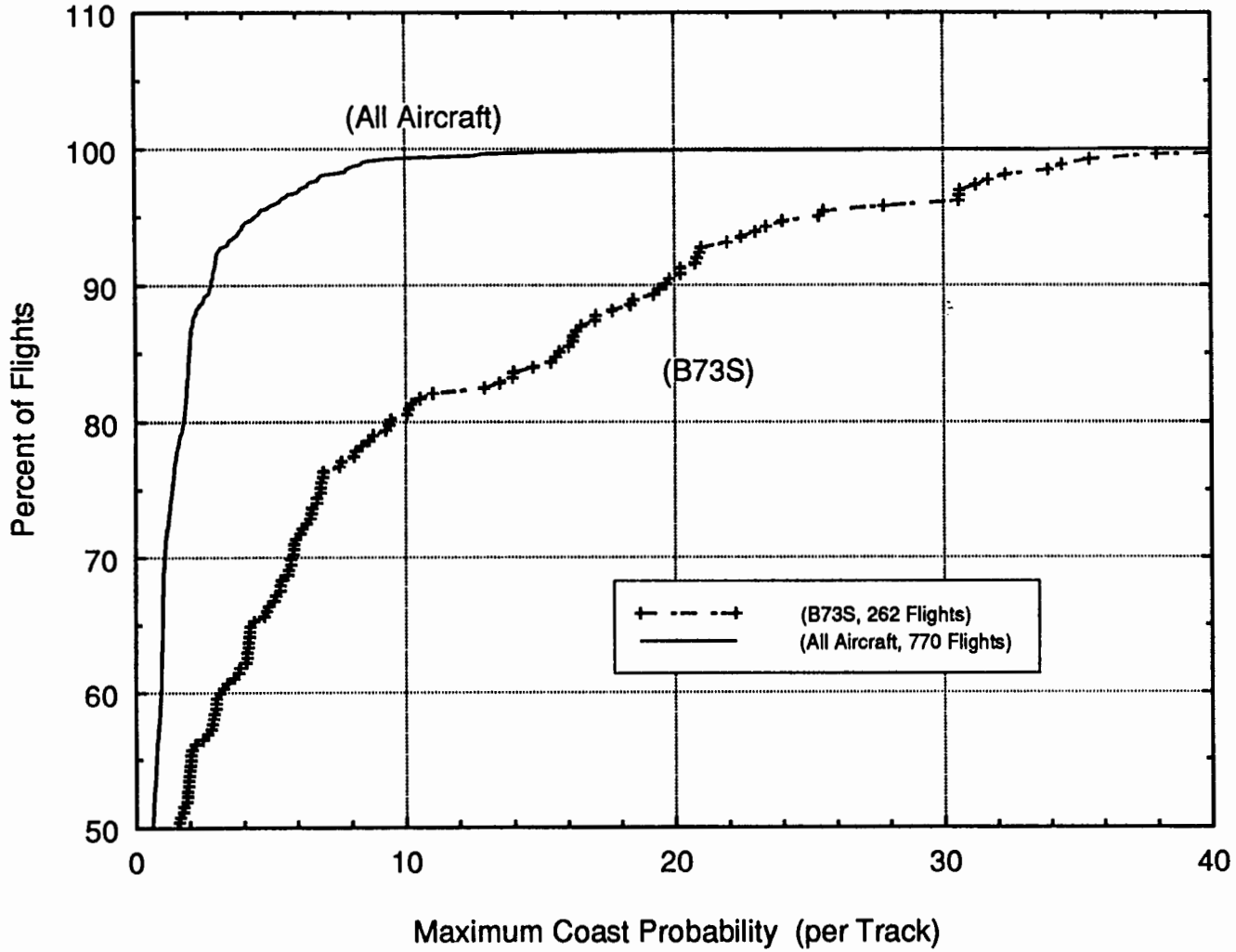

Figure 42. Maximum Single Track Coast Probabilities. Coasting Compared Between B73S and All Aircraft / Chicago CDR Data Sample - 6:42 pm 10/21/91 to Noon 10/23/91.

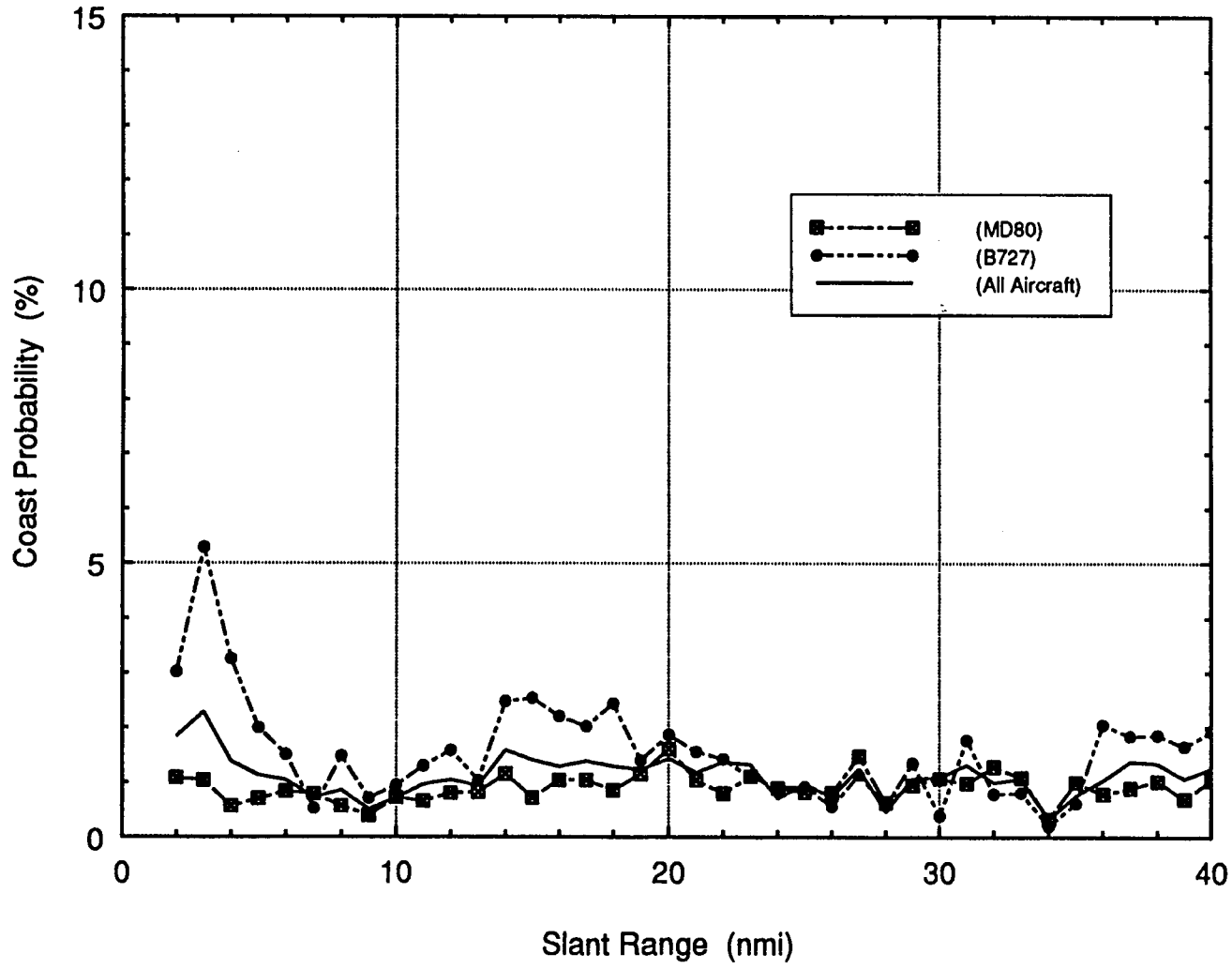

Figure 43. Probability of Coasting vs Slant Range for Selected Airline and Aircraft Type. Principal Airlines Aircraft Types / Chicago CDR Sample - 6:42 pm 10/21/91 to Noon 10/23/91.

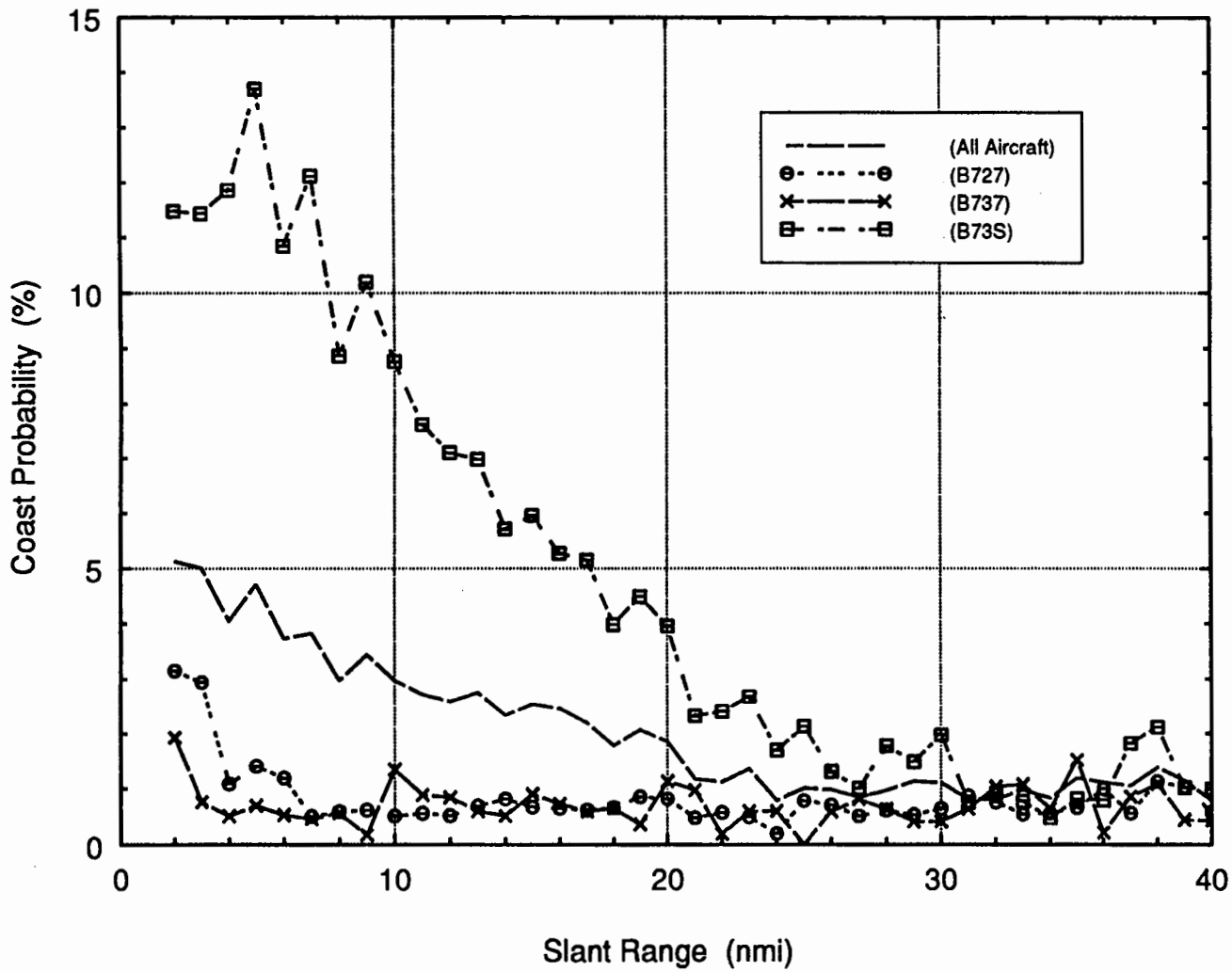

Figure 44. Probability of Coasting vs Slant Range for Selected Airline and Aircraft Type. Principal Airlines Aircraft Types / Chicago CDR Sample - 6:42 pm 10/21/91 to Noon 10/23/91.

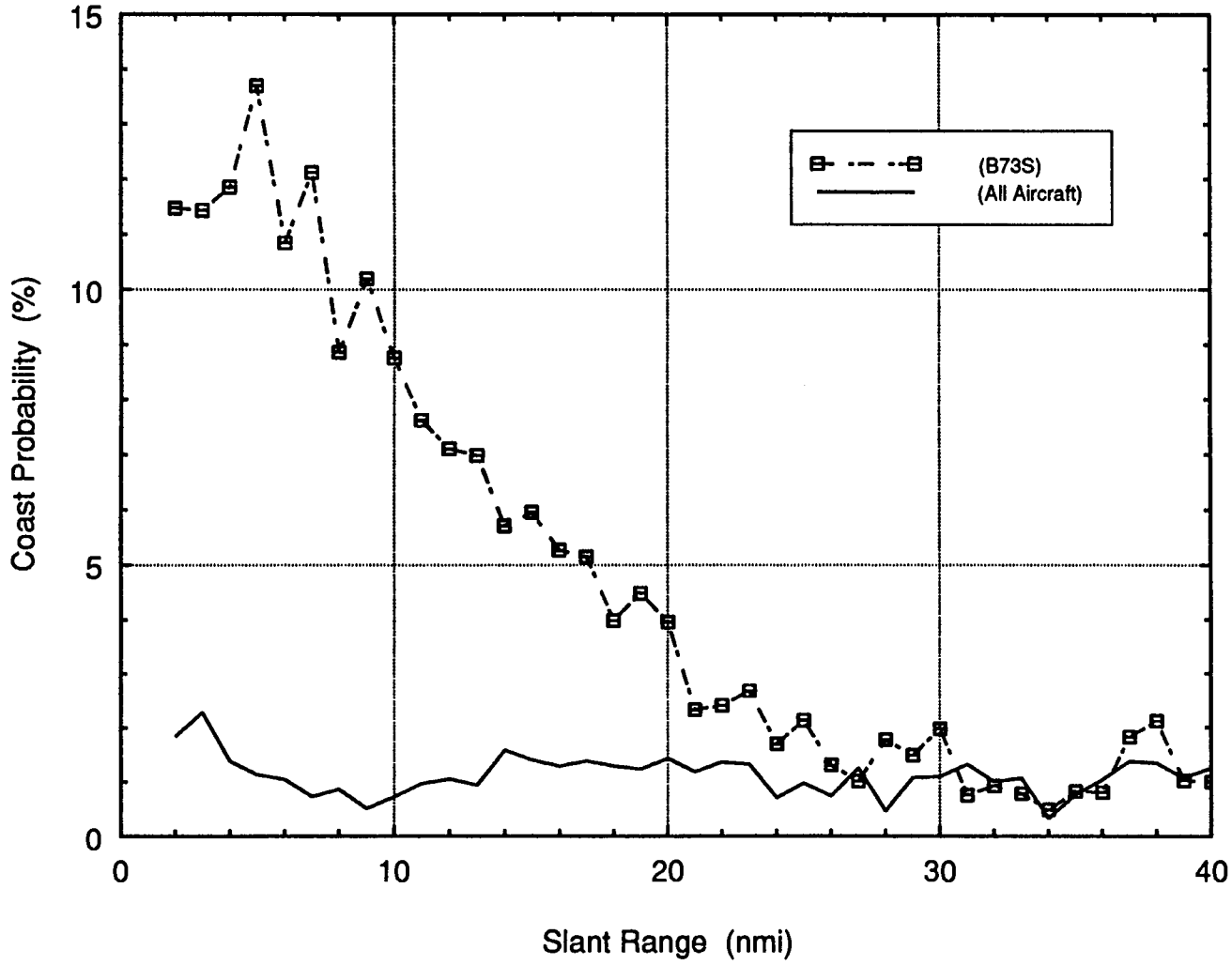

Figure 45. Probability of Coasting vs Slant Range for Selected Airline and Aircraft Type. Comparison Between B73S and All Aircraft / Chicago CDR Sample - 6:42 pm 10/21/91 to Noon 10/23/91.

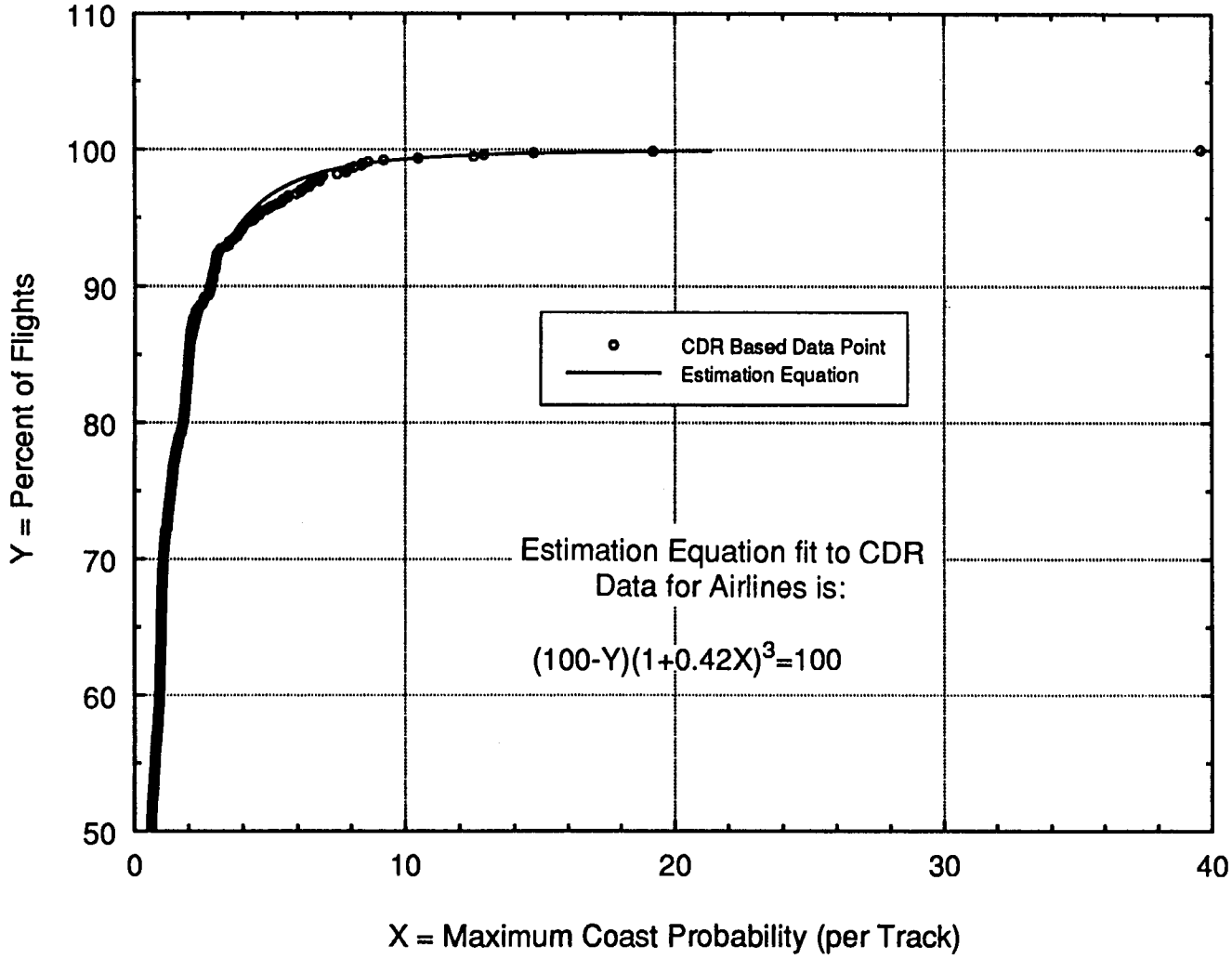

Figure 46. Maximum Single Track Coast Probabilities. Estimation Equation Derived by Fit to All Aircraft Coasting / Chicago CDR Data Sample - 6:42 pm 10/21/91 to 7:13 am 10/23/91.

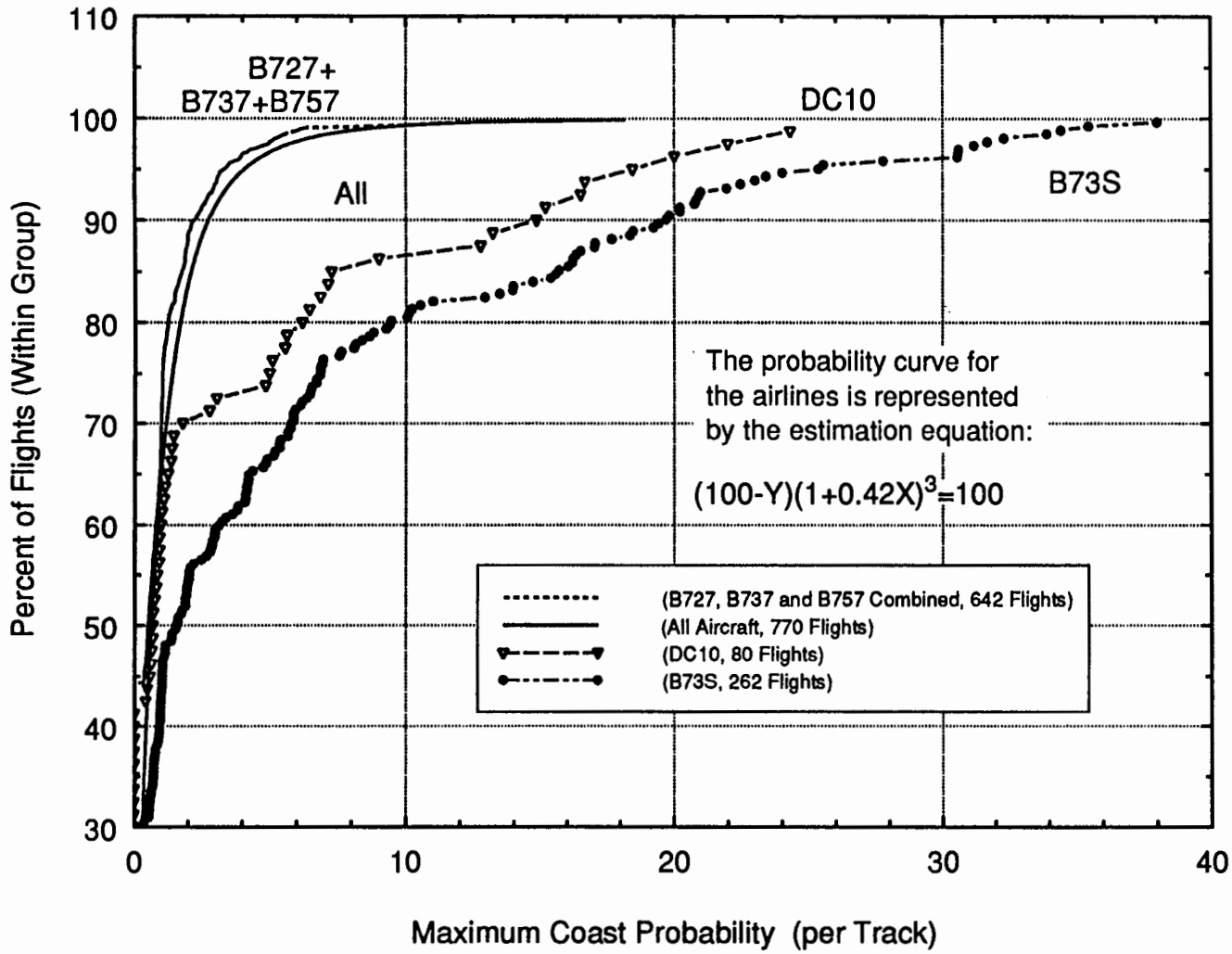

Figure 47. Maximum Single Track Coast Probabilities. Comparison Between Airlines / Chicago CDR Data Sample - 6:42 pm 10/21/91 to 7:13 am 10/23/91.

When the CDR database is screened to remove both valid reports and coasts that fall outside the active surveillance region, the remaining reasons for a coast are defined as follows:

(a) Uncorrelated Target Reports: If a coast is posted during a scan, the target report data within that scan are screened for a possible target report with the appropriate range, azimuth, and transponder code. If one is found the coast is flagged to show that a target report was available, but did not correlate.

(b) Crossing Tracks (Synchronous Garble): The aircraft tracks are examined for crossing situations that would produce synchronous garble. The track histories of both aircraft are examined to insure that both tracks are true aircraft and not false tracks produced by code garbling.

(c) False Tracks Produced by Transponder Code Garble: Since the ARTS tracker relies heavily upon the validity of the Mode 3/A code to update an active track, a new (false) track can be initiated and the original (true) track coasted one scan if the target report code is garbled (typically by 1 bit). On the following scan, a valid target report is again received and the true track is updated, while the false track is coasted. In subsequent scans, the true track continues to be updated while the false track is coasted until it is dropped. The track histories of both aircraft are examined to determine if both tracks are true aircraft or if one is a false track produced by code garbling.

(d) Low P1-P3 Antenna Gain on the Interrogation Uplink: The AMF data results described previously pointed out the multipath lobing in the antenna elevation pattern due to the mainbeam ground reflection. The net result of the lobing pattern nulls is the lack of available P1-P3 power at the target aircraft transponder antenna at particular elevation angles. The range dependence of the measured AMF data of Figure 1 was removed to produce the antenna gain pattern as a function of elevation angle illustrated in Figure 25. The azimuth regions of 30-90 degrees and 115-145 degrees are viewed as potential vertical lobing areas because of the flat ground surrounding the SSR antenna at these azimuths. Targets within these azimuth regions were evaluated in terms of their elevation relative to the expected antenna null locations. Coasts with lower than a specified value were flagged as possible low P1-P3 amplitude candidates.

(e) Low P1/P2 Power Ratio: If a transponder receives a P1/P2 signal ratio of 9 dB or greater it must reply, and conversely if the received P1/P2 ratio is 0 dB or less the transponder must suppress. P1/P2 ratios between 0 and 9 dB are not defined and whether or not a reply is issued is transponder dependent. The antenna patterns generated from the AMF data of Figure 25 show multipath and differential lobing due to the ground reflection and difference in height between the 5-ft array and the omni antenna. For this study, P1/P2 values of both 5 and 10 dB were used to evaluate the effects of antenna pattern on the tracking. It should be noted that the differences in actual aircraft altitudes and the reported quantized altitudes will make a noticeable difference in the P1/P2 ratio. This is due to the sensitivity of the lobing structure to variations in path length differences on the order of wavelengths.

(f) Aircraft Maneuvering: Since the aircraft ATCRBS transponder antenna is typically located on the fuselage underside, certain aircraft maneuvers (primarily turning) can cause shadowing of the antenna from the interrogation signals. At the moment, a

reliable automated method for determining the aircraft maneuver and the aircraft antenna blockage relative to the SSR is still being developed. However, a reasonable assessment has been made by visual inspection to determine turning aircraft and possible shadowing.

(g) Standby Antenna Blockage: AMF data showed severe signal fading due to the Standby ASR antenna along the 170-degree radial. Coasts in the azimuth sector from 165 to 175 degrees were flagged for possible signal fading.

(h) Aircraft Specific/Equipment: The CDR evaluation in the previous section brought to light coasting associated with specific aircraft types and onboard equipment. These coasts are associated with some Airline-H B73S and DC10 aircraft. The results of the previous section were used to determine the percentage contribution due to the aircraft specific coasting.

The above causes are lumped together by their net effect on the radar link performance. For instance, aircraft maneuvering and standby antenna blockage both affect the link performance by reducing the available signal strength at the transponder antenna terminals, therefore, these two causes are lumped into the category of "signal fading." The four categories comprise the following coast causes.

Garble	Synchronous garble Code garble Uncorrelated target reports
Signal Fading	Standby Antenna Blockage Aircraft maneuvering Low P1 signal power
Differential Lobing	Low P1/P2 power ratio
Aircraft Specific	Aircraft Equipment Problems

Tables 4-1 and 4-2 summarize the results of associating the coast data with the phenomena described above for both the high- and low-density samples, respectively. The coast associations are not unique in the sense that each coast may be associated with more than one possible cause. For instance, low P1 power will increase the possibility for a low P1/P2 ratio as well. However, over 90% of the coasts have been associated with at least one explanation. It should be noted that short tracks (less than 10 reports) were not eliminated. Their elimination will tend to improve the statistics overall, especially the blip/scan ratios. For a more accurate blip/scan ratio assessment refer to Section 4.3.

Table 4-1. Coast Associations for High-Density Sample (0700-0930)

Possible Cause of Coast	Percentage of Total Coasts
Garble	40%
Signal Fading	20%
Differential Lobing	30%
Aircraft Specific	5%

Table 4-2. Coast Associations for Low-Density Sample (0000-0700)

Possible Cause of Coast	Percentage of Total Coasts
Garble	60%
Signal Fading	20%
Differential Lobing	10%
Aircraft Specific	<1%

The P1/P2 association with differential lobing in the low-density sample is significantly lower due to the absence of aircraft approaching from the northeast quadrant where most of the lobing patterns occur. The low-density sample was taken late at night after noise abatement procedures went into effect limiting the aircraft in the northeast sector.

4.4.1 Track Data Samples

A select few of the track data samples are shown in the following figures. Figure 48 shows all tracks within the surveillance area for a 10-minute segment of the high-density sample. Figure 49 shows the same for the low-density sample. Both plots show the entire 10-minute CDR data sample with "Xs indicating a coast.

Figure 50 illustrates those coasts associated with a low P1/P2 ratio (indicated by the letter D) based on elevation angle to the sensor. As shown, many of the coasts in both the northeast and east-southeast wedges can be attributed to low P1/P2 power.

Figure 51 illustrates the blip/scan ratios for selected azimuth sectors for the 10 minute sample. The azimuth sectors coincide with the differential lobing regions (30-90 degrees and 115-145 degrees) and the blockage region (165-175 degrees). The table at the bottom shows the associated blip/scan ratios for the various sectors. Note the disproportionate number of coasts to track updates for the differential lobing and blockage regions as compared to the remaining region, indicating the effect of the current SSR configuration on track performance.

Figure 52 illustrates the aircraft specific problems associated with Airline-H B-737S and DC-10 aircraft. It shows an ARTS radar track of a Airline-H B-737S aircraft into and out of O'Hare Airport. Serious track coasting is observed within approximately 20 nmi of the airport SSR. The extent of coasting and its occurrence within 20 nmi of the SSR is typical of all aircraft coasts that are identified to be equipment specific. The problem appears to be due to a deficiency in the design of the reply rate limiting function in earlier models of one particular manufacturer's Mode S transponder, which occasionally prevents the transponder from replying to SSR interrogations. The problem is under investigation by the manufacturer and plans are to replace the defective transponders as quickly as possible.*

---

* This assertion was verified and the defective transponders repaired soon after the results of this study were announced.

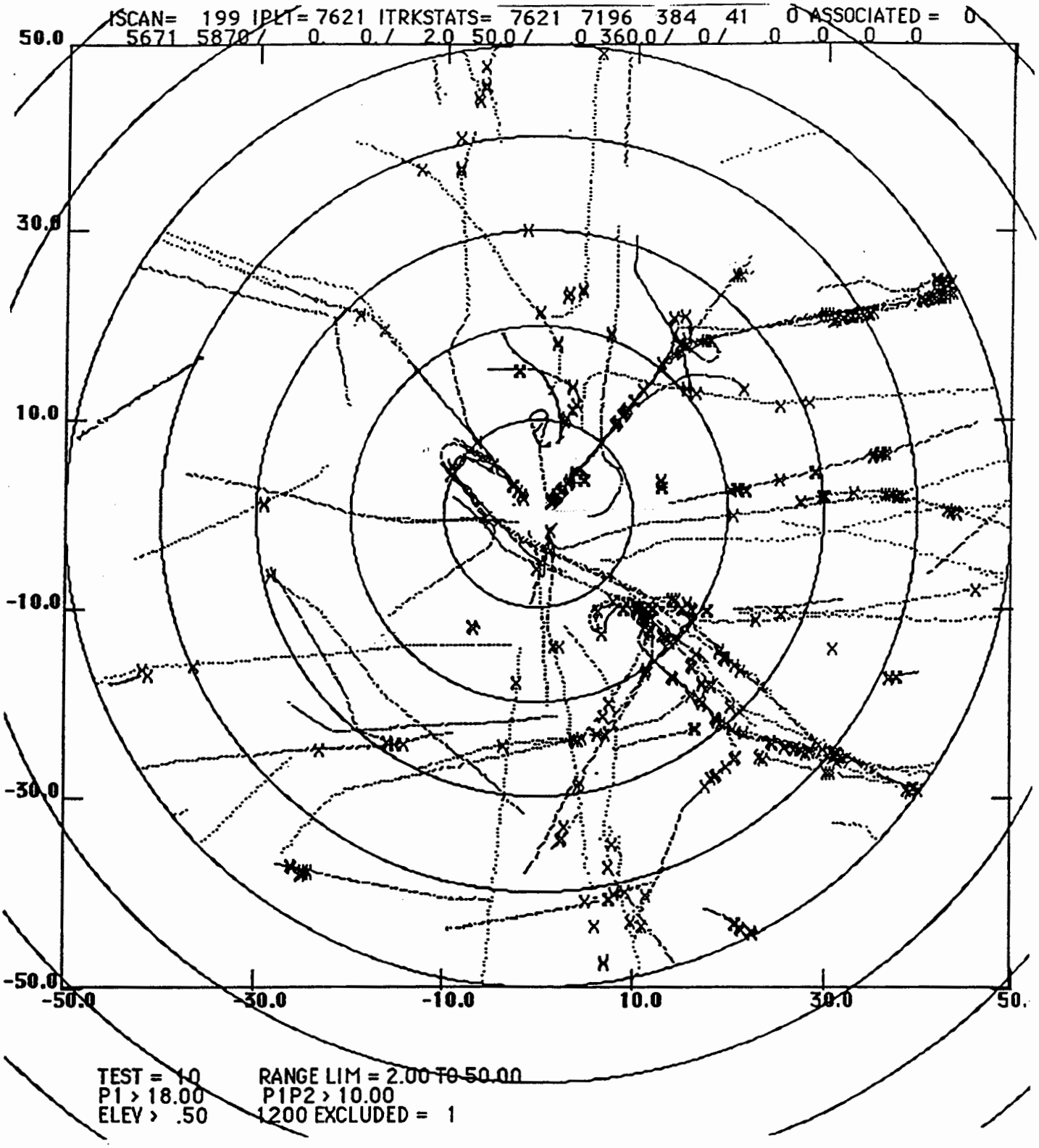

Figure 48. High-Density Data Sample. All tracks within surveillance area.

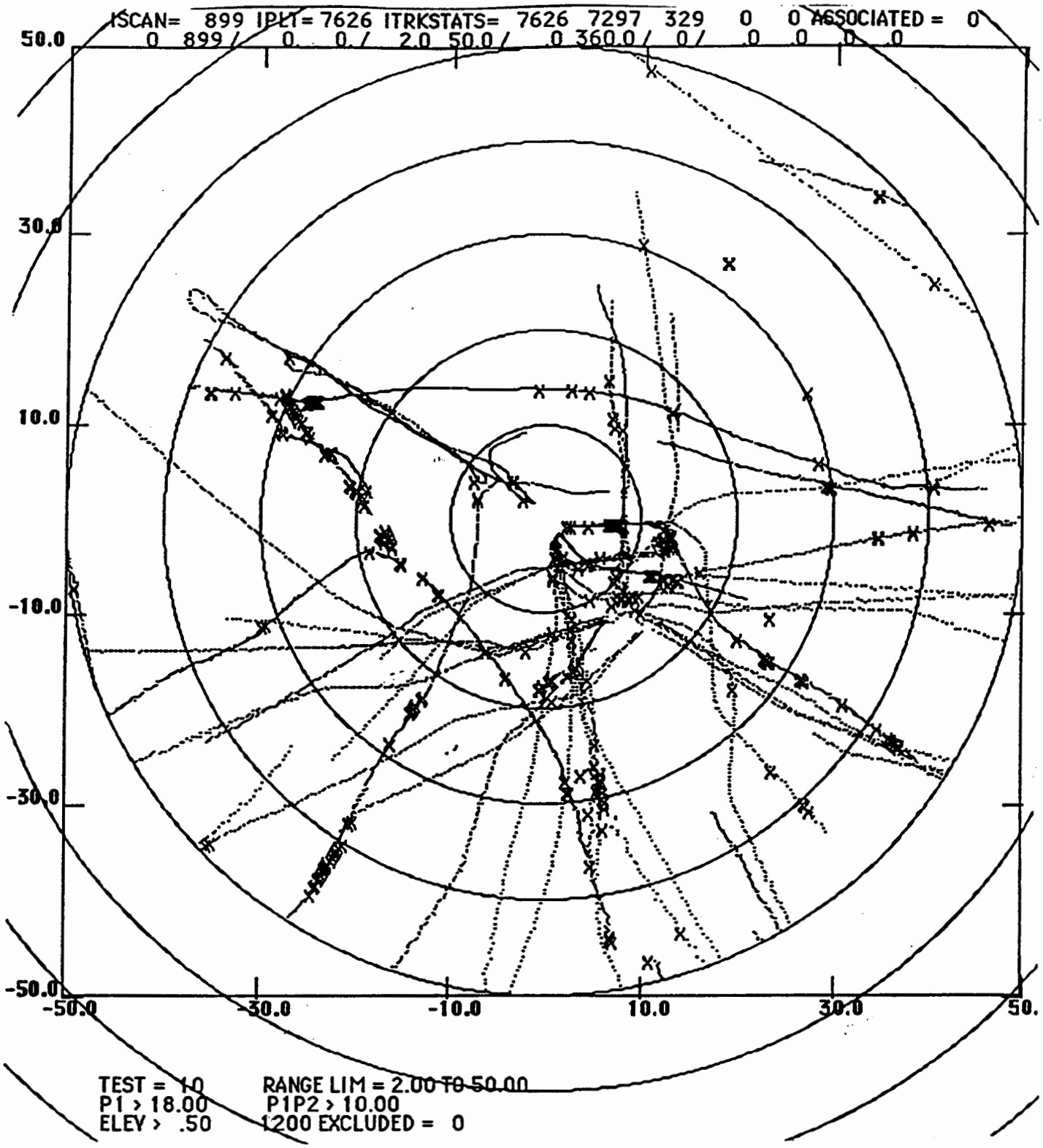

Figure 49. Low-Density Data Sample. All tracks within surveillance area.

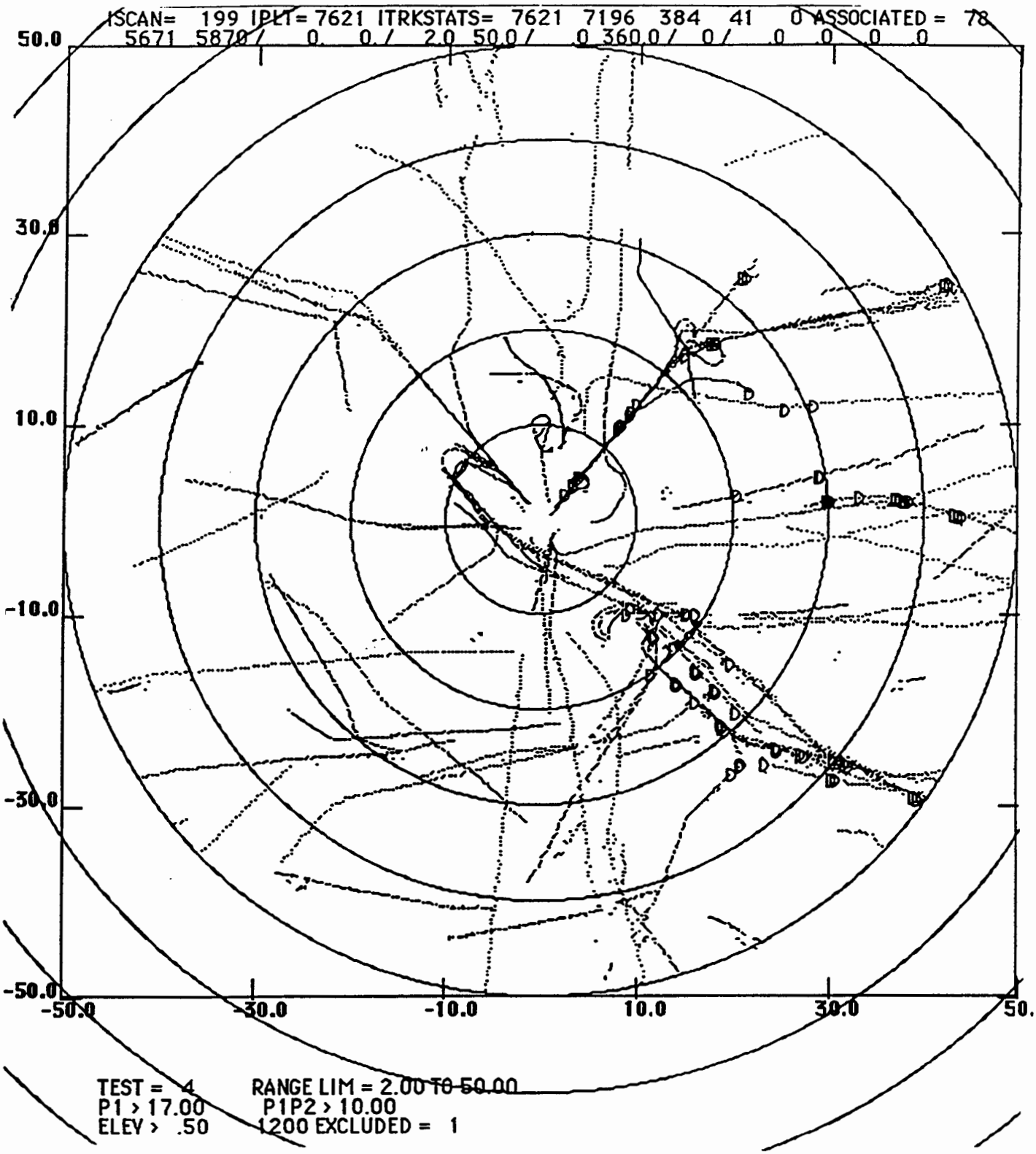

Figure 50. Coasts Associated with Low P1/P2 Ratio - High-Density Sample.

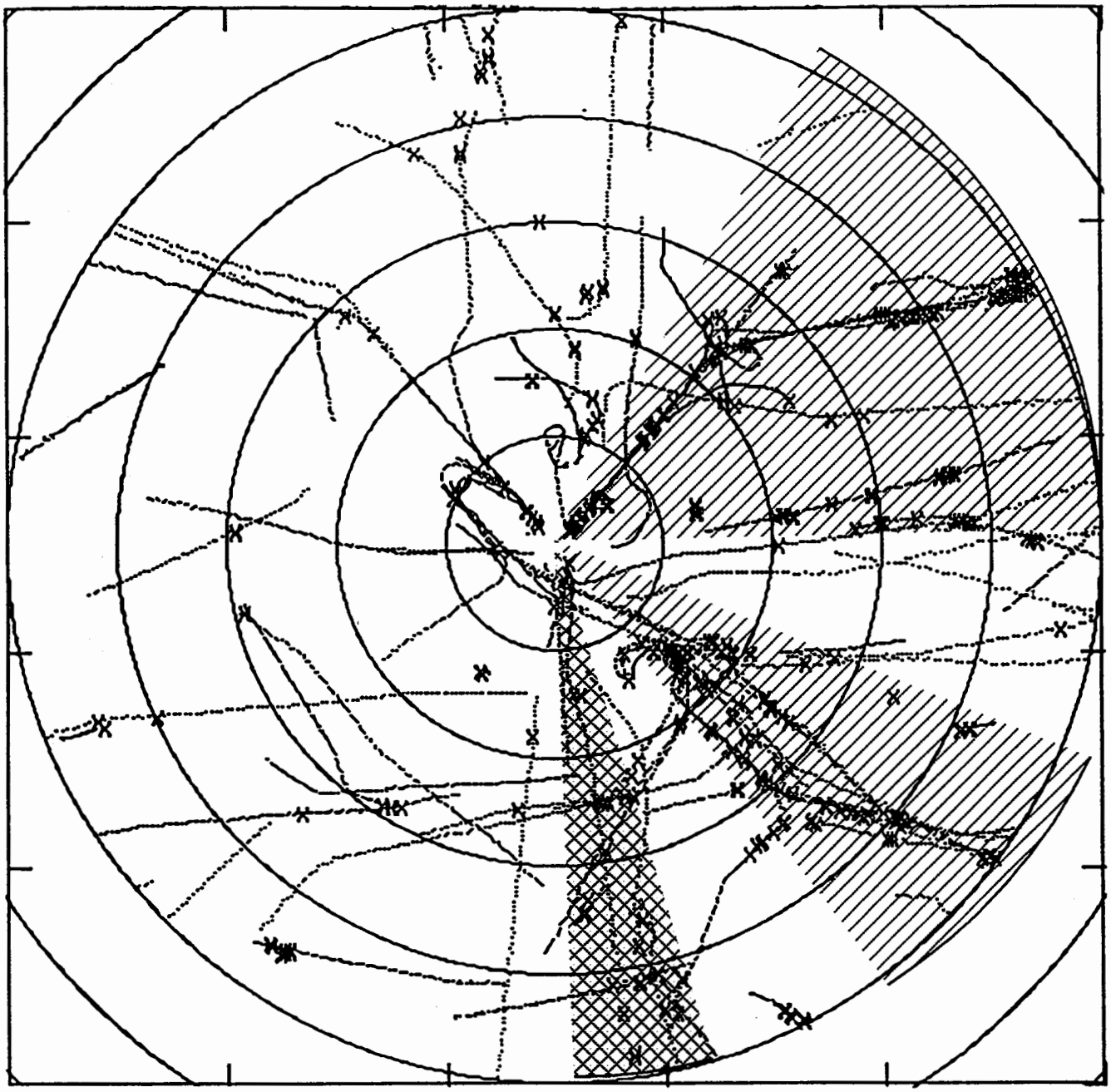

Figure 51. ARTS Track Data — 22 October 1991 - 7:45 to 7:54 am.

	UPDATES	COASTS	BLIP/SCAN
OVERALL	7196	384	94.9%
	2848	244	92.1%
	310	22	93.3%
REMAINING	4038	118	97.2%

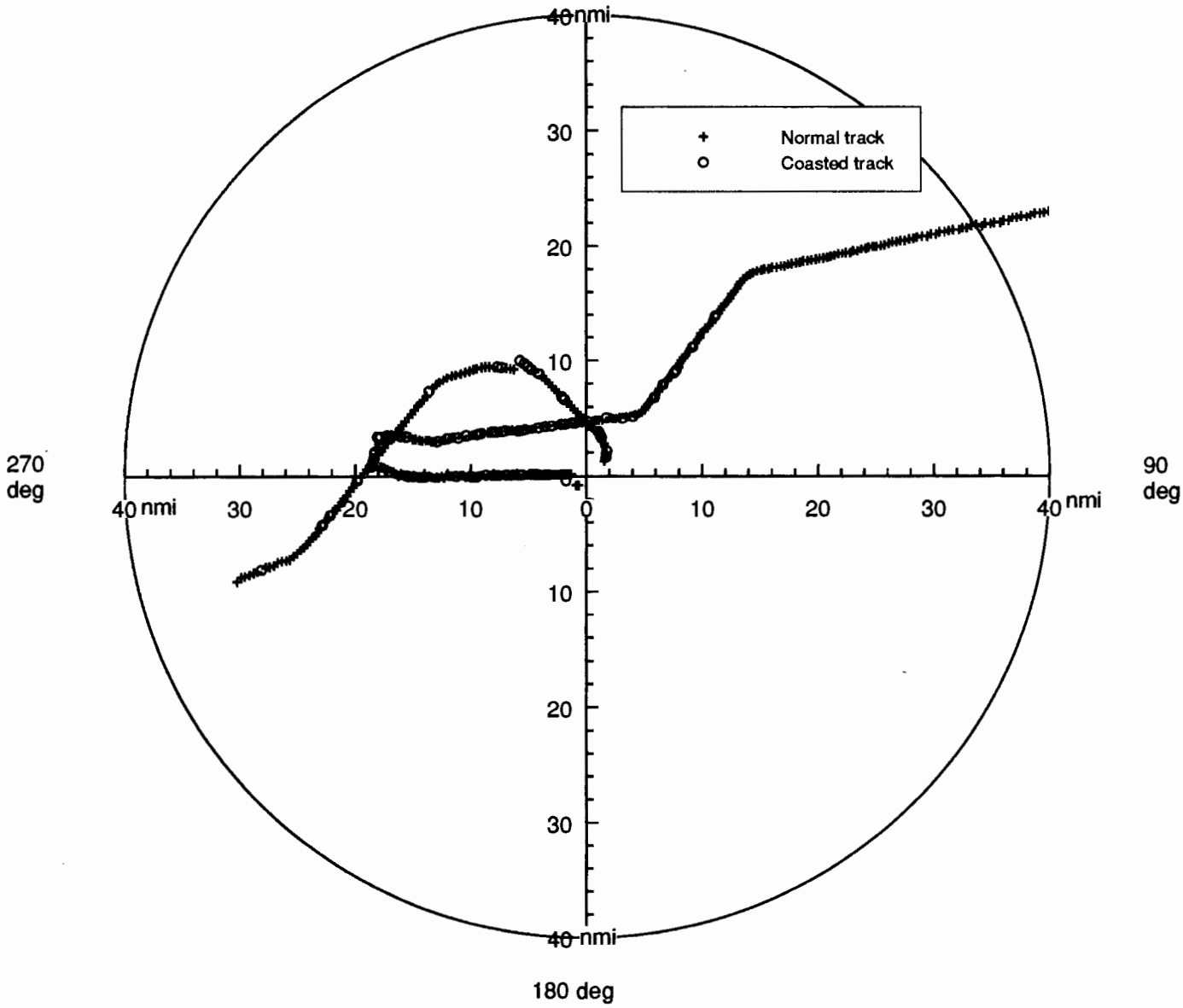

Figure 52. Chicago Radar Track. Chicago 12/2/91 from 15:00 to 19:08.

5. CONCLUSIONS

5.1 IMPACT OF TCAS ON SSR PERFORMANCE

Examination of AMF data collected during the busy morning traffic period of 22 October 1991 shows an acceptable TCAS total interrogation rate at the location of the AMF aircraft. AMF was flown in the most dense and problematical traffic areas as defined by the O'Hare controllers and the number of TCAS-equipped aircraft within the Chicago terminal area at the time is estimated to vary between 14 and 16. The number of TCAS was derived from an association of flight numbers to airline TCAS equipage lists.

In one initial 9-minute segment, the total number of TCAS interrogations observed by AMF during the observation period was 82,211 which results in an average TCAS interrogation rate of 152.3/sec due to all TCAS units in the vicinity. Assuming that a TCAS interrogation "ties up" a transponder for 50 sec and that the TCAS interrogation rate was poisson distributed, a victim transponder would be unavailable for a single SSR interrogation 0.76% of the time because of TCAS. During this 9-minute segment, a preemption of an SSR interrogation received at the AMF by a TCAS interrogation actually occurred 153 times in 25,346 opportunities or 0.6% of the time. This value agrees with the poisson assumption above and is considerably less than the 1% average interference limit allocated to TCAS.

It is interesting to note that the ground interrogator activity during this period would have occupied a victim transponder 1.6% of the time.

To ensure that the initial 9-minute segment is representative of a longer period, ATCRBS and TCAS interrogations were counted over the entire 2 1/2 hours of data. During this longer period, the total TCAS interrogation rate exhibited occasional peaks with the highest peak reaching about 500 TCAS interrogations per sec. The ARTS track performance was not noticeably affected by the peak values in the TCAS interrogation rate.

The peak values coincide with the times that the AMF aircraft is closest to the O'Hare SSR and conceivably close to many TCAS aircraft such that it could briefly observe most of the interrogations from each nearby TCAS regardless of the direction of the interrogation and therefore see an occasional peak above 280/sec. This is still an acceptable condition for a victim transponder since the TCAS interference limiting design philosophy is concerned with the average effect of the total of all TCAS interrogations on the reply reliability of transponders under SSR surveillance.

To illustrate the insignificant impact to SSR of a total TCAS interrogation rate of 500/sec at a victim transponder under full TCAS implementation, an analysis was performed that shows that the TCAS interrogation rate would have to reach 10,000 interrogations per sec (20 times higher) before it would degrade the SSR surveillance track reliability of a transponder by 2%.

The AMF also measured the ATCRBSE interrogation rates and the suppression rates produced by all SSRs in the Chicago vicinity during the 2 1/2-hour period. The SSR transmission activity in terms of occupation of transponder availability is nearly twice that of the TCAS interrogation activity.

5.2 SSR INTERROGATION PERFORMANCE

Severe differential lobing in elevation is observed along an azimuth of 65 degrees relative to the SSR and is seen to result in target coasting. The character of the terrain surrounding the SSR and analysis of coasting observed on AMF and ARTS targets-of opportunity suggest that differential lobing can occur within an azimuth region of 40 to 85 degrees. There is evidence to indicate that the differential lobing observed in Chicago degrades the overall track blip/scan ratio 1 to 2%.

Differential lobing occurs when interrogation signals from vertically displaced mainbeam and omni antennas are subject to in-beam multipath reflections. At some elevation angles the null of the mainbeam signal can coincide with a peak of the omni signal causing mainbeam suppression of the transponder. Examination of the data indicates that differential lobing can also result in P1 pulse reduction near beam edges because of destructive interference between comparable levels of mainbeam P1 pulse and omni ISLS P1 pulse. This has been seen to result in either a shortening of the scan runlength or transponder rejection of interrogations because of out-of-tolerance relative P1 and P3 values.

Differential lobing can be eliminated in Chicago by operating with the integral omni function of the 5-ft array. It is understood that this is not a desirable option because of the increase in reflections caused by the inadequate SLS pattern coverage at the ends of the array and the current limits on transmit power. Also, the negative tilt of the 5-ft array exacerbates the lobing problem by decreasing the advantages of the underside cutoff characteristic. It is understood that the tilt is desired in order to increase low angle, long range coverage, again because of current limits on transmit power. This is a bad trade-off since the free-space power gain of 1.5 dB is offset by a large increase in the depths of the lobing nulls. It is understood that eventually the current SSR function in Chicago will be transferred to the ATCBI-5, and that the added power capability of the BI-5 will allow operation with the integral omni and an antenna tilt of 0 degrees. It is also recommended that the RF phase between the mainbeam P1 signal and P1 omni signal be phased to prevent destructive interference.

An alternative solution to the differential lobing problem is the placement of fences at appropriate locations to prevent reflections. A complete analysis of the reflection phenomena using target track data may provide sufficiently accurate information on reflection points in order to establish locations for a reflection fence.

Less severe problems of signal fading were observed at azimuths of 170 degrees and 300 degrees and are attributed to blockage by the standby radar and a lightning support pole respectively. Fading on the order of 8 to 12 dB occurs because of the standby radar and 8 dB because of the support pole.

5.3 ARTS TRACK PERFORMANCE

Blip/scan ratios computed from the ARTS data indicate reasonable overall track performance. A blip/scan ratio computed using all tracks within the ARTS surveillance area resulted in values of 93.9% and 95.4% for the high-density and low-density sampled periods respectively. When short tracks (less than 10 track reports) and tracks outside of 0.5- to 40-degrees elevation and 2- to 45-nmi range are excluded, the blip/scan ratios become 97.6% and 98%, respectively, for the high and low densities. These values compare favorably with the performance measured at other high-density terminal areas.

Detailed examination of blip/scan ratios for individual air carrier aircraft indicate that the track performance associated with a few specific aircraft is substantially poorer than the average air carrier performance. Analysis of 36 hours of ARTS data collected from 21 to 23 October 1991, shows that 67% of one Airlines B-737S and DC-10 aircraft in the Chicago area experience severe coasting within about 20 nmi of the terminal SSR. This coasting is characterized by extended periods of time during which altitude information is not available to controllers. These particular aircraft exhibit coast probabilities about five times greater than other air carrier aircraft. The cause of this coasting appears to be due to a fault in the design of the reply rate limiting function in early versions of one manufacturers Mode S transponder which occasionally prevents the transponder from replying to SSR interrogations. Although this cause accounts for only 5% of the total coasts seen by controllers, its persistence during a track deprives the controller of necessary altitude information especially during critical terminal approach and departure periods. As a result, every effort is being made to resolve this particular problem quickly.

The association of ARTS target track coasts to probable reasons for the coast was successful for over 90% of the coasted scans of air carrier aircraft tracks recorded during both the high traffic density and the low-density traffic periods of 22 October 1991.

Of the associated coasts, about 30% appear to be caused by the differential lobing problem. If this problem were eliminated, the blip/scan ratio of the Chicago ARTS would improve by about 1 to 2%.

APPENDIX A

FLIGHT TEST SCENARIOS

Airborne Measurement Facility (AMF) flight tests were conducted at Chicago O'Hare Airport on 21 October 1991. This appendix gives a brief summary of the tests conducted during that time frame.

Basically three objectives were accomplished over two flights within the ORD TCA. The objectives are outlined below.

A. 1030 MHZ UPLINK MEASUREMENTS ALONG APPROACH/DEPARTURE PATHS

This test acquired uplink interrogation data along approaches to all active runways at ORD. The MIT aircraft was sequenced with air carriers during high-density traffic periods. The purpose of these measurements was to obtain transponder suppression rates, TCAS whisper/shout interrogations and ground sensor performance.

B. 1030 MHZ TCAS INTERROGATION MEASUREMENTS

This test acquired TCAS interrogation data within the Chicago surveillance area by orbiting the airport from approximately 15 nmi at 6500-ft altitude. The purpose was to obtain measurements of TCAS whisper/shout interrogations and interference limiting performance within the 1030 MHz environment.

C. ASR ANTENNA PATTERN AND VERTICAL LOBING STRUCTURE ASSESSMENT

This test measured the SSR 5-ft array and stick omni pattern at various azimuths and elevations to characterize the antenna mainbeam, Sidelobe Suppression (SLS) with the omni antenna, and the elevation pattern vertical lobing structure.

Tests A and B were conducted simultaneously during the morning rush from 0700-0940 CST. Data were taken on approaches to runways 22R and 14L and departures on runway 09. Data were also taken in the vicinity of TCAS equipped aircraft on approaches to 22R and 14L at approximately 25-nmi radius at 6500 ft.

Test C was conducted at night during low operations from 2230-0030. Figure A-1 depicts the relation between the radial tests and the ORD airport runway configuration. The radial flights were flown at several different altitudes to collect data over a range of elevation angles. Table A-1 displays the altitudes and ranges that were flown to cover the elevation angle range of 1-4 degrees.

Table A-1. Altitudes and Ranges for Radial Runs (Test C)

Altitude	Range (from ORD)	Max Ground Speed
3000	25 - 7 nmi	124 kts.
4000	32 - 9 nmi	160 kts
5000	38 - 12 nmi	160 kts
6000	44 - 14 nmi	160 kts
8000 (065 radial only)	56 - 18 nmi	160 kts

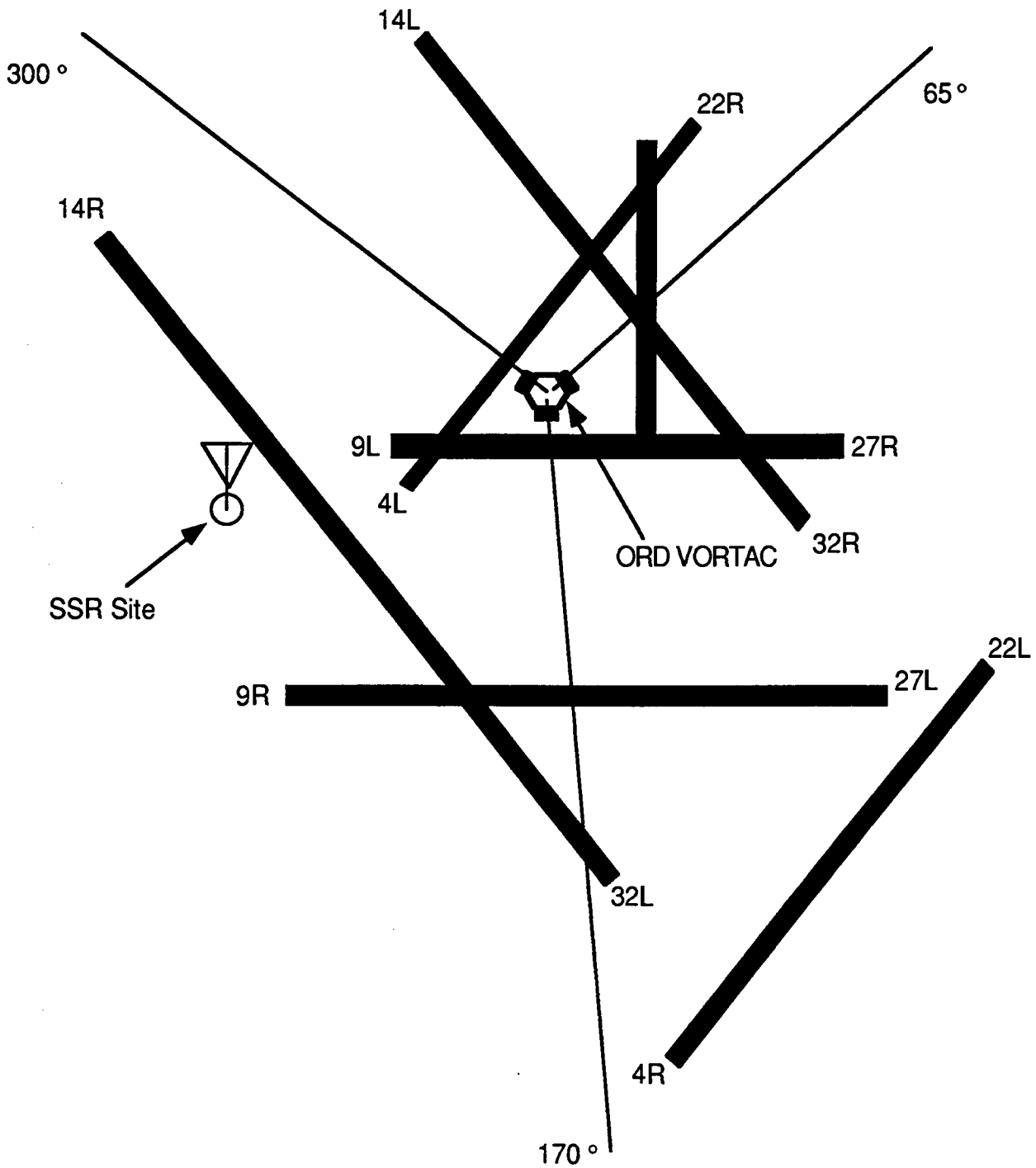

Figure A-1. AMF Flight Test - Radials for Vertical Lobing Assessment (Test C).

APPENDIX B

ORD ARTS III/A ATCRBS RADAR PARAMETERS*

Secondary Surveillance Radar Parameters

Transmitter:

Type:	ATCBI-4
Nominal PRF:	424 pps
PRF Stagger Sequence (msec):	1897
	1981
	2411
	3003
	2348
	1937
	2002
	3286
P1/P3 Power into Mainbeam antenna:	141 Watts (51.5 dBm)
P2 SLS Power into Omni antenna:	229 Watts (53.6 dBm)
P1 ISLS Power into Omni antenna:	114.5 Watts (50.6 dBm)
Interlace:	3A,3A,C
SSR Antenna:	
Tower Height:	67-ft. AGL (664-ft. MSL)
Antenna Tilt:	-1 degree
5-Ft Array:	FA9764 Texas Instruments
Gain	+ 21 dBi at peak-of-beam
Antenna Height (MSL):	745.8 ft. to array center
Omni Antenna:	FA8044 Vertical Collinear Array, 20" tall
Gain	+ 4 dBi
Antenna Height (MSL):	748.3 ft. to array base

From Don Hahn, AGL-463 FAA Regional Office, Chicago.

APPENDIX C

SSR UPLINK POWER CALCULATION

The following calculation of received interrogation power levels at the AMF receiver for a range of 15 nmi is intended to illustrate the assumptions and the parameters used to compute the comparative theoretical values of received power used in the report.

SSR UPLINK POWER CALCULATION

		Main Beam	Omni	
SSR Transmit Power	(dBm)	+51.5	+53.6	
SSR Transmit Ant Gain (1)		(dBi)	+19.0	+4.0
Free-Space-Path Loss (2)	(dB)	-122.0	122.0	
AMF Antenna Gain	(dBi)	+3.0	3.0	
Rec. Pwr. at AMF	(dBm)	-48.5	-61.4	

(1) SSR antenna gain at 2-degree elevation with -1 degree antenna tilt. Peak-of-beam gain is +21 dBi with a 1.5 dB/degree lower edge cutoff at 0-degree elevation.

(2) Free-space path loss = 20 log ($4\pi R/\lambda$) where R = 15 nmi.

APPENDIX D

AMF DESCRIPTION

The Airborne Measurement Facility (AMF) is a data collection and conversion system that provides a means for obtaining recorded data representing pulsed electromagnetic signal received on one of the two ATC radar beacon frequency bands (1030 or 1090 MHz) that is selected for a given data collecting mission. The facility consists of two subsystems:

1. The airborne subsystem provides for the reception of signals in the selected band, their conversion to digital data samples and storage on an instrumentation-type magnetic tape, see Figure D-1.
2. The ground post-processing subsystem provides a means for playing back the instrumentation tape and subsequent storage onto a computer readable format 9-track tape.

The airborne subsystem basically contains a receiver/digitizer box, which houses two (2) pulse amplitude measuring channels, one for each of the top and bottom aircraft omni antennas, and one angle-of-arrival measuring channels. The analog pulse data are digitized and stored in words of 48 bits in length which include measured items such as top and bottom channel pulse widths, amplitudes, and angle-of-arrival (relative to aircraft heading). Along with the pulse data is a time stamp to indicate the initiating time of the received pulse. The pulse data are then stored on a high speed instrumentation tape.

The instrumentation tape is then processed by filtering and sorting the pulse data words then storing the remaining pulse data onto 9-track tape. The 9-track tape can then be processed using computer based analysis to recreate the timeline of events, events being a particular interrogation format, to assess interrogation rates, ATCRBS radar performance, TCAS whisper/shout interrogations, etc.

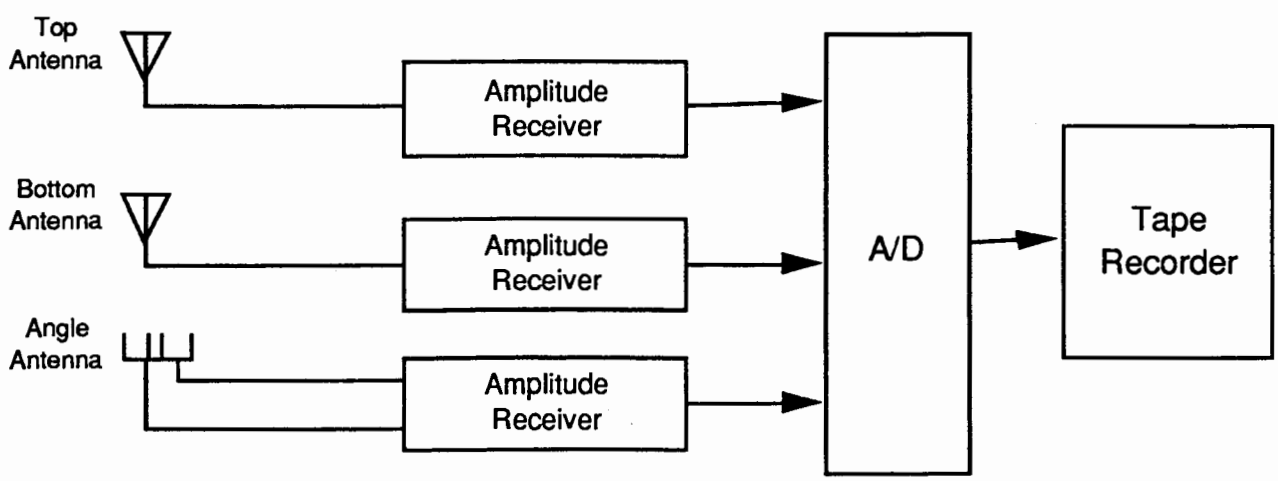

Figure D-1. AMF Airborne Subsystem Block Diagram.